UNIVERSITY OF TURIN

DOCTORAL SCHOOL

PhD in
AGRICULTURAL, FOREST AND FOOD SCIENCES

CYCLE: XXXIII

"*SWEETIES VINIFERA*: THE ROLE OF SUGAR METABOLISM AND SIGNALLING IN GRAPEVINE RESPONSES TO BIOTIC AND ABIOTIC STRESSES"

Cristina Morabito

Supervisor:
Prof. Andrea Schubert

Ph.D. Coordinator:
Prof. Eleonora Bonifacio

YEARS
2018; 2019; 2020

Meravigliarsi di tutto è il primo passo

della ragione verso la scoperta.

Louis Pasteur

CONTENTS

INTRODUCTION

Carbohydrates synthesis and sucrose distribution in the plant

Plants synthesize sugars from photosynthesis, and leaf sugars are transported to the whole plant allowing growth. Sugar distribution regulates growth of plant organs and sucrose is the main sugar transported along the phloem. Plants fix atmospheric carbon dioxide into triose phosphates in the chloroplast. Triose phosphates are transported into the cytosol and then converted into fructose bisphosphate by aldolase. A phosphatase converts fructose bisphosphate into fructose 6-phosphate, which can be transformed into glucose 6-phosphate by phosphoglucoisomerase. Phosphoglucomutase is then responsible for interconversion of glucose 6-phosphate into glucose 1-phosphate. The enzyme UGPase synthetizes UDP-glucose from glucose 1-phosphate and UTP, and sucrose derives from dephosphorylation of sucrose 6-phosphate, obtained from UDP-glucose and fructose 6-phosphate.

Sucrose moves from the mesophyll cells to phloem parenchyma cells through plasmodesmata. Then, sucrose uploading into the phloem follows either the symplastic or the apoplastic pathway. In the first case, sucrose reaches companion cells and then sieve elements hrough plasmodesmata, following a concentration gradient. In absence of plasmodesmata connecting cells, sucrose is transported inside the phloem cells through the sucrose-proton cotransporter (SUC1) situated on the phloem plasma membranes. In grapevine, such as in many other plant species, phloem loading is mainly apoplastic. Phloem unloading may also be symplastic or apoplastic. In both situations, unloading is enhanced when sucrose is fast metabolized. Invertases and sucrose synthase are the enzymes involved in sucrose cleavage. Invertases are located in the cell wall, inside the vacuole and in the cytoplasm, while sucrose synthase is cytoplasmic only. Activity of these enzymes converts sucrose into hexose sugars, which are stored in the vacuoles or subjected to phosphorylation.

Plant organs function as sinks or as sources of carbohydrates. Even the leaf, which is the main source tissue, can actually function as a sink at the early stages of development. Branches and roots are primarily sources at the onset of the season, while turn into sinks later. Fruits, even if containing chlorophyll at the beginning of the development, are always considered as sinks. Carbohydrates distribution along the plant is thus fundamental in driving growth of some organs in comparison to others. Sugar supply depends on the ability of each sink of unloading sucrose, or rather on faster metabolizing sucrose. Therefore, organs exhibiting a higher activity of those enzymes responsible for sucrose degradation and transport are considered as strong sinks. In grapevine plants, berries are the strongest sinks and, due to their economic importance, delivering in their direction is favored by agronomic practices.

Stress induces a reprogramming of the carbohydrate status of the leaf

Plants are exposed to several stresses during their whole life. Overcoming stresses requires the activation of numerous metabolic pathways, inevitably causing a new arrangement of carbohydrate distribution among different organs. Energetic resources are used to face the stress or kept as a reserve available for recovery. Moreover, the stress itself can alter environmental conditions, affecting photosynthesis and sugar metabolism consequently.

All over the world and in Europe in particular, viticulture constitutes a key agronomic production for its economic importance and value. Factors negatively influencing the correct physiological functioning of grapevine directly affect final yields in terms of quantity and quality. During the past years, research concerning carbohydrate metabolism in grapevine has been mainly focused on sugar allocation in the berry and on how stress could negatively affect the mechanisms involved. Nevertheless, many different studies conducted on various plant species, including *Vitis vinifera*, demonstrated the pivotal role of leaf sugar content in driving stress adaptation processes. Grapevine productivity is affected

by wide range of biotic and abiotic stresses, which induce severe biochemical and molecular modifications. Drought, cold and soil salinity are the principal agents of osmotic stress, the main causing factor of physiological alterations. Besides, plants have to deal with multiple issues of biotic origin and the combined effect of environmental stresses and biological threats. *Vitis vinifera* is the host of several pathogens, including bacteria, fungi, viruses and phytoplasmas.

As it has been already underlined, previous literature confirmed the involvement of carbohydrate metabolism in stress response mechanisms. Plants exposed to water, salt, cold or freezing stress are reported to increase soluble sugars and starch concentration in leaf (Medici *et al*., 2014), with the main role of maintaining osmotic balance, but also contributing to carbon storage and to free radical scavenging. Changes in sugar composition in leaf are also normally associated with pathogen infection. Grapevine red blotch-associated virus (GRBaV) causes a significant increment of glucose (Wallis and Sudarshana, 2016). Botrytis colonization is followed by strong accumulation of starch, sucrose and glucose in the inflorescences, coupled with a significant reduction of starch synthesis and an increased content of hexoses in leaf, suggesting that organs can actuate different responsive strategies to pathogen attacks, enhancing resource mobilization (Vatsa-Portugal *et al*., 2015). Nevertheless, stresses can reduce photosynthetic activity and, as a consequence, carbohydrates synthesis, conducting plants to carbon starvation (McDowell *et al*., 2011). Under such conditions, sugar metabolism is redirected towards storage and secondary metabolism, with the aim of promoting adaptive and recovering mechanisms. High activation of sucrose hydrolyzing enzymes (Prezelj *et al*., 2016; Proels and Hückelhoven, 2014) and transporters is a frequent response to stress, which leads to a switch from source to sink of the leaves (Roitsch, 1999; Vatsa-Portugal *et al*., 2015). The central role of sugars in enhancing recovery from biotic and abiotic stress is then further explained by their interdependence with other molecules and signaling pathways directly linked to stress. Drought and salinity

conditions are frequently associated with strong accumulation of abscisic acid (Downtown *et al*., 1990; Tombesi *et al*., 2015). In many woody species, including grapevine, ABA has emerged as a key factor in carbohydrate mobilization during recovery, in particular in starch-to-sugars conversion and by enhancing metabolic enzymes activity (Murcia *et al*., 2016; Pan *et al*., 2005; Perrone *et al*., 2012; Thalmann *et al*., 2016). Jasmonate-dependent pathways are also known to be co-regulated by sugars (Reinbothe *et al*., 1994). Furthermore, carbohydrate metabolism alterations are also intimately correlated to target gene expression and transcription factor regulation. A recent work by Hou *et al*. (2020) demonstrates the involvement of the transcription factor *VvWRKY13* in response to drought stress by reducing metabolism of proline and soluble sugars. A *VvWRKY13*-overexpressing line of Arabidopsis exhibited a higher expression of this transcription factor and a simultaneous reduction of soluble sugars content. Moreover, grapevine varieties more sensitive to drought showed a higher level of *VvWRKY13* transcripts. In many other studies, a cultivar-dependent tolerance to stress appeared to be correlated with higher sugar contents (Beheshti Rooy *et al*., 2017; Gamm *et al*., 2011; Ripamonti *et al*., 2020) and with an enhanced activity of carbohydrate-related enzymes (Prezelj *et al*., 2016; Proels and Hückelhoven, 2014) and genes (Hayes *et al*., 2007; Pagliarani *et al*., 2020; Santi *et al*., 2013). In diseased plants, pathogenesis-related (*PR*) genes are activated by increasing sugar concentration (Xiao *et al*., 2000), while transcription of other genes is triggered by carbohydrate starvation (Ho *et al*., 2001). Carbohydrates are not only crucial in activating complex regulatory cascade pathways, but they can also act as signaling molecules themselves (Rolland *et al*., 2006). Glucose signal is displayed through the conserved glucose sensor hexokinase activity (Sheen, 2014), while sucrose regulates translation of basic leucine zipper (bZIP)-type transcription factors (Wiese et al., 2004). Trehalose-6-phosphate plays a crucial role in plant development and stress response and tolerance, influencing gene

expression and metabolic pathways in a direct or indirect manner (Chary *et al*., 2008; Figueroa *et a*l., 2016; Figueroa and Lunn, 2016; Lunn *et al*., 2014).

Outline of the thesis

Purpose of this PhD thesis was to elucidate the involvement of sugar metabolism and signaling in response to abiotic and biotic stresses in source tissues of *Vitis vinifera*. The results will further reveal efficient strategies to help plants facing stress, improving tolerance and promoting adaptation mechanisms.

Chapter I presents an evaluation of physiology and xylem sap biochemistry alterations of the grapevine cultivar Grenache under slow and fast rates of water stress and during recovery. Intensity and duration of drought affected sugar accumulation in the sap and in the stem tissues, therefore differently influencing recovery mechanisms of the plants. Slow developing stress allowed grapevines to accumulate soluble sugar in the xylem sap, coupled with pH acidification, promoting stem priming to fulfill recovery, likely delaying stomata closure and limiting ABA accumulation. During fast stress progression, huge amount of ABA were measured in the sap and there was no evidence of sugar accumulation, suggesting plants adopted a sugar-independent strategy to recover.

Description of the trehalose-6-phosphate synthase gene family in grapevine is discussed in **chapter II**. After bioinformatics research, expression of the identified genes was assessed in different tissues and developmental stages. In order to confirm the consistence of the T6P-sucrose nexus in the grapevine system, a sucrose treatment on leaves was applied and changes of *TPS* gene expression and soluble sugar content were studied. Finally, considering the potential roles of trehalose and T6P under osmotic stress, we investigated the expression of the *VvTPS* genes, and the concentration of soluble sugars, under drought stress and a subsequent recovery.

Aim of **chapter III** is to investigate the role of sucrose metabolism and signalling in response to *Flavescence dorée*, a phytoplasma-derived disease severely affecting grapevine. The project followed two parallel strategies. Effect of sucrose treatments on FDp-infected leaves was evaluated in correspondence of the disease peak during the vegetative season in vineyard conditions. Comparison of two different sucrose treatments (spray and infusion application) was performed, aiming to identify the most suitable and efficient operative strategy. Both treatments were effective in activating activity of carbohydrate-related enzymes, and expression of sucrose metabolism-dependent genes. The putative role of sucrose-related metabolism in conferring a diverse grade of tolerance was also assessed by performing sugar quantification, enzymatic activity and target gene expression analyses on tolerant and susceptible grapevine varieties in healthy conditions. Results showed a clear discrimination between tolerant and susceptible grapevines, further underlying how plants can embrace multiple approaches towards stress tolerance.

References

Beheshti Rooy, S.S., Hosseini Salekdeh, G., Ghabooli, M., Gholami, M., Karimi, R., 2017. Cold-induced physiological and biochemical responses of three grapevine cultivars differing in cold tolerance. Acta Physiologiae Plantarum **39**. https://doi.org/10.1007/s11738-017-2561-z

Chary, S.N., Hicks, G.R., Choi, Y.G., Carter, D., Raikhel, N. v., 2008. Trehalose-6-Phosphate Synthase/Phosphatase Regulates Cell Shape and Plant Architecture in Arabidopsis. Plant Physiology **146**. https://doi.org/10.1104/pp.107.107441

Downtown, W.J.S., Loveys, B.R., Grant, W.J.R., 1990. Salinity effects on the stomatal behaviour of grapevine. New Phytologist **116**. https://doi.org/10.1111/j.14698137.1990.tb00535.x

Figueroa, C.M., Feil, R., Ishihara, H., Watanabe, M., Kölling, K., Krause, U., Höhne, M., Encke, B., Plaxton, W.C., Zeeman, S.C., Li, Z., Schulze, W.X., Hoefgen, R., Stitt, M., Lunn, J.E., 2016. Trehalose 6-phosphate coordinates organic and amino acid metabolism with carbon availability. The Plant Journal **85**. https://doi.org/10.1111/tpj.13114

Figueroa, C.M., Lunn, J.E., 2016. A Tale of Two Sugars: Trehalose 6-Phosphate and Sucrose. Plant Physiology **172**. https://doi.org/10.1104/pp.16.00417

Gamm, M., Héloir, M.-C., Bligny, R., Vaillant-Gaveau, N., Trouvelot, S., Alcaraz, G., Frettinger, P., Clément, C., Pugin, A., Wendehenne, D., Adrian, M., 2011. Changes in Carbohydrate Metabolism in *Plasmopara viticola*–Infected Grapevine Leaves. Molecular Plant-Microbe Interactions® **24**. https://doi.org/10.1094/MPMI-02-11-0040

Hayes, M.A., Davies, C., Dry, I.B., 2007. Isolation, functional characterization, and expression analysis of grapevine (*Vitis vinifera* L.) hexose transporters: differential roles in sink and source tissues*. Journal of Experimental Botany **58**. https://doi.org/10.1093/jxb/erm061

Ho, S.-L., Chao, Y.-C., Tong, W.-F., Yu, S.-M., 2001. Sugar Coordinately and Differentially Regulates Growth- and Stress-Related Gene Expression via a Complex Signal Transduction Network and Multiple Control Mechanisms. Plant Physiology **125**. https://doi.org/10.1104/pp.125.2.877

Hou, L., Fan, X., Hao, J., Liu, G., Zhang, Z., Liu, X., 2020. Negative regulation by transcription factor VvWRKY13 in drought stress of *Vitis vinifera* L. Plant Physiology and Biochemistry **148**. https://doi.org/10.1016/j.plaphy.2020.01.008

Lunn, J.E., Delorge, I., Figueroa, C.M., van Dijck, P., Stitt, M., 2014. Trehalose metabolism in plants. The Plant Journal **79**. https://doi.org/10.1111/tpj.12509

McDowell, N.G., Beerling, D.J., Breshears, D.D., Fisher, R.A., Raffa, K.F., Stitt, M., 2011. The interdependence of mechanisms underlying climate-driven vegetation mortality. Trends in Ecology & Evolution **26**.

Medici, A., Laloi, M., Atanassova, R., 2014. Profiling of sugar transporter genes in grapevine coping with water deficit. FEBS Letters **588**. https://doi.org/10.1016/j.febslet.2014.09.016

Murcia, G., Pontin, M., Reinoso, H., Baraldi, R., Bertazza, G., Gómez-Talquenca, S., Bottini, R., Piccoli, P.N., 2016. ABA and GA_3 increase carbon allocation in different organs of grapevine plants by inducing accumulation of non-structural carbohydrates in leaves, enhancement of phloem area and expression of sugar transporters. Physiologia Plantarum **156**. https://doi.org/10.1111/ppl.12390

Pagliarani, C., Gambino, G., Ferrandino, A., Chitarra, W., Vrhovsek, U., Cantu, D., Palmano, S., Marzachì, C., Schubert, A., 2020. Molecular memory of *Flavescence dorée* phytoplasma in recovering grapevines. Horticulture Research **7**. https://doi.org/10.1038/s41438-020-00348-3

Pan, Q.-H., Li, M.-J., Peng, C.-C., Zhang, N., Zou, X., Zou, K.-Q., Wang, X.-L., Yu, X.-C., Wang, X.-F., Zhang, D.-P., 2005. Abscisic acid activates acid invertases in developing grape berry. Physiologia Plantarum **125**. https://doi.org/10.1111/j.1399-3054.2005.00552.x

Perrone, I., Pagliarani, C., Lovisolo, C., Chitarra, W., Roman, F., Schubert, A., 2012. Recovery from water stress affects grape leaf petiole transcriptome. Planta **235**. https://doi.org/10.1007/s00425-011-1581-y

Prezelj, N., Covington, E., Roitsch, T., Gruden, K., Fragner, L., Weckwerth, W., Chersicola, M., Vodopivec, M., Dermastia, M., 2016. Metabolic Consequences of Infection of Grapevine (*Vitis vinifera* L.) cv. "Modra frankinja" with *Flavescence Dorée* Phytoplasma. Frontiers in Plant Science **7**. https://doi.org/10.3389/fpls.2016.00711

Proels, R.K., Hückelhoven, R., 2014. Cell-wall invertases, key enzymes in the modulation of plant metabolism during defence responses. Molecular Plant Pathology **15**. https://doi.org/10.1111/mpp.12139

Reinbothe, S., Mollenhauer, B., Reinbothe, C., 1994. JIPs and RIPs: the regulation of plant gene expression by jasmonates in response to environmental cues and pathogens. The Plant Cell **6**. https://doi.org/10.1105/tpc.6.9.1197

Ripamonti, M., Pegoraro, M., Morabito, C., Gribaudo, I., Schubert, A., Bosco, D., Marzachì, C., 2020. Susceptibility to *Flavescence dorée* of different *Vitis vinifera* genotypes from north-western Italy. Plant Pathology. https://doi.org/10.1111/ppa.13301

Roitsch, T., 1999. Source-sink regulation by sugar and stress. Current Opinion in Plant Biology **2**. https://doi.org/10.1016/S1369-5266(99)80036-3

Rolland, F., Baena-Gonzalez, E., Sheen, J., 2006. SUGAR SENSING AND SIGNALING IN PLANTS: Conserved and Novel Mechanisms. Annual Review of Plant Biology **57**. https://doi.org/10.1146/annurev.arplant.57.032905.105441

Santi, S., Grisan, S., Pierasco, A., De Marco, F., Musetti, R., 2013. Laser microdissection of grapevine leaf phloem infected by stolbur reveals site specific gene responses associated to sucrose transport and metabolism. Plant, Cell & Environment **36**. https://doi.org/10.1111/j.1365-3040.2012.02577.x

Sheen, J., 2014. Master regulators in plant glucose signaling networks. Journal of Plant Biology **57**. https://doi.org/10.1007/s12374-014-0902-7

Thalmann, M., Pazmino, D., Seung, D., Horrer, D., Nigro, A., Meier, T., Kölling, K., Pfeifhofer, H.W., Zeeman, S.C., Santelia, D., 2016. Regulation of Leaf Starch Degradation by Abscisic Acid Is Important for Osmotic Stress Tolerance in Plants. The Plant Cell **28**. https://doi.org/10.1105/tpc.16.00143

Tombesi, S., Nardini, A., Frioni, T., Soccolini, M., Zadra, C., Farinelli, D., Poni, S., Palliotti, A., 2015. Stomatal closure is induced by hydraulic signals and maintained by ABA in drought-stressed grapevine. Scientific Reports **5**. https://doi.org/10.1038/srep12449

Vatsa-Portugal, P., Walker, A.-S., Jacquens, L., Clément, C., Barka, E.A., Vaillant Gaveau, N., 2015. Inflorescences vs leaves: a distinct modulation of

carbon metabolism process during *Botrytis* infection. Physiologia Plantarum **154**. https://doi.org/10.1111/ppl.12287

Wallis, C.M., Sudarshana, M.R., 2016. Effects of Grapevine red blotch-associated virus (GRBaV) infection on foliar metabolism of grapevines. Canadian Journal of Plant Pathology **38**. https://doi.org/10.1080/07060661.2016.1227374

Wiese, A., Elzinga, N., Wobbes, B., Smeekens, S., 2004. A Conserved Upstream Open Reading Frame Mediates Sucrose-Induced Repression of Translation. The Plant Cell **16**. https://doi.org/10.1105/tpc.019349

Xiao, W., Sheen, J., Jang, J.-C., 2000. The role of hexokinase in plant sugar signal transduction and growth and development. Plant Molecular Biology **44**. https://doi.org/10.1023/A:1026501430422

CHAPTER I

Do the ends justify the means? Impact of drought progression rate on stress response and recovery in *Vitis vinifera* cv Grenache

Cristina Morabito

Jessica Orozco, Giulia Tonel, Silvia Cavalletto, Giovanna Roberta Meloni, Andrea Schubert, Maria Lodovica Gullino, Maciej Zwieniecki, Francesca Secchi

Summary

Plants are frequently exposed to prolonged and intense drought events. To survive, species must implement strategies to overcome progressive drought while maintaining sufficient resources to sustain the recovery of function. Our objective was to understand how stress rate development modulates energy reserves and affects the recovery process.

Grenache *Vitis vinifera* cultivar was exposed to either fast developing drought (within few days; FDD), typical of pot experiments, or slow developing drought (few weeks, SDD), more typical for natural conditions.

FDD was characterized by fast (2-3 days) stomatal closure in response to increased stress level, high ABA accumulation in xylem sap (>400 μg/L) without the substantial changes associated with stem priming for recovery (no accumulation of sugar or drop in xylem sap pH). In contrast, SDD was characterized by gradual stomatal closure, low ABA accumulation (<100 μg/L) and changes that primed the stem for recovery (xylem sap acidification from 6 to 5.5 pH and sugar accumulation from 1 to 3 g/L). Despite FDD and SDD demonstrating similar trends over time in the recovery of stomatal conductance, they differed in sensitivities to xylem ABA. Grenache showed near-isohydric and

near-anisohydric behavior depending on the rate of drought progression gauging the risk between hydraulic integrity and photosynthetic gain. Isohydry observed during FDD could potentially provide protection from large sudden swings in tension whilst switching to anisohydry during SDD could prioritize the maintenance of photosynthetic activity over hydraulic security that is not threatened by a gradual increase in tension.

1. Introduction

Over the course of their life, plants experience a wide range of climatic conditions, fluctuations in temperature, nutrient and water availability that are often suboptimal and can severely constrain their growth and reproductive development (Zeppel *et al*. 2014, Yuan *et al*. 2019). Perennial species in particular are left increasingly vulnerable to additional abiotic and biotic stressors, greatly limiting productivity (Allen *et al*. 2010). Amongst abiotic stressors drought is the most pervasive; plants recurrently face alternating periods of drought, varying in length and intensity, followed by the sudden availability of water often in the form of rain. Typically, under natural conditions, slow-developing drought spans weeks if not months (Zargar *et al*. 2011). Initially, the onset of drought leads to a drop-in plant water potential and stomatal conductance consequently hindering photosynthesis and impeding growth. Prolonged exposure to stress results in xylem embolism formation thus interrupting and/or completely halting water transport, which if not ameliorated may culminate in plant death (Tyree and Sperry 1989, Zwieniecki and Secchi 2015). Plant stress response strategies emerged to account for drought severity, duration, and frequency typical of their respective environments, with the goal of utilizing the sudden burst of water supply to resume physiological activity. Therefore, species survival strategies to cope with drought stress cannot just be seen as passive, but rather as proactive preparations for recovery prompted by the sudden availability

of water. This novel premise stipulates that drought and recovery are not dichotomous and independent but should be considered as one interwoven continuous process (Ruehr *et al*. 2019).

Processes that lay the foundation for facilitating recovery may be activated alongside conventional stress response mechanisms. Given that preparation for recovery is initiated during drought, its course and effectiveness may be impacted by features characteristic of temporal stress dynamics such as rate, and duration, which may dictate the ultimate success of post-drought recovery (Anderegg *et al*. 2013). Unfortunately, much of our current understanding rests upon studies performed on plants, more than often maintained in pots and greenhouses, wherein drought is simulated by an abrupt discontinuity in water supply, which can skew or even completely overlook the processes at play during the natural trajectory of drought stress (Romero *et al*. 2017). In nature, stress usually develops gradually over the course of weeks or months as effective soil volume per plant is large, while in experimental settings large negative tensions are often achieved in a matter of a few days or even hours, thus altering or inhibiting acclimation responses and limiting our ability to reliably assess recovery dynamics (Ingrisch and Bahn 2018). In order to survive, species must be able to coordinate an arsenal of multiscale responses, including adjustments to their biochemistry and physiology that can concurrently address the progressive drought while maintaining sufficient resources to sustain the prospective recovery of plant function. These adjustments include changes in levels of stress hormones (Daszkowska-Golec and Szarejko 2013), osmolytes and protective chemicals (Blum 2017), xylem sap pH (Secchi and Zwieniecki 2012), metabolism of nonstructural carbohydrates (NSC) (Trifilo *et al*. 2017, Tomasella *et al*. 2019), and expression of genes (Cramer *et al*. 2007). Therefore, the length and severity of stress incurred by plants can have downstream ramifications on the degree and path of recovery. How and which aspects of stem biochemistry

and whole plant physiology are affected by the rate of drought stress progression and how these changes impact recovery remains an open question.

Mounting evidence points to the linkage between NSC metabolism and a plant's capacity to cope and recover from drought stress (O'Brien *et al*. 2014, Schwalm *et al*. 2017, Trugman *et al*. 2018). Amidst periods of water scarcity, during which stomatal closure prevents photosynthetic carbon uptake (McDowell *et al*. 2008, McDowell *et al*. 2011), stored NSC can act as a buffer providing carbon to maintain basic metabolism and defense processes (McDowell and Sevanto 2010, Sala *et al*. 2012). Drought affects not only the total carbohydrates amount, but also the allocation and composition of NSCs, all of which can be linked to concurrent changes in xylem sap chemistry (Savi *et al*. 2016, Tomasella *et al*. 2017, Ivanov *et al*. 2019). Specifically, in some species, a drop in xylem sap pH induces an accumulation of soluble sugars in the apoplast that can promote recovery by serving as osmolytes generating a gradient to refill embolized conduits; processes that are associated with 'stem priming' for recovery (Secchi and Zwieniecki 2012, Pagliarani *et al*. 2019, Tomasella *et al*. 2021). Given that sugar depletion is expected during prolonged drought stress, rapid recovery of plant photosynthetic capacity might be a crucial adaptation that would confer plants with a competitive advantage. However, a gradual reinstatement of pre-stress functions may be necessary to afford sufficient time to repair drought stress related damage. For example, delaying stomatal opening despite tension alleviation may reduce transpirational demand and provide additional time for the slow osmotically driven removal of embolism to occur. In this respect, ABA-mediated control of stomatal aperture may be more important over passive turgor and water potential-driven responses. Thus, the objective of this study was to understand how plants use their time under stress to modulate their energy reserves (mostly carbohydrate supply) and xylem chemistry (pH and ABA content) to enhance recovery processes.

While duration and magnitude are defining features of drought, the rate of stress progression is seldom considered despite its potential importance for the acclimation of plants to stress and their subsequent recovery. Therefore, we hypothesized that a slow developing drought (SDD) would permit the time for changes in the xylem sap chemistry to prime the stem for recovery while delaying stomatal opening. A fast-developing drought (FDD) would be limited to prioritizing the conservation of water by shutting stomata without the changes associated with stem priming. Given that stomatal behavior can have large implications for NSC and water-loss dynamics, we tested our hypothesis on *Vitis vinifera* cultivar Grenache purported to be near-isohydric (Shelden *et al*. 2017). We evaluated stress responses and recovery by analyzing both physiological and chemical parameters in response to fast and natural timing of drought occurrence, thus investigating the specific drought response strategies.

2. Materials and Methods

2.1 Plant materials and experimental set up

Vitis vinifera cv Grenache cuttings were provided by the nursery Vivai Cooperativi Rauscedo-San Giorgio della Richinvelda (PN), Italy. These commercially available plants are typically grafted on rootstock 1130P (*V. berlandieri* cv. Resseguier nr. 2 × *V. rupestris* cv. Du Lot.). In this study, we refer to the plants simply as Grenache.

Two-year-old grapevines were grown in a greenhouse under partially controlled climatic conditions. Temperature was maintained in the range of 25–32°C and natural daylight was supplemented, when necessary, with light from metal halogen lamps to maintain a minimum of 500–600 mmol photons m^{-2} s^{-1} during a 12-h-light/12-h-dark cycle. Each plant grew in a 4-L pot filled with a substrate composed of sandy-loam soil/expanded clay/peat mixture (2:1:1 by

weight). A total of 25 grafted grapevines were used in this study; at the beginning of the experiment Grenache plants had an average height of 87.05 ± 11.8 cm.

The 25 grapevines were further divided in 3 groups: 10 plants were exposed to SDD treatment, 10 plants to a FDD and the remaining 5 grapevines were kept as controls (CTR), these plants were irrigated to field capacity every morning during the whole experimental period. The SDD was achieved by progressively reducing the amount of water provided to the plants along the experiment (20% less of water used every day), while the FDD was induced by interrupting irrigation. In both treatments, water stress was imposed until stem water potential reached the average level of -2 MPa. Once water stress levels were reached, the grapevines were re-watered in the morning up to field capacity and for the following ten days (REC).

Xylem sap and stem tissues were collected from the treated (SDD, FDD and REC) and control plants (CTR) throughout the experiment duration and the samples were stored for further chemical analyses. Physiological parameters (stem water potential, stomatal conductance and photosynthesis) were monitored during the entire experiment (i.e. from the start of the stress treatments until full recovery of physiological functions) in both droughted and control plants.

2.2 Measurement of leaf gas exchange and xylem pressure

Stomatal conductance (g_s) and net photosynthesis (A_n) were measured on fully expanded leaves exposed to direct sunlight, using a portable infrared gas analyzer (ADC-LCPro+ system, The Analytical Development Company Ltd, Hoddesdon, UK). Measurements were performed using a 6.25 cm^2 leaf chamber equipped with artificial irradiation (1200 µmol photon m^{-2} s^{-1}), set with a chamber temperature of 25°C to avoid overheating. CO_2 values were maintained at greenhouse conditions (400-450 ppm). Leaf gas exchange was monitored daily (between 10:00 am and 12:00 pm) for the whole duration of the experimental

trial; meanwhile several leaves were collected for xylem pressure measurements (stem water potential).

Xylem pressure measurements were performed on fully expanded non-transpiring leaves. Prior to taking the measurements, leaves were placed in humidified aluminum foil-wrapped plastic bags for 20 minutes before excision. After excision, leaves were allowed to equilibrate for an additional 15 minutes and water potential was measured using a Scholander-type pressure chamber (Soil Moisture Equipment Corp., Santa Barbara, CA, USA).

2.3 Sap and stem sampling procedure

Xylem sap was collected from treated (SDD, FDD and REC) and control (CTR) plants, according to a previously described method (Secchi and Zwieniecki 2012). Briefly, a branch was attached through a plastic tube to a syringe needle. The needle was threaded through a rubber cork to a vacuum chamber, with the needle tip placed in a 1.5-mL plastic tube. After a vacuum suction was generated, pieces of stem were consecutively cut from the top, allowing liquid from open vessels to be sucked out of the stem and collected in the tube. Sap samples were stored at -20°C until analyses of pH and NSC content were conducted.

The stems sampled for sap collection were cut in small sections using a fresh razor blade and microwaved at 700 W for 3 min to stop enzymatic activities. Samples were then oven-dried at 70 °C for 24 h, ground to fine powder (particle size < 0.15 mm) using a tissue lyser system (TissueLyser II, Qiagen), and kept for further analyses (starch and soluble sugar content) at room temperature.

2.4 Measurements of pH and soluble carbohydrates in xylem sap

Variations in xylem sap pH during SDD and FDD and along recovery period in comparison to control plants were evaluated using a micro pH electrode (PerpHect® ROSS®, Thermo Fischer Scientific, Waltham, MA USA). Non-structural carbohydrates (NSC) content in xylem sap samples was quantified following the anthrone-sulfuric acid assay described by Leyva et al. (2008) with the modifications indicated in Secchi and Zwieniecki (2012). In short, 50 µL samples were mixed with 150 µL of anthrone in sulfuric acid (0.1%, w/v) in a 96-well micro-plate (iMark Microplate Absorbance Reader, BioRad). The plate was cooled on ice for 10 minutes, heated at 100 °C for 10 minutes, and then equilibrated to room temperature for 10 minutes. A glucose standard curve was used to compare the colorimetric response of the samples, whose absorbance was read at 620 nm. Soluble carbohydrates concentration was expressed as g L^{-1} of glucose.

2.5 Analysis of soluble sugars and starch concentration in stem samples

25 ± 4 mg of powdered sample materials were transferred into a 1.5 mL Eppendorf test tube. To extract soluble sugars, 1 mL of 0.2 M sodium acetate buffer solution (pH= 5.5) was added to each sample, vortexed and incubated at 70°C for 10 minutes. The NSC were quantified following the procedure described above and the sugar concentration was expressed as mg g^{-1} dry weight. For starch analyses, the remaining pellet was exposed to 100°C for 10 minutes and submitted to enzymatic digestion for 4 h at 37°C in 0.2 M sodium acetate buffer (pH = 5.5) with 0.7 U of amylase and 7 U of amyloglucosidase. Once the digestion was completed, samples were centrifuged for 5 minutes at 21 000 *g*, and the supernatant was diluted 1: 20 and quantified using the method described above for determining soluble carbohydrates content.

2.6 HPLC-MS/MS analysis of sap abscisic acid (ABA) content

ABA concentration was quantified following the method described by Siciliano *et al*. (2015) with minor changes. Xylem sap samples were centrifuged at 13000 *g* and 4 °C for 5 minutes. From the obtained supernatant, a total volume of 50 µL for each sample was collected in a 1 mL amber glass vial containing an appropriate glass insert (Supelco, Sigma-Aldrich) for small sample volumes and analyzed by HPLC-MS/MS. High Performance Liquid Chromatography was carried out using a 1260 Agilent Technologies (Waldbronn, Germany) system equipped with a binary pump and a vacuum degasser. Sample aliquots (20 µL) were injected on a Luna C18 (150 × 2 mm i.d., 3 µm Phenomenex, Torrance, CA) and ABA was eluted in isocratic conditions of 65:35 (H2O:CH3CN v/v acidified with HCOOH 0.1%) under a flow of 200 µL min^{-1} for 5 minutes. Using an electrospray (ESI) ion source operating in negative ion mode, samples were introduced into a triple-quadruple mass spectrometer (Varian 310-MS TQ Mass Spectrometer). Analyses were conducted in MRM mode using two transitions: 263>153 (CE 12V) for quantification, 263>219 (CE 12V) for monitoring, with 2 mbar of Argon (Ar) as collision gas. The external standard method was applied to quantify ABA concentration in target samples. In detail, a standard curve was generated using an original ABA standard (Sigma Aldrich, St Louis, MO, USA; purity 98.5 %), with concentrations ranging from 10 to 500 µg L^{-1}. The detection (LOD) and quantification (LOQ) limits were calculated based on the standard deviation of the response (σ) and slope of the calibration curve (S) ratio in accordance with the ICH Harmonized Tripartite Guideline expressed as: LOD=3.3σ/S; LOQ=10σ/S. Calculated final values were as follows: LOD = 0.87 ng mL^{-1}; LOQ = 2.90 ng mL^{-1}.

2.7 Statistical analyses

Significant differences among treatments were analyzed by applying a one-way analysis of variance. Tukey's honestly significant difference post-hoc test was used for separating means when analysis of variance results was significant ($P < 0.05$). The SPSS statistical software package (v24.0, SPSS Inc., Cary, NC) was used to run the statistical analyses, and Sigma Plot software (Systat Software Inc., San Jose, CA) was used to create figures.

3. Results

3.1 Physiological Changes in Response to SDD, FDD and Recovery

At the end of the treatments, well irrigated plants were longer than the stressed ones (165.67 ± 15.04 cm versus 107 ± 5.3 cm and 132.25 ± 11.32 cm, respectively for SDD and FDD treatments). The plants exposed to SDD at the end of experiment showed a 23% of length while Grenache exposed to FDD were about 52% longer than plants at the beginning of experiment (Fig. 1). Moreover, SDD grapevines grew only the first 13 days from the beginning of the stress.

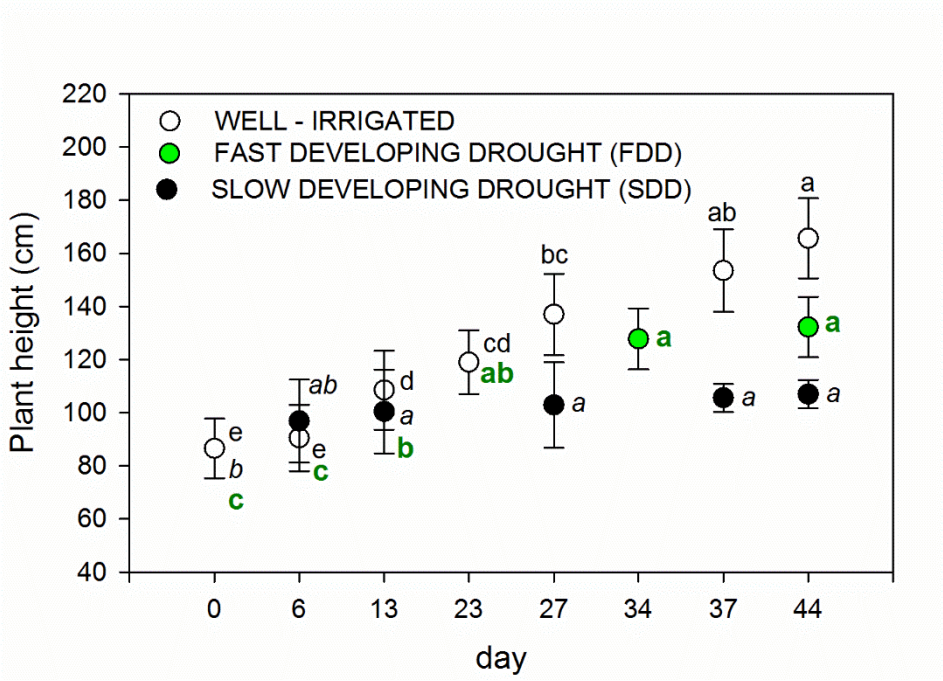

Fig. 1 – Temporal plant growth (height) during fast developing drought (FDD; green circles) and slow developing drought (SDD; black circles). White circles denote well-irrigated grapevine plants. Letters denote statistical differences according to Fisher LSD test ($P < 0,05$).

Grenache plants exposed to SDD reached the stress level of approximately -2 MPa in 44 days (ψ stem: -2.06 ± 0.40 MPa), while in FDD water stress was achieved within 18 days (ψ stem: -1.85 ± 0.07 MPa; Fig. 2a). The rate of water stress progression was significantly different between treatments and was ~0.09 and ~0.025 (MPa day^{-1}) respectively for FDD and SDD (Fig. 2a). Stomatal conductance (gs) progressively decreased during SDD treatment, while it seemed to collapse within 1 day in FDD treatment (Fig. 2c).

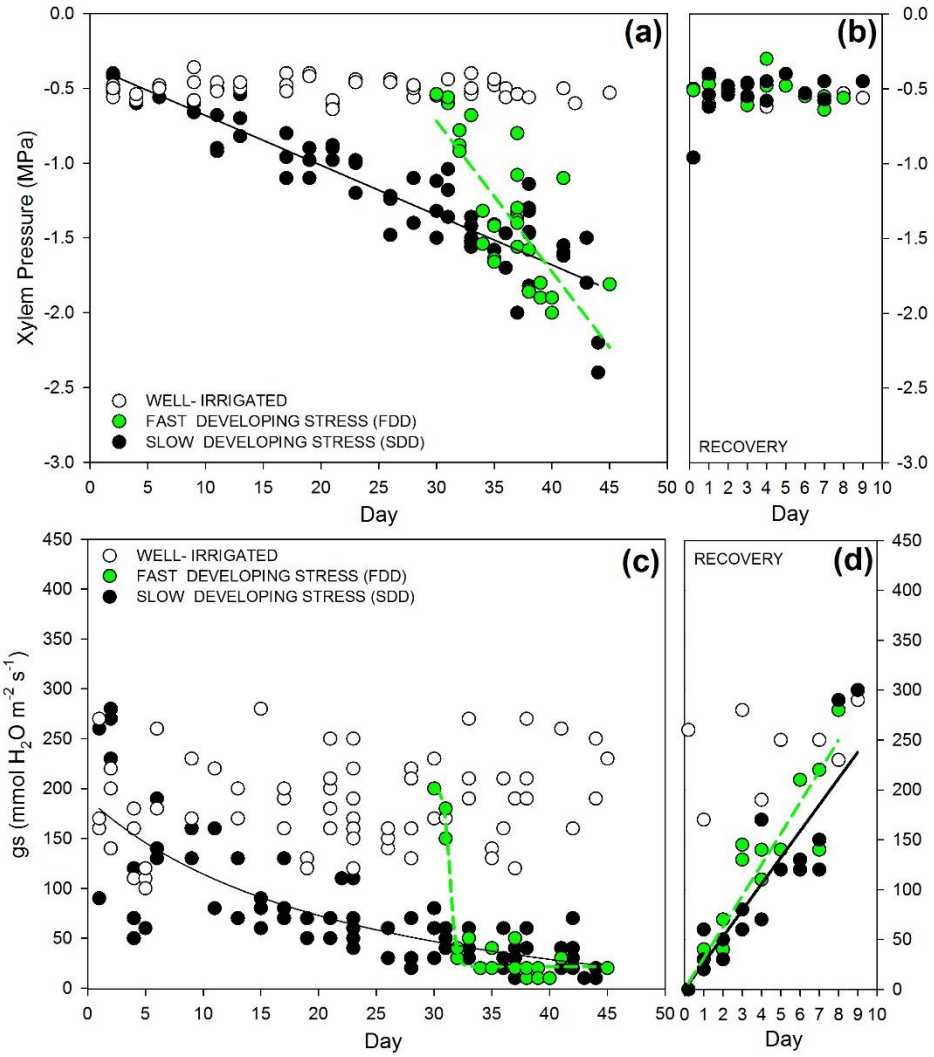

Fig. 2 – Temporal dynamics of **(a-b)** stem water potential (xylem pressure) and **(c-d)** stomatal conductance (gs) during fast developing drought (FDD) and slow developing drought (SDD), and during recovery respectively from FFD and SDD. Each circle represents a plant.

The response of gs to xylem pressure was different between the two treatments; in the SDD treatment plants gradually shut stomata in response to

increment of stress level and remain partially open even at -1 MPa, while in FDD stomata closure occurred at the onset of low stress around -0.6 MPa. (Fig. 3a).

Post-rewatering, water potential recovered within the first day in both treatments. (Fig. 2b). Recovery of gs was much slower than that of water potential but was not significantly affected by treatment (Fig. 2d). Recovery of gs expressed as a response to water potential revealed no relationship (Fig. 3b).

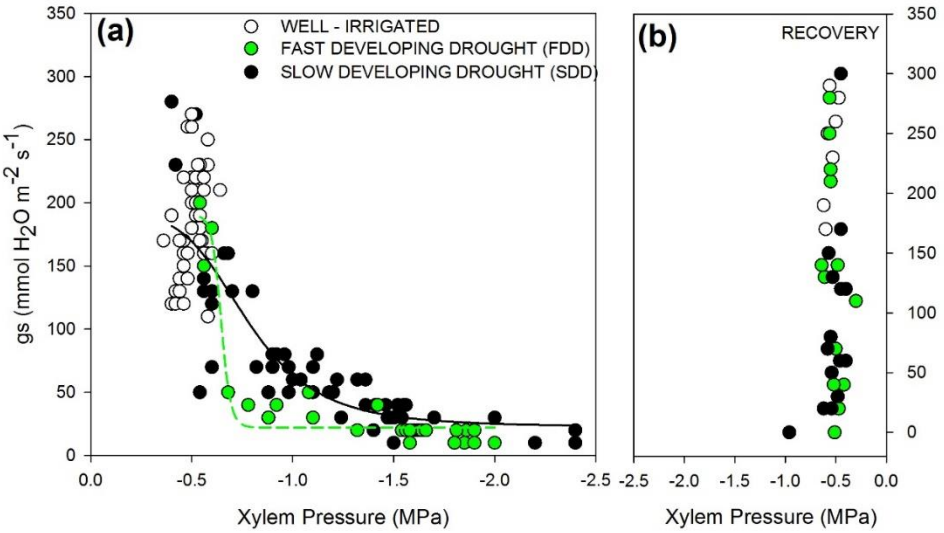

Fig. 3 – Stomatal conductance (gs) in relation to xylem pressure in Grenache plants during (**a**) fast developing drought (FDD) and slow developing drought (SDD) and during (**b**) recovery from FDD and SDD. Data were fitted with the four-parameter logistic curves (dose-response curve; black and green lines for respectively SDD and FDD treatment; for more details see Secchi and Zwieniecki, 2014. Parameters that describe curves for the two stressed populations are statistically different (FDD-EC50gs = -0.645 MPa and SDD-EC50gs = -0.777 MPa; Paternoster t test, $P < 0.01$).

As expected, net photosynthesis and stomatal conductance were well correlated; a constant reduction of net photosynthesis was in fact coupled with a progressive reduction of gs. Rewatering completely restored photosynthetic activity to pre-stress measurements after stomata were fully open (Fig. 4a-b).

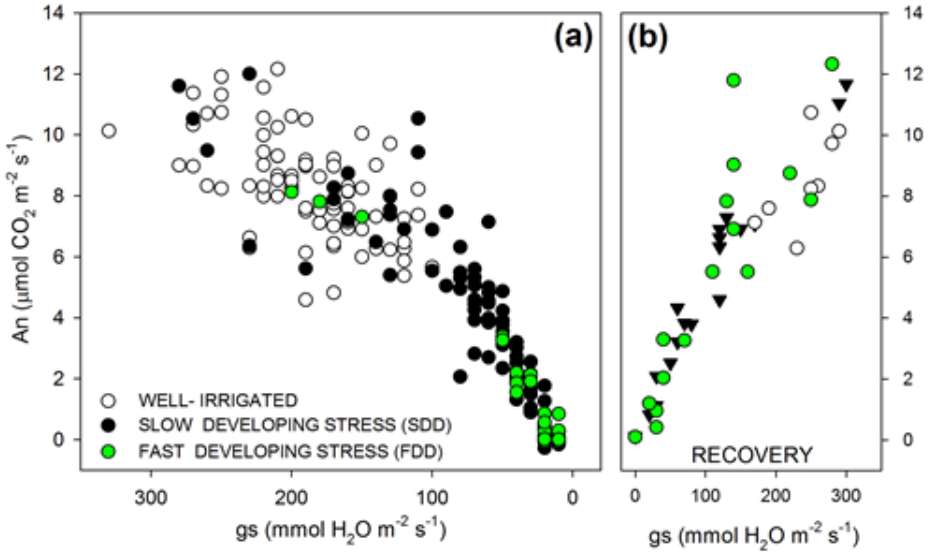

Fig. 4 – Net photosynthesis (An) in relation to stomatal conductance (gs) during (**a)** fast and slow developing drought (FDD and SDD) followed by **(b)** recovery (REC) from fast and slow developing drought treatments. White circles represent well-irrigated plants (CTR).

3.2 Biochemical Changes in xylem sap in Response to Stresses and Recovery

ABA, pH and soluble sugar contents in the xylem sap are represented as average values at different xylem pressure intervals (MPa; Fig. 5a-d). Xylem sap ABA increased with the increment of drought level for both stresses (Fig. 5b), however ABA was highly accumulated at the end of FDD treatment (FD3, Fig. 5b). The ABA accumulation to 60-90 μg/L forced complete stomatal closure (Fig. 2c), but ABA continued accumulation under FDD treatment and reached values 10 times higher than those under SDD conditions. During the recovery phase, xylem pressure recovered within one day, however ABA concentrations during 1-3 days post recovery (R1, Fig. 5b) remained high at the level of FDD and SDD under drought. Drop in ABA content did not occur until 8-10 days post

rehydration. At that time, ABA concentration decreased to pre-stress values in both treatments (R2, Fig. 5b).

Fast developing drought did not significantly affect the pH of xylem sap. Sap acidification was observed after one day of relief from slow developing drought, Xylem sap pH changed from of 5.92 ± 0.042 in control plants to 5.46 ± 0.12 in recovered plants (Fig. 5c). The acidification of xylem sap occurred in parallel with a significant increase in soluble carbohydrate content (from 0.51 ± 0.079 g L^{-1} in control plants to 3.82 ± 1.16 g L^{-1} in recovered plants; Fig. 5d). The total amount of carbohydrates in the sap returned to pre-stress levels after 10 days of rehydration (0.44 ± 0.056 g L^{-1}), when pH values were higher and overlapping those of irrigated plants (pH: 5.75 ± 0.053; Fig. 5d).

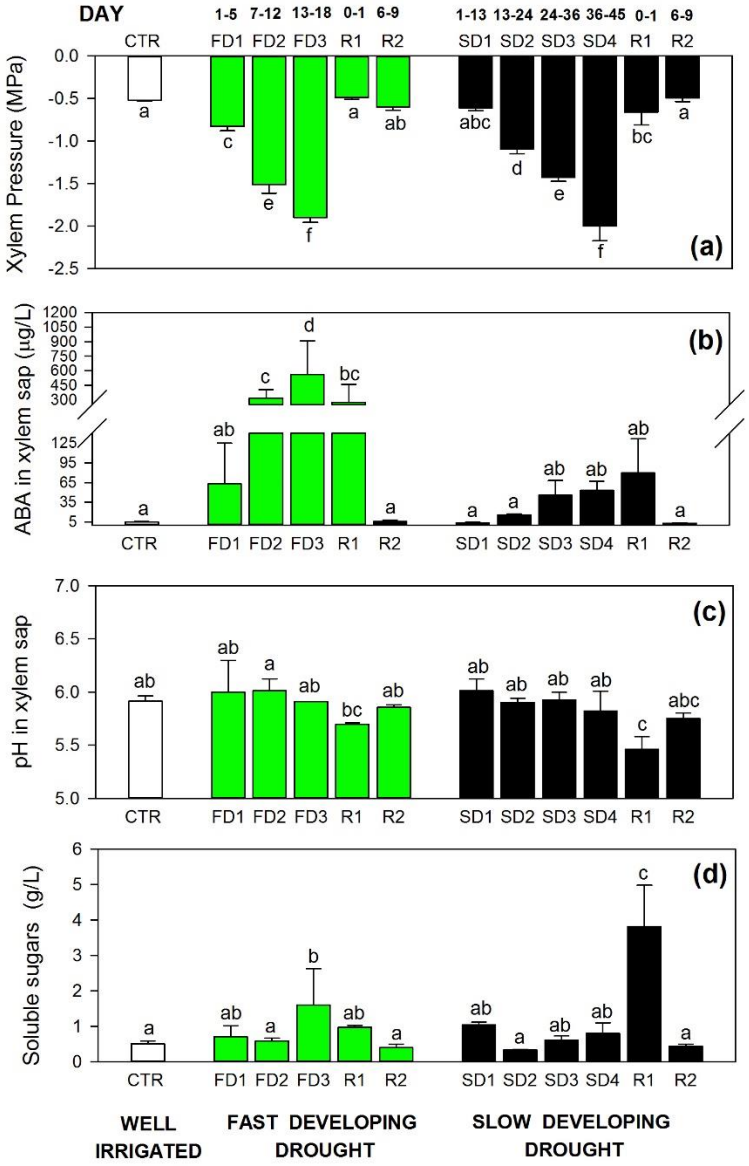

Fig. 5 – **(a)** Xylem pressure, **(b)** abscisic acid (ABA) concentration, **(c)** pH values and **(d)** soluble sugar content measured from xylem sap collected from plants exposed to a fast developing drought (FDD; green bars) and to a slow developing drought (SDD; black bars). White bars indicate average values measured in well-irrigated plants (CTR). Letters denote homogeneous groups based on the Fisher LSD method. Data are mean values and bars are SE.

During FDD and SDD, the response of ABA to stomatal conductance was well correlated in both drought treatments; FDD: $R^2 = 0.98$ $P < 0.001$, SDD: $R^2 = 0.92$ $P < 0.001$ (Fig. 6). The ABA concentration increased significantly in the xylem sap of the stems while gs decreased and a maximum level of ABA was reached when stomata were closed.

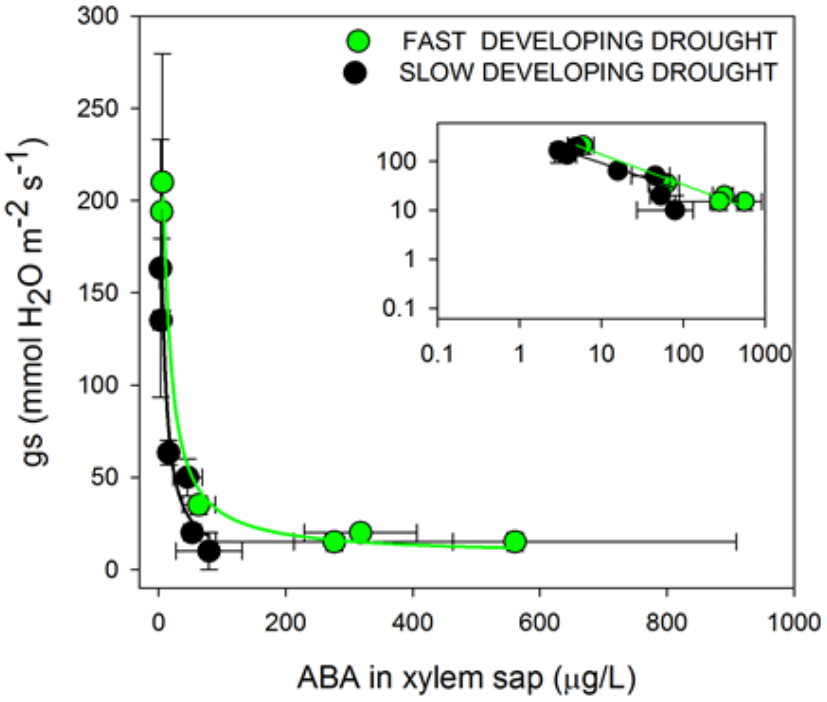

Fig. 6 – Relationship between stomatal conductance (gs) and abscisic acid (ABA) content in xylem sap during fast developing drought (FDD, green circles) and slow developing drought (SDD; black circles). Insets depict stomatal conductance (g_s) *vs* ABA represented with log scale values. Green lines represent the curves obtained for FDD and black lines for SDD treatment. Data are mean values and bars are SE.

During the drought experiments, sugar concentration was low and not correlated with pH values (Fig.7). However, Grenache SDD stressed plants showed high carbohydrate content only at lower pH values during the first day of recovery (R1) that was significantly different from the rest of the measurements (Fig. 7).

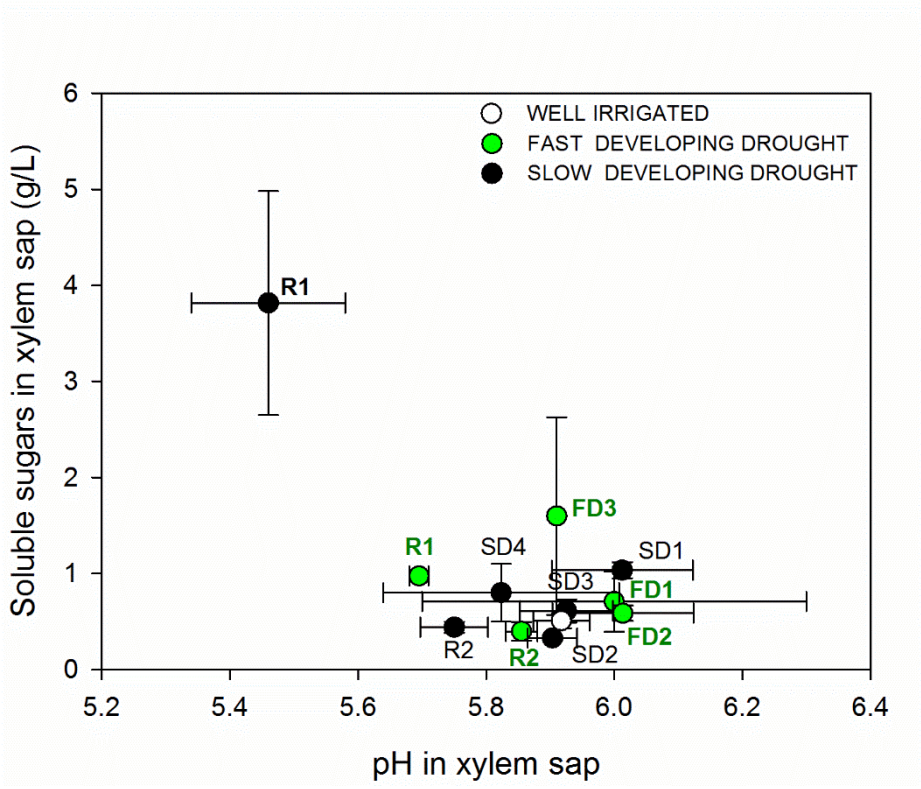

Fig. 7 – Xylem soluble sugar content related to pH values during fast developing drought (FDD; green circles) and slow developing drought (SDD; black circles). Data are mean values and bars are SE.

3.3 Biochemical Changes in stem tissues in Response to Stresses and Recovery

Drought treatments affected differently the total NSC contents in the stems; plants exposed to FDD treatment did not modify the total carbohydrates (starch plus soluble sugars) content in stem tissues during both stress and recovery (Fig.8a). However, plants exposed to SDD showed an increase of total NSC content during stress and the values returned to pre-stress levels when water was alleviated, with sugar concentration overlapping those of well-watered grapevines, (SDD: 94.32 ± 26.40, 157.97 ± 19.55 and 105.23 ± 2.75 mg g^{-1} of total sugars respectively for well-watered, SD4 stress and recovered plants; Fig.8a).

In details, the FDD treatment increased the content of starch in the stems during the drought imposition (FD3, 1.5-fold more than controls) and after one day of rewatering (2.2-fold more, Fig. 8b), while the accumulation of soluble sugars did not change over the experiment (Fig. 8c). Plants from SDD treatment accumulated slightly more starch compared to well-watered conditions (Fig. 8b) and significantly more soluble sugars (1.7-fold more). Interestingly, during the recovery phase stem sugars in SDD plant return to pre-stress level within one day (Fig. 8c).

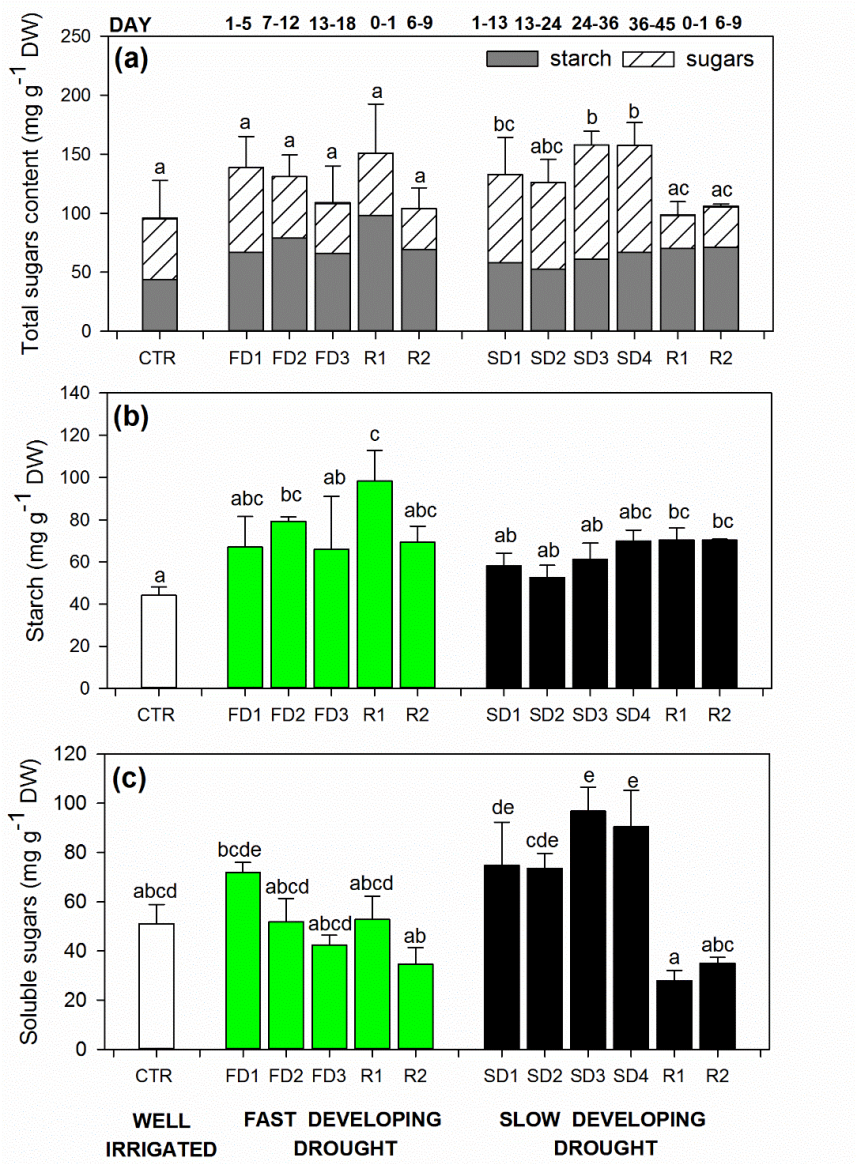

Fig. 8 – **(a)** Total carbohydrates (starch plus soluble sugars), **(b)** starch content and **(c)** soluble sugars content measured from stem tissues collected from plants exposed respectively to a fast developing drought (FDD; green bars) and to a slow developing drought (SDD; black bars). White bars bars indicate average values measured in well-irrigated plants (CTR). Letters denote homogeneous groups based on the Fisher LSD method. Data are mean values and bars are SE.

4. Discussion

Using two distinct methods to impose drought onto potted plants: (1) an immediate interruption of irrigation resulting in fast developing drought (FDD) and (2) a constant reduction in available water resulting in slow-developing drought (SDD), we successfully implemented two rates of drought progression allowing us to test the proposed hypotheses. The two methods were chosen to simulate the fast water potential decline, rates of ~0.09 (MPa day^{-1}), typical of most drought experiments conducted on potted plants (Griesser *et al*. 2015) and the gradual decline, rates of ~0.025 (MPa day^{-1}), more typical of drought under field and natural conditions (Romero *et al*. 2017). We found significant differences between the fast and slow rates of drought progression, among set of measured water stress related physiological responses including stomatal conductance, xylem sap ABA concentration, xylem sap pH, and soluble sugar concentrations in xylem sap, as well as modifications in the content of stem carbohydrates. Furthermore, we observed that not only was each drought rate accompanied by distinct xylem biochemical changes but in addition, the respective changes also set the precedent for their corresponding recovery. Our findings suggest that the evaluation of plant response to stress should be analyzed in the context of plant water potential, while the subsequent recovery from stress should be evaluated in the context of time (Fig. 2-3). In addition, our findings can be analyzed in the context of impact of drought progression rate on protective strategy (isohydric vs anisohydric behavior) and subsequent recovery process.

As sessile organisms subjected to a wide range of constantly changing environmental conditions, plants' survival depends on their capacity to integrate information about their surroundings, gauge potential trade-offs and adjust their physiology accordingly, all the while optimizing resources especially under water stress. Therefore, mechanisms that regulate gas exchange and restrict water loss

are imperative for adapting and thriving in these conditions. A binomial method of classification, isohydric and anisohydric (Schultz 2003), has been used to explain differences in stomatal behavior between *Vitis vinifera* varieties in response to water stress. However this classification should not be decisive (Hochberg *et al*. 2018), and recently it has been shown that isohydric and anisohydric behavior is not constitutive for a characteristic variety but rather it is environmentally dependent (Martorell *et al*. 2015). In general, anisohydric plants, withstand a wide variation of water potential but promote photosynthetic gains, thus maintaining higher stomatal aperture and exhibiting substantial reduction in xylem pressure (Coupel-Ledru *et al*. 2017). In contrast, isohydric plants should limit water potential variation to protect hydraulic integrity at the cost of photosynthetic output and are more exposed to carbon starvation risk when compared to anisohydric plants, due to the prompt stomatal closure in the case of water stress (Tardieu and Simonneau 1998). Grenache is typically considered to show near-isohydric response. Indeed, when exposed to FDD, Grenache shut stomata in a step-like manner in response to small drops in water potential (within 0 to -0.6 MPa) in a manner to the typical isohydric stomatal behaviors. However, Grenache's isohydric behavior disappeared under SDD treatment. Such dual response contradicts popular approaches that ascribe species or varieties' dominant adaptive stomatal responses to be inherent and independent of environmental conditions (Dal Santo *et al*. 2016).

Some previous studies have reported switching between iso- and anisohydric behavior even within the same cultivar (Franks *et al*. 2007, Chaves *et al*. 2010, Rogiers *et al*. 2012, Zhang *et al*. 2012), but the circumstances promoting this behavioral ambiguity in response to drought remained unclear (Domec and Johnson 2012, Klein 2014). Considering stress development dynamics may reconcile the apparent inconsistencies and provide insight into the benefits that come from a shifting strategy that adjusts along a stress continuum as opposed to being constrained to an archetypal response. Isohydricity may be a

beneficial response under FDD regimes when sudden unanticipated deviations from typical transpirational demand risk exposure to tensions that can endanger xylem functionality (Tyree and Sperry 1988) or accelerate senescence. Under SDD conditions a near-anisohydric response can dominate, as a slow buildup of tension affords plants the time and security to better acclimate under the reduced risk of sudden hydraulic failure, all the while preserving photosynthetic activity. In this study, Grenache exemplifies such flexibility by modulating stomatal conductance in accordance with drought length and rate. Thus, we suggest that iso- and anisohydric behaviors bound an array of facultative behaviors imposed by different rates and length of drought stress that permit plants to shift priorities and coordinate responses to optimize the tradeoff between carbon gain and hydraulic function, and analysis of stomatal response to water stress should account for the rate of stress development.

Xylem sap ABA and pH have been shown to mediate stomatal closure and associated with aniso- and isohydric behavior (Davies *et al*. 2002, Sharp and Davies 2009, Marusig and Tombesi 2020). In fact, both strategies are often associated with different degrees of ABA concentration and sensitivity (Coupel-Ledru *et al*. 2017). Under FDD, a large sudden accumulation of ABA in xylem sap was observed, reflected in a steep stomatal conductance decline, following a moderate decrease in water potential. Under SDD treatment accumulation of ABA was very slow and reached levels 10 times lower then under FDD treatment. It seems that complete stomatal closure was observed under similar ABA concentration in both treatments (60-80 μg/L), although observed excessive increasing accumulation of ABA in FDD treatment might suggest lower sensitivity of stomata to ABA concentration under sudden drought (see slight shift in response of gs to ABA in Fig. 5 inset). This might indicate that ABA sensitivity is not an intrinsic varietal property but can be associated with the rate of water stress development. Therefore, ABA sensitivity may not be the best indicator to differentiate between iso/anisohydricity given that stress rate

progression might alter ABA sensitivity and patterns of accumulation. We think that this notion is a novel concept that should be further explored as previous studies have found that experimental conditions influence stomatal behavior and apparent sensitivity to ABA (Lavoie-Lamoureux *et al*. 2017, Martinez-Vilalta and Garcia-Forner 2017).

Moreover, the ABA concentration in the xylem sap and plant sensitivity acquired during stress may also play an important part in recovery from stress. There is an increasing appreciation for the fact that the recovery of water potential does not result in immediate stomatal opening (Blackman *et al*. 2009, Martorell *et al*. 2014) and delay is often observed. Such time-lag may be an evolved trait that provides additional time for the restoration of hydraulic plant capacity (Martorell *et al*. 2014, Pagliarani *et al*. 2019). This delay has been associated with lingering ABA concentrations post-tension-release (Lovisolo *et al*. 2008, Brodribb and McAdam 2013). Indeed, in the present study we observed the presence of lingering ABA following rehydration. One might expect that gas exchange recovery from fast induced stress would be hastened by the quick improvement in water potential. Surprisingly, the recovery of leaf gas exchange was slow and not related to the recovery of water potential in both drying regimes despite levels of lingering ABA being drastically lower in SDD than in FDD. It can be speculated that recovery in Grenache might be linked to its sensitivity to ABA and xylem sap pH acclimation. Photosynthetic recovery is an important competitive advantage of any species; thus, the observed delay can be seen as a disadvantageous behavior. However, this delay might be necessary to assure that xylem transport capacity is restored to its maximum prior to an increase in transpiration demand. It is imperative to reconsider the way we represent recovery from assessing it in terms of water potential to looking at it from the perspective of time passing.

Although in this study we did not assess hydraulic losses due to tension, applied stress was shown to cause embolism in grapevine (Brodersen *et al*. 2013,

Pratt *et al*. 2020, Brodersen *et al*. 2018, Tombesi *et al*. 2014). Furthermore, it has been shown that recovery processes resulting in the restoration of hydraulic capacity require both energy and time to utilize the sudden occurrence of high water potential (Salleo *et al*. 2004, Secchi and Zwieniecki 2016, Savi *et al*. 2016, Trifilò *et al*. 2017). As drought decreases photosynthetic output and growth, consequently it is thought that the NSC storage pool may initially increase due to a reduction in sink activities but subsequently decrease due the expenditure required to maintain metabolic activity (Trifilo *et al*. 2017). It might be expected that such behavior would be more pronounced in SDD as a slow decrease in plant water potential would allow more time between the halting of growth and total stomata shutdown, while in FDD both growth and stomata shutdown may occur almost simultaneously and no accumulation should be detected. Grenache indeed increased soluble sugar and starch contents under SDD conditions and did not change sugar content under FDD conditions even if an increased in starch level was observed. It is assumed that the restoration of xylem functional capacity post stress-exposure requires a pH driven accumulation of sugars in xylem sap, which creates an osmotic gradient that stimulates embolism recovery (Salleo *et al*. 2004, Secchi and Zwieniecki 2016). Such dependency has been previously observed and further supports the notion that under natural drought conditions the pH of xylem sap stimulates an efflux of soluble sugars to the xylem (Secchi *et al*. 2017). Interestingly, during SDD, this accumulation of sugar in sap was imperceptible; however, during recovery there was a significant increase which was associated with a drop in pH (Fig. 4). Nevertheless, this increase only persisted for a few days. In FDD no significant changes in xylem sap soluble sugar levels were detected and no relationship between sap pH and SC concentration was present. This differential response between SDD and FDD may suggest that SDD results in physiological preparations aimed at reinstating their hydraulic system while FDD (most likely not a realistic drought treatment) can result in artifactual responses that may not facilitate full physiological recovery. Taken together, it

seems that the length and rate of drought stress affects xylem sap soluble sugar concentration such that longer and slower stress stimulates processes associated with recovery from embolism, while fast stress progression may hinder physiological preparations for recovery

5. Conclusions

Our results suggest that, in the case of Grenache, isohydric and anisohydric behaviour are facultative responses that can be linked to the rate of drought progression. The isohydric behaviour can be a useful strategy against a sudden increase in tension, while anisohydric response can be linked to a more gradual tension increase that promotes maintenance of photosynthetic activity.

Stress progression rate affects xylem sap ABA concentration and sensitivity of stomata to ABA.

Post-stress recovery occurs in two phases: (1) fast (hours) recovery of water potential and (2) slow (days) yet continuous recovery of stomatal conductance. Recovery rate was independent from the stress progression rate and could be linked to lingering ABA concentrations in xylem sap and respective sensitivities.

Concentration of stem NSC were minimally affected by stress progression rates. However, xylem sap soluble sugar content increased in SDD in correspondence to lower pH, suggesting that slow developing stress might prime plants for restoring hydraulic capacity.

References

Allen CD, Macalady AK, Chenchouni H, Bachelet D, McDowell N, Vennetier M, Kitzberger T, Rigling A, Breshears DD, Hogg EH (Ted), et al. 2010. A global overview of drought and heat-induced tree mortality reveals emerging climate change risks for forests. Forest Ecology and Management **259**: 660–684.

Anderegg LDL, Anderegg WRL, Berry JA. 2013. Not all droughts are created equal: Translating meteorological drought into woody plant mortality. Tree Physiology **33**: 701–712.

Blackman CJ, Brodribb TJ, Jordan GJ. 2009. Leaf hydraulics and drought stress : response , recovery and survivorship in four woody temperate plant species. : 1584–1595.

Blum A. 2017. Osmotic adjustment is a prime drought stress adaptive engine in support of plant production. Plant Cell and Environment **40**: 4–10.

Brodersen CR, McElrone AJ, Choat B, Lee EF, Shackel KA, Matthews MA. 2013. In Vivo Visualizations of Drought-Induced Embolism Spread in Vitis vinifera. Plant Physiology **161**(4)1820-1829

Brodersen CR, Knipfer T, McElrone AJ. 2018. In vivo visualization of the final stages of xylem vessel refilling in grapevine (*Vitis vinifera*) stems. New Phytologist **217**(1)117-126

Brodribb TJ, McAdam SAM. 2013. Abscisic acid mediates a divergence in the drought response of two conifers. Plant Physiology **162:** 1370–1377.

Chaves MM, Zarrouk O, Francisco R, Costa JM, Santos T, Regalado AP, Rodrigues ML, Lopes CM. 2010. Grapevine under deficit irrigation: hints from physiological and molecular data. Annals of botany **105**: 661–676.

Coupel-Ledru A, Tyerman S, Masclef D, Lebon E, Christophe A, Edwards EJ, Simonneau T. 2017. Abscisic acid down-regulates hydraulic conductance of grapevine leaves in isohydric genotypes only. Plant Physiology: pp.00698.2017.

Cramer GR, Ergül A, Grimplet J, Tillett RL, Tattersall EAR, Bohlman MC, Vincent D, Sonderegger J, Evans J, Osborne C, et al. 2007. Water and salinity stress in grapevines: early and late changes in transcript and metabolite profiles. Functional and Integrative Genomics **7**: 111–134.

Dal Santo S, Palliotti A, Zenoni S, Tornielli GB, Fasoli M, Paci P, Tombesi S, Frioni T, Silvestroni O, Bellincontro A, et al. 2016. Distinct transcriptome responses to water limitation in isohydric and anisohydric grapevine cultivars. BMC Genomics **17**: 1–19.

Daszkowska-Golec A, Szarejko I. 2013. Open or close the gate - stomata action under the control of phytohormones in drought stress conditions. Frontiers in Plant Science **4**: 1–16.

Davies WJ, Wilkinson S, Loveys B. 2002. Stomatal control by chemical signalling and the exploitation of this mechanism to increase water use efficiency in agriculture. New Phytologist **153**: 449–460.

Domec JC, Johnson DM. 2012. Does homeostasis or disturbance of homeostasis in minimum leaf water potential explain the isohydric versus anisohydric behavior of *Vitis vinifera* L. cultivars? Tree Physiology **32**: 245–248.

Franks PJ, Drake PL, Froend RH. 2007. Anisohydric but isohydrodynamic: seasonally constant plant water potential gradient explained by a stomatal control mechanism incorporating variable plant hydraulic conductance. Plant, Cell and Environment **30**: 19–30.

Griesser M, Weingart G, Schoedl-Hummel K, Neumann N, Becker M, Varmuza K, Liebner F, Schuhmacher R, Forneck A. 2015. Severe drought stress is affecting selected primary metabolites, polyphenols, and volatile metabolites in grapevine leaves (*Vitis vinifera* cv. Pinot noir). Plant Physiology and Biochemistry **88**: 17–26.

Hochberg U, Rockwell FE, Holbrook NM, Cochard H. 2018. Iso/Anisohydry: a plant environment interaction rather than a simple hydraulic trait. Trends in Plant Science **23**: 112–120.

Ingrisch J, Bahn M. 2018. Towards a comparable quantification of resilience. Trends in Ecology and Evolution **33**: 251–259.

Ivanov YV., Kartashov AV., Zlobin IE, Sarvin B, Stavrianidi AN, Kuznetsov VV. 2019. Water deficit-dependent changes in non-structural carbohydrate profiles, growth and mortality of pine and spruce seedlings in hydroculture. Environmental and Experimental Botany **157**: 151–160.

Klein T. 2014. The variability of stomatal sensitivity to leaf water potential across tree species indicates a continuum between isohydric and anisohydric behaviours. Functional Ecology **28**: 1313–1320.

Lavoie-Lamoureux A, Sacco D, Risse PA, Lovisolo C. 2017. Factors influencing stomatal conductance in response to water availability in grapevine: a meta analysis. Physiologia Plantarum **159**: 468–482.

Leyva A, Quintana A, Sánchez M, Rodríguez EN, Cremata J, Sánchez JC. 2008. Rapid and sensitive anthrone-sulfuric acid assay in microplate format to quantify carbohydrate in biopharmaceutical products: method development and validation. Biologicals **36**: 134–141.

Lovisolo C, Perrone I, Hartung W, Schubert A. 2008. An abscisic acid-related reduced transpiration promotes gradual embolism repair when grapevines are rehydrated after drought. New Phytologist **180**: 642–651.

Martínez-Vilalta J, Garcia-Forner N. 2017. Water potential regulation, stomatal behaviour and hydraulic transport under drought: deconstructing the iso/anisohydric concept. Plant Cell and Environment **40**: 962–976.

Martorell S, Diaz-Espejo A, Medrano H, Ball MC, Choat B. 2014. Rapid hydraulic recovery in *Eucalyptus pauciflora* after drought: linkages between stem hydraulics and leaf gas exchange. Plant, Cell and Environment **37**: 617–626.

Martorell S, Diaz-Espejo A, Tomas M, Pou A, El Aou-Ouad H, Escalona JM, Vadell J, Ribas-Carbo M, Flexas J, Medrano H. 2015. Differences in water-use-efficiency between two *Vitis vinifera* cultivars (Grenache and Tempranillo) explained by the combined response of stomata to hydraulic and chemical signals during water stress. Agric Water Manage **156**: 1-9.

Marusig D, Tombesi S. 2020. Abscisic acid mediates drought and salt stress responses in V*itis vinifera*—a review. International Journal of Molecular Sciences **21**: 116.

McDowell NG, Beerling DJ, Breshears DD, Fisher RA, Raffa KF, Stitt M. 2011. The interdependence of mechanisms underlying climate-driven vegetation mortality. Trends in Ecology and Evolution **26**: 523–532.

McDowell NG, Pockman WT, Allen CD, Breshears DD, Cobb N, Kolb T, Plaut J, Sperry J, West A, Williams DG, et al. 2008. Mechanisms of plant

survival and mortality during drought : why do some plants survive while others succumb to drought ? New Phytologist **178**: 719–739.

McDowell NG, Sevanto S. 2010. The mechanisms of carbon starvation : how, when, or does it even occur at all? New Phytologist **186**: 264–266.

O'Brien MJ, Leuzinger S, Philipson CD, Tay J, Hector A. 2014. Drought survival of tropical tree seedlings enhanced by non-structural carbohydrate levels. Nature Climate Change **4**: 710–714.

Pagliarani C, Casolo V, Ashofteh Beiragi M, Cavalletto S, Siciliano I, Schubert A, Gullino ML, Zwieniecki MA, Secchi F. 2019. Priming xylem for stress recovery depends on coordinated activity of sugar metabolic pathways and changes in xylem sap pH. Plant Cell and Environment **42**: 1775–1787.

Pratt RB, Castro V, Fickle JC, Madsen A, Jacobsen Al. 2020. Factors controlling drought resistance in grapevine (*Vitis vinifera*, chardonnay): application of a new microCT method to assess functional embolism resistance. American Journal of Botany **107**(4):618-627

Rogiers SY, Greer DH, Hatfield JM, Hutton RJ, Clarke SJ, Hutchinson PA, Somers A. 2012. Stomatal response of an anisohydric grapevine cultivar to evaporative demand, available soil moisture and abscisic acid. Tree Physiology **32**: 249-261.

Romero P, Botía P, Keller M. 2017. Hydraulics and gas exchange recover more rapidly from severe drought stress in small pot-grown grapevines than in field-grown plants. Journal of Plant Physiology **216**: 58–73.

Ruehr NK, Grote R, Mayr S, Arneth A. 2019. Beyond the extreme: recovery of carbon and water relations in woody plants following heat and drought stress. Tree Physiology: 1–15.

Sala A, Woodruff DR, Meinzer FC. 2012. Carbon dynamics in trees: feast or famine? Tree Physiology **32**: 764–775.

Salleo S, Lo Gullo MA, Trifilò P, Nardini A. 2004. New evidence for a role of vessel associated cells and phloem in the rapid xylem refilling of cavitated stems of *Laurus nobilis* L. Plant, Cell and Environment **27**: 1065–1076.

Savi T, Casolo V, Luglio J, Bertuzzi S, Trifilò P, Lo Gullo MA, Nardini A. 2016. Species-specific reversal of stem xylem embolism after a prolonged

drought correlates to endpoint concentration of soluble sugars. Plant Physiology and Biochemistry **106**: 198–207.

Schultz HR. 2003. Differences in hydraulic architecture account for near-isohydric and anisohydric behaviour of two field-grown *Vitis vinifera* L. cultivars during drought. Plant, Cell and Environment **26**: 1393–1406.

Schwalm CR, Anderegg WRL, Michalak AM, Fisher JB, Biondi F, Koch G, Litvak M, Ogle K, Shaw JD, Wolf A, et al. 2017. Global patterns of drought recovery. Nature **548**: 202–205.

Secchi F, Pagliarani C, Zwieniecki MA. 2017. The functional role of xylem parenchyma cells and aquaporins during recovery from severe water stress. Plant Cell and Environment **40**: 858–871.

Secchi F, Zwieniecki MA. 2012. Analysis of xylem sap from functional (nonembolized) and nonfunctional (embolized) vessels of *Populus nigra*: chemistry of refilling. Plant Physiology **160**: 955–964.

Secchi F, Zwieniecki MA. 2014. Down-regulation of PIP1 aquaporin in poplar trees is detrimental to recovery from embolism. Plant Physiology **164**: 1789-1799

Secchi F, Zwieniecki MA. 2016. Accumulation of sugars in the xylem apoplast observed under water stress conditions is controlled by xylem pH. Plant Cell and Environment **39**: 2350–2360.

Sharp RG, Davies WJ. 2009. Variability among species in the apoplastic pH signaling response to drying soils. Journal of Experimental Botany **60**: 4363–4370.

Shelden MC, Vandeleur R, Kaiser BN, Tyerman SD 2017. A Comparison of Petiole Hydraulics and Aquaporin Expression in an Anisohydric and Isohydric Cultivar of Grapevine in Response to Water-Stress Induced Cavitation. Frontiers in Plant Science 8

Siciliano I, Amaral Carneiro G, Spadaro D, Garibaldi A, Gullino ML. 2015. Jasmonic acid, abscisic acid, and salicylic acid are involved in the phytoalexin responses of rice to *Fusarium fujikuroi*, a high gibberellin producer pathogen. Journal of Agricultural and Food Chemistry **63**: 8134–8142.

Tardieu F, Simonneau T. 1998. Variability among species of stomatal control under fluctuating soil water status and evaporative demand: modelling isohydric and anisohydric behaviours. Journal of Experimental Botany **49**: 419–432.

Tomasella M, Häberle KH, Nardini A, Hesse B, Machlet A, Matyssek R. 2017. Post drought hydraulic recovery is accompanied by non-structural carbohydrate depletion in the stem wood of Norway spruce saplings. Scientific Reports **7**: 113.

Tomasella M, Casolo V, Aichner N, Petruzzellis F, Savi T, Trifilo P, Nardini A. 2019. Non-structural carbohydrate and hydraulic dynamics during drought and recovery in *Fraxinus ornus* and *Ostrya carpinifolia* saplings. Plant Physiology and Biochemistry **145**: 1-9

Tomasella M, Casolo V, Natale S, Petruzzellis F, Kofler W, Beikircher B, Mayr S, Nardini A. 2021. Shade-induced reduction of stem nonstructural carbohydrates increases xylem vulnerability to embolism and impedes hydraulic recovery in *Populus nigra*. New Phytologist **231**(1): 108-121

Tombesi S, Nardini A, Farinelli D, Palliotti A. 2014. Relationships between stomatal behavior, xylem vulnerability to cavitation and leaf water relations in two cultivars of *Vitis vinifera*. Physiologia Plantarum **152**(3)453-464

Trifilò P, Casolo V, Raimondo F, Petrussa E, Boscutti F, Lo Gullo MA, Nardini A. 2017. Effects of prolonged drought on stem non-structural carbohydrates content and post-drought hydraulic recovery in *Laurus nobilis* L.: the possible link between carbon starvation and hydraulic failure. Plant Physiology and Biochemistry **120**: 232–241.

Trugman AT, Detto M, Bartlett MK, Medvigy D, Anderegg WRL, Schwalm C, Schaffer B, Pacala SW. 2018. Tree carbon allocation explains forest drought kill and recovery patterns. Ecology Letters **21**: 1552–1560.

Tyree MT, Sperry JS. 1988. Do woody plants operate near the point of catastrophic xylem dysfunction caused by dynamic water stress? Plant Physiology **88**: 574-580.

Tyree MT, Sperry JS. 1989. Vulnerability of xylem to cavitation and embolism. Water: 19–38.

Yuan W, Zheng Y, Piao S, Ciais P, Lombardozzi D, Wang Y, Ryu Y, Chen G, Dong W, Hu Z, et al. 2019. Increased atmospheric vapor pressure deficit reduces global vegetation growth. Science Advances **5: 1–13.**

Zargar A, Sadiq R, Naser B, Khan FI. 2011. A review of drought indices. Environmental Reviews **19**: 333–349.

Zeppel MJB, Wilks J V, Lewis JD. 2014. Impacts of extreme precipitation and seasonal changes in precipitation on plants. Biogeosciences **11**: 3083–3093.

Zhang Y, Oren R, Kang S, Niinemets Ü. 2012. Spatiotemporal variation of crown-scale stomatal conductance in an arid *Vitis vinifera* L. cv. Merlot vineyard: direct effects of hydraulic properties and indirect effects of canopy leaf area. Tree Physiology **32**: 262–279.

Zwieniecki MA, Secchi F. 2015. Threats to xylem hydraulic function of trees under 'new climate normal' conditions. Plant, Cell and Environment **38**: 1713–1724.

CHAPTER II

Grapevine TPS (trehalose-6-phosphate synthase) family genes are differentially regulated during development, upon sugar treatment and drought stress

Cristina Morabito

Francesca Secchi, Andrea Schubert

Summary

Trehalose-6-phosphate synthase (TPS) performs the first step in the biosynthetic pathway of trehalose-6-phosphate and trehalose. These two molecules play key roles in the control of carbon allocation and of stress responses in plants. We investigated the organization of the *TPS* gene family and its developmental and environmental expression regulation in grapevine, a major horticultural crop. We identified three novel genes in the family, and assessed the expression of the 11 family members in tissues and developmental phases. Two potentially biosynthetic *TPS* isoforms belonging to Class I were preferentially expressed in leaf (*VvTPS1_A*) and in fruit (*VvTPS1_B*) respectively. Sucrose treatment induced expression of *VvTPS1_B*, but not of *VvTPS1_A*, and a progressive decrease of sucrose concentration. Expression of a few Class II genes was affected by sucrose treatment. Application of osmotic stress by withdrawing irrigation also induced a decrease in sucrose and an increase of glucose content, and down-regulation of the *VvTPS1_A* gene. We discuss the possible role of these potential biosynthetic *TPS* genes. Subgroups of *TPS* genes, including both Class I and Class II isoforms, followed a co-expression pattern in different conditions, suggesting that Class II TPS proteins may directly or indirectly interact with *TPS* biosynthetic genes. Our results pave the way for clarification of the role of *TPS* isoforms in grapevine responses to environmental stress.

1. Introduction

The disaccharide trehalose and its phosphorylated form trehalose 6-phosphate (T6P) control many aspects of plant development and adaptation to stress. Trehalose was identified in fungi, mosses, and ferns where it may have a protective role against protein and membrane denaturation, especially during desiccation events, preventing protein aggregation and free radical diffusion (Brumfield, 2004). In higher plants, trehalose was initially thought to be present only as a result of fungal interactions (Schubert *et al*., 1992), but later on, albeit at low concentration, it was detected in Angiosperms (Goddijn and van Dun, 1999). Increase of trehalose concentration, following over-expression of biosynthetic genes, results in enhanced tolerance to osmotic stress in dicots and monocots (Jang *et al*., 2003).

T6P is present in plant tissues at even lower levels than trehalose and plays complex regulatory roles. Concentration of T6P is highly regulated and linked to the concentrations of sucrose: T6P accumulates following sucrose application in Arabidopsis and in other plants (Figueroa and Lunn, 2016). Sucrose content in the shoot apical meristem of *A. thaliana* is correlated to T6P content, and a relative stability of the T6P/sucrose ratio has been observed also in crop plants (Dai *et al*., 2013; Du *et al*., 2017). The strong relationship linking sucrose and T6P lead to the formulation of the "sucrose-T6P nexus" model, which postulates that T6P concentration is induced by sucrose, while it feeds back on sucrose levels, maintaining sucrose concentration at optimal ranges, whose values depend on cell type, developmental stage and environmental conditions (Yadav *et al*., 2014). T6P is involved in the activation of a wide range of plant growth-related processes. In source leaves, T6P induces a decrease in sucrose levels by diverting metabolic sucrose to metabolic pathways alternative to phloem loading (Figueroa and Lunn, 2016). In sinks, T6P activates growth by repressing Sucrose-non-fermenting-1-Related Kinase1 (SnRK1) (Delatte *et al*.,

2011; Zhang *et al*., 2009), which inhibits growth of sink tissues by phosphorylating a range of target proteins, including the transcription factor bZIP11, indirectly repressing T6P accumulation (Ma *et al*., 2011) and the TARGET OF RAPAMYCIN (TOR) kinase (Nietzsche *et al*., 2016).

Trehalose and T6P are synthesized in plants following a two-step pathway, where trehalose 6-phosphate synthase (TPS: not to be confounded with terpene synthases, which share the same acronym) catalyses the condensation reaction of uridine diphosphate (UDP)-glucose and glucose 6-phosphate (G6P), forming trehalose 6-phosphate (T6P) and uridine diphosphate (UDP); then, trehalose phosphate phosphatase (TPP) dephosphorylates T6P to form trehalose and inorganic phosphate (Goddijn and van Dun, 1999). TPS is thus of particular interest as potentially being able to affect the concentration of both sugars and, as a consequence, to control an ample array of physiological processes in plants.

The *TPS* gene family in Arabidopsis and in rice consists of 11 members (Vandesteene *et al*., 2010; Zang *et al*., 2011). Poplar (Yang *et al*., 2012) and winter wheat (XIE *et al*., 2015) have 12 *TPS* genes, whereas in *Malus domestica* 13 genomic sequences compose the *TPS* gene family (Du *et al*., 2017). The grapevine *TPS* family was described by Fernandez *et al*. (2012) as consisting of 7 genes. Arabidopsis *TPS* genes possess two domains, TPS and TPP, which bear homology to the bacterial *OtsA* and *OtsB* genes, respectively responsible for TPS and TPP activity in *E. coli*. The TPP domain of Arabidopsis *TPS* genes however is not functional and only separated *TPP* genes (lacking the TPS domain) perform the TPP reaction in plants (Vandesteene *et al*., 2010). The *TPS* family is divided into two distinct clades, class I and class II, based on distinct gene structures, patterns of gene expression, and enzymatic activities of the encoded proteins (Lunn, 2007). Class I members encode TPS proteins with demonstrated biosynthetic activity (Blázquez *et al*., 1998; Vandesteene *et al*., 2010), while class II proteins lack both TPS and TPP activity and, notwithstanding several investigation efforts, their functions remain still unresolved (Ramon *et al*., 2009).

TPS gene expression is organ- and developmental stage-specific (Ramon *et al*., 2009) and is affected by stress (drought, salt, temperature, and chilling) and sucrose treatments (Du *et al*., 2017; Fernandez *et al*., 2012; Mu *et al*., 2016).

Vitis vinifera is a worldwide cultivated plant species, extremely important from an economic point of view. Grapevines are often exposed to drought stress, and in such conditions, its vegetative organs undergo important variations in sugar concentration (Cramer *et al*., 2007; Hochberg *et al*., 2013). Given the known roles of T6P and of trehalose in the control of soluble sugar concentration and in responses to stress in plants, regulation of *TPS* expression in these processes is conceivable and worthy investigation.

Here, we performed a deeper characterization of the *VvTPS* gene family in grapevine; we identified three novel genes, and we assessed their expression in different tissues and developmental stages. To directly test the dependency of T6P on sucrose concentration, a sucrose treatment on leaves was applied and changes of *TPS* gene expression and soluble sugar content were studied. Finally, considering the potential roles of trehalose and T6P under osmotic stress, we investigated the expression of the *VvTPS* genes, and the concentration of soluble sugars, under drought stress and a subsequent recovery. We identified novel genes of the *TPS* family in grapevine and we show that *TPS* genes are regulated by drought stress. We further show that a potentially biosynthetic *TPS* isoform preferentially expressed in leaves is not regulated by sucrose and is strongly downregulated by drought stress.

2. Materials and methods

2.1. Identification of VvTPS genes

The eleven sequences of the *Arabidopsis thaliana TPS* gene family were downloaded from the TAIR genome database (www.arabidopsis.org) and were

used as a query in a BLAST analysis against the *Vitis vinifera* genome (http://genomes.cribi.unipd.it/grape/). Final identification of grapevine *TPS* gene sequences was achieved comparing information from different databases, such as CRIBI (http://genomes.cribi.unipd.it/grape/), Genoscope (http://www.cns.fr/externe/GenomeBrowser/Vitis/) and Ensembl Plants (https://plants.ensembl.org/Vitis_vinifera/Info/Index).

The resulting grapevine TPS protein sequences, downloaded from the Grape Genome Database (12X V2 version), were further confirmed using the Conserved Domain search tool (https://www.ncbi.nlm.nih.gov/Structure/cdd/wrpsb.cgi), and proteins lacking TPS domains were rejected.

2.2. Phylogenetic and gene structure analyses

The TPS protein sequences of *A. thaliana* were aligned to those of grapevine using Muscle software (https://www.ebi.ac.uk/Tools/msa/muscle/) and a phylogenetic tree was generated using MEGA X software (Kumar *et al*., 2018), applying the neighbor-joining method and the Jones-Taylor-Thornton model for amino acid substitutions. Bootstrap support values were estimated using 1000 pseudo-replicates. A pairwise comparison was performed among full-length protein sequences from *V. vinifera* and *A. thaliana TPS* family, first within the same class, I and II separately, and then between the two classes. Identification and sequence alignment of conserved motifs containing active sites were performed using DNAMAN software (https://www.lynnon.com/).

The structure of *VvTPS* genes was analyzed and graphically represented using the Gene Structure Display Server 2.0 (GSDS; http://gsds.cbi.pku.edu.cn/). Protein molecular weight and isoelectric point were calculated using ProParam (https://web.expasy.org/protparam/). Protein subcellular localization was predicted *in silico* with BUSCA software (http://busca.biocomp.unibo.it/). *TPS* genes were localized on grapevine chromosomes and mapping results were

graphically annotated using the vector graphics editor Inkscape, version 0.92.4 (https://inkscape.org/).

2.3. Plant material and sample collection

Plant material at different developmental stages was collected in 2018 from twelve, ten-year-old *Vitis vinifera* plants cv. Barbera, randomly distributed in an experimental vineyard located at the Department of Agricultural, Forest and Food Sciences campus in Grugliasco (45°03'57.9"N 7°35'32.9"E). Samples collected from the different plants were pooled in order to perform gene expression analyses. Flowers and setting pistils were collected on 10 May and 10 June respectively; green berries, young (node 3 from apex) and mature (node 15 from apex) leaves on 24 July; *véraison* and ripening berries on 1 August and 28 August, respectively; lignified one-year canes on 27 September. Samples were ground in liquid nitrogen and stored at -80°C for further analysis.

Sucrose treatments were performed by spraying a 1% sucrose solution on cv Barbera leaves in vineyard conditions. Six grapevines were treated with the sucrose solution and six were used as not-treated controls. One hour after treatment, the excess of sucrose was removed by spraying and rinsing leaves with distilled water. Six fully expanded sun-leaves were randomly collected from different points of the canopy of each treated and not-treated plant after one and twenty-four hours after sucrose treatment, in order to perform sugar quantification and gene expression analyses.

In order to test the effects of drought stress, twelve one-year-old Barbera plants grafted on SO4 were grown in a glasshouse under partially controlled climatic conditions. Temperature was maintained in the range of 25–32°C. Each plant grew in a 4 L-pot filled with a substrate composed of sandy-loam soil/ expanded clay/peat mixture (2:1:1 by weight), and daily irrigated to substrate capacity. Starting on 20 July 2018, six plants were kept as controls and daily

irrigated to substrate capacity (CTR), while six plants were exposed to a progressive drought stress (DS) induced by withholding irrigation for 13 consecutive days; at the end of the drought period and for further 7 days, these plants were daily re-watered to substrate capacity (REC).

Leaf samples were collected after 0, 5 and 13 days of drought stress, and after 1, 3 and 7 days from re-watering. At each sampling date, three fully expanded leaves were sampled from three out of the six available plants per treatment for assessment of stem water potential, while three leaves were sampled from the other three plants for determination of sugars content and gene expression. Collected leaf samples were ground in liquid nitrogen and stored at -80°C for further analyses.

2.4. Gas exchange and water potential measurements

Stomatal conductance (g_s) and net photosynthesis (A_n) were measured on fully expanded leaves exposed to direct sunlight, using a portable infrared gas analyzer (LCPro+ system, The Analytical Development Company Ltd, Hoddesdon, UK). Measurements were performed using a 6.25 cm^2 leaf chamber equipped with artificial irradiation (1200 µmol photons m^{-2} s^{-1}), set with a chamber temperature of 25°C to avoid overheating. Ambient CO_2 values were 400-450 ppm. Leaf gas exchange was assessed daily between 10:00 am and 12:00 pm.

Stem water potential measurements were performed on non-transpiring leaves. To this aim, each leaf was enclosed in a humidified aluminium foil-wrapped plastic bag for 20 minutes before excision. After excision, leaves were allowed to equilibrate in the closed bag for an additional 15 minutes and water potential was measured using a Scholander-type pressure chamber (Soil Moisture Equipment Corp., Santa Barbara, CA).

2.5. Measurement of sugar content and gene expression

50 mg-aliquots of ground leaf tissue were extracted with deionized water for 15 min at 70°C and then centrifuged at 10000 g for 20 min. Glucose concentration was assessed on a fraction of the supernatant using the glucose-oxidase Glucose Assay kit (GAGO-20, Merck, Darmstadt, Germany), reading absorbance at 540 nm. Another fraction of the supernatant was digested with 15 units of invertase (I4504, Merck, Darmstadt, Germany) and total glucose level was measured. The sucrose level was then calculated as total glucose minus free glucose.

Total RNA was extracted from 200 mg tissue aliquots of each leaf sample, using a CTAB-based protocol adapted to grapevine tissues (Carra et al., 2007). RNA quantification and quality evaluation were performed using a NanoDrop™ 2000 spectrophotometer (ThermoFisher Scientific, Massachusetts, United States). RNA samples integrity was further checked through electrophoresis on a 1% agarose gel.

In order to avoid genomic DNA contamination, total RNA was treated with RNase-free DNase (DNase I, Amplification Grade Invitrogen, ThermoFisher Scientific, Massachusetts, United States). Then, 500 ng of DNase I-treated RNA was reverse-transcribed into cDNA using the High Capacity cDNA Reverse Transcription Kit (Applied Biosystems, California, United States).

Gene-specific primers were designed with Primer3 program (http://primer3.ut.ee/) (Tab. 1). Annealing temperatures, GC content (%) and absence of primer dimers or not specific secondary structures were confirmed through Oligo Evaluator (SIGMA-Aldrich; http://www.oligoevaluator.com/). The geometric average of *VvUbiquitin and VvActin* expression was used as reference in order to normalise gene expression data. Primer specificity and efficiency were assayed to ensure measurement accuracy.

RT-qPCR analyses were performed in a StepOnePlus™ Real-time PCR detection system (Applied Biosystems, California, United States), supported by the StepOne software, version 2.3. Reactions were carried out in a final volume of 10 µl, consisting of 1 µl diluted cDNA, 1 µl of primer mix (10 µM), 5 µl Luna® Universal qPCR Master Mix (BioLabs Inc., Massachusetts, United States) and 3 µl DEPC-treated ultrapure water. The PCR program was set as follows: 95°C for 10 min (initial holding stage); 45 cycles of 95°C for 15 sec, 63°C for 1 min. For melting curve analysis, the temperature was set at 95°C for 15 sec and at 63°C for 1 min. The Ct method was used to calculate normalized gene expression levels for family characterization work, while gene expression results from drought experiment were normalized on control samples. Analyses were performed in three technical replicates.

The heatmap summarizing the *TPS* family characterization results was realized with GraphPad Prism8 program (https://www.graphpad.com/scientific-software/prism/) on a z-score normalized data matrix (mean-centered data, normalized on standard deviation). Euclidean distance was applied to accomplish cluster analysis.

Tab. 1 – Specific primers sequence list.

Gene name	Gene ID (CRIBI)	Primer name	Forward primer sequence	Reverse primer sequence	Amplicon size (bp)
VvTPS1_A	VIT_10s0003g02160	***VvTPS1_A***	CTCACAAGCCAGGTTCATGA	GGCCACAAACTCATAGCTAACA	192
VvTPS1_B	VIT_19s0014g00300	***VvTPS1_B***	CCCGCTTAAAGTTTTGCCCT	CCTTCTGGCCTTCTTCCCTT	153
VvTPS5	VIT_02s0012g01680	***VvTPS5***	GTGTTCTTGCCAATGAGCCA	TGCCGCATTGTTACAAGGAG	115
VvTPS6	VIT_01s0011g05960	***VvTPS6***	TGCCTCCTGATCTGTTTACCA	CCTGCCATAGAGAACGGTTG	126
VvTPS7_A	VIT_10s0003g01680	***VvTPS7_A***	GGACAGAAACCAAGTAAAGCCA	GAGATGGGGAAGGGTCTGAA	100
VvTPS7_B	VIT_12s0028g01670	***VvTPS7_BC***	GAAGGGAAAACGGTGTTGCT	CGGTCTTTCCTTGCCACTTT	118
VvTPS7_C	VIT_03s0063g01510				
VvTPS8_A	VIT_14s0036g01210	***VvTPS8_AB***	TGTTTAGTGTCGCTGATACG	TGTAGTGATCTTTGCATGCC	162
VvTPS8_B	VIT_07s0005g05690				
VvTPS9	VIT_17s0000g08010	***VvTPS9***	GGAGCACTGGTTTTAGCCTG	GCCCTTCTATTCGCCCTCTT	109
VvTPS10	VIT_01s0026g00280	***VvTPS10***	TTATGCTCGCCACTTCCTGT	CACAGTCCGACCCGAGTAAT	100
VvCWINV1	VIT_09s0002g02320	***VvCWINV1***	TCTATCAACAGCTCTACGGGT	TCTCACGGTTGTAGCTTCCA	124
VvSUSY2	VIT_07s0005g00750	***VvSUSY2***	GCCCTGCATGGTTCAATTGA	GTCAAGCCTTGCCATGGAAA	114
VvActin	VIT_04s0044g00580	***VvACT***	GCCCCTCGTCTGTGACAATG	CCTTGGCCGACCCACAATA	101
VvUbiquitin	VIT_16s0098g01190	***VvUBI***	TGAGGCTTCGTGGTGGTATT	GCGGCAGATCATTTTGTCCT	80

2.6. Statistical analyses

In the sucrose treatment experiment, a Student t-test ($P < 0.05$) was performed to evaluate statistical difference among treated and not-treated samples at each time point respectively. In the drought stress experiment, data were submitted to one-way analysis of variance (ANOVA) and means were compared using Tukey's post hoc test. Statistical significance was set at $P < 0.05$. Three replicates were used. Sigma Plot® software (Systat Software Inc.) was used to perform statistical analyses and to create figures. Graphical implementation of figures was carried out with Inkscape software version 0.92.4 (https://inkscape.org/).

3. Results

3.1. Identification and characterization of grapevine TPS genes

Using *A. thaliana TPS* sequences (*AtTPS1-AtTPS11*) as BLAST queries against the grapevine genome, 11 putative grape *TPS* genes were identified and named following the similarity with Arabidopsis *TPS* genes (Tab. 2).

Conserved domain search allowed the localization of both TPS and TPP domains on nine of the eleven identified sequences. *VvTPS8_A* and *VvTPS8_B* only display the TPS domain. Predicted molecular weight is above 80 kDa for most of the proteins; *VvTPS1_A* shows a lower predicted weight of 60 kDa, and the two proteins lacking the TPP domain have an average molecular weight of 36 kDa. Coding sequences range from 1608 to 2787 bp with the exception of *VvTPS8_A* and *VvTPS8_B* whose coding sequences are 543 and 1347 bp long respectively. The *in silico* predicted localization of TPS proteins includes cytoplasm and nucleus.

3.2. Chromosome localisation, phylogenetic and gene structure analyses

The eleven putative genes are localised on 9 different chromosomes of the grapevine genome (Fig.1A). Phylogenetic analysis confirmed an organization into two classes as reported for *TPS* gene families from Arabidopsis and other plant species (Fig. 1B, 2). *VvTPS1_A* and *VvTPS1_B* belong to Class I, while the remaining *VvTPS* genes belong to Class II. Class II is divided into two main clusters; the first includes *VvTPS5* and *VvTPS6*, and the second is organized in two further subgroups, respectively composed of the three genes annotated as *VvTPS7*, and of the cluster including *VvTPS9*, the two isoforms of *VvTPS8*, and *VvTPS10*. *VvTPS8_A and VvTPS8_B*, respectively localized on chromosome 14 and 7, are confined to a distal region of the phylogenetic tree: this outlying position could be explained by the lack of the TPP domain in these two genes. Gene structure (Fig. 1C) confirms the TPS domain as N-terminal and the TPP

domain as C-terminal. Exon/intron structure is markedly different in *VvTPS1_A* and *VvTPS1_B*, where introns are more numerous and more extended, compared to Class II members.

Tab. 2 - The trehalose-6-phosphate synthase (*TPS*) gene family in *Vitis vinifera*.

Gene name	Gene ID (CRIBI)	Genome location	MW (kDa)	pI	AA	Subcellular localization (score)	Coding sequence (bp)	TPS domain location	TPP domain location	N° of exons/introns
VvTPS1_A	VIT_10s0003g02160	chr10:388361-3911610	60	7,65	535	Cyto (0.7)/nucl (0.3)	1608	18-163	192-382	12/11
VvTPS1_B	VIT_19s0014g00300	chr19:291985-313231	104	6,55	927	Nucl (1)	2784	88-553	582-797	19/18
VvTPS5	VIT_02s0012g01680	chr2:8014367-8023721	97	5,86	864	Cyto (0.7)/nucl (0.3)	2595	60-546	591-842	3/2
VvTPS6	VIT_01s0011g05960	chr1:5722102-5727217	97	5,45	854	Cyto (0.7)/nucl (0.3)	2565	61-550	597-845	3/2
VvTPS7_A	VIT_10s0003g01680	chr10:3105364-3114457	96	5,57	853	Cyto (0.7)/nucl (0.3)	2562	59-542	586-837	4/3
VvTPS7_B	VIT_12s0028g01670	chr12:2329757-2333598	97	5,39	855	Nucl (1)	2568	60-543	587-838	3/2
VvTPS7_C	VIT_03s0063g01510	chr3:4947898-4950033	80	5,67	705	Nucl (1)	2118	60-543	587-655	1
VvTPS8_A	VIT_14s0036g01210	chr14:12064993-12065680	21	8,75	180	Nucl (1)	543	36-80		1
VvTPS8_B	VIT_07s0005g05690	chr7:9969828-9970515	51	8,68	448	Nucl (1)	1347	304-348		1
VvTPS9	VIT_17s0000g08010	chr17:8993307-8996192	91	5,83	809	Cyto (0.7)/nucl (0.3)	2430	63-493	537-7889	4/3
VvTPS10	VIT_01s0026g00280	chr1:8955542-8962419	105	5,86	928	Cyto (0.7)/nucl (0.3)	2787	56-540	587-837	7/6

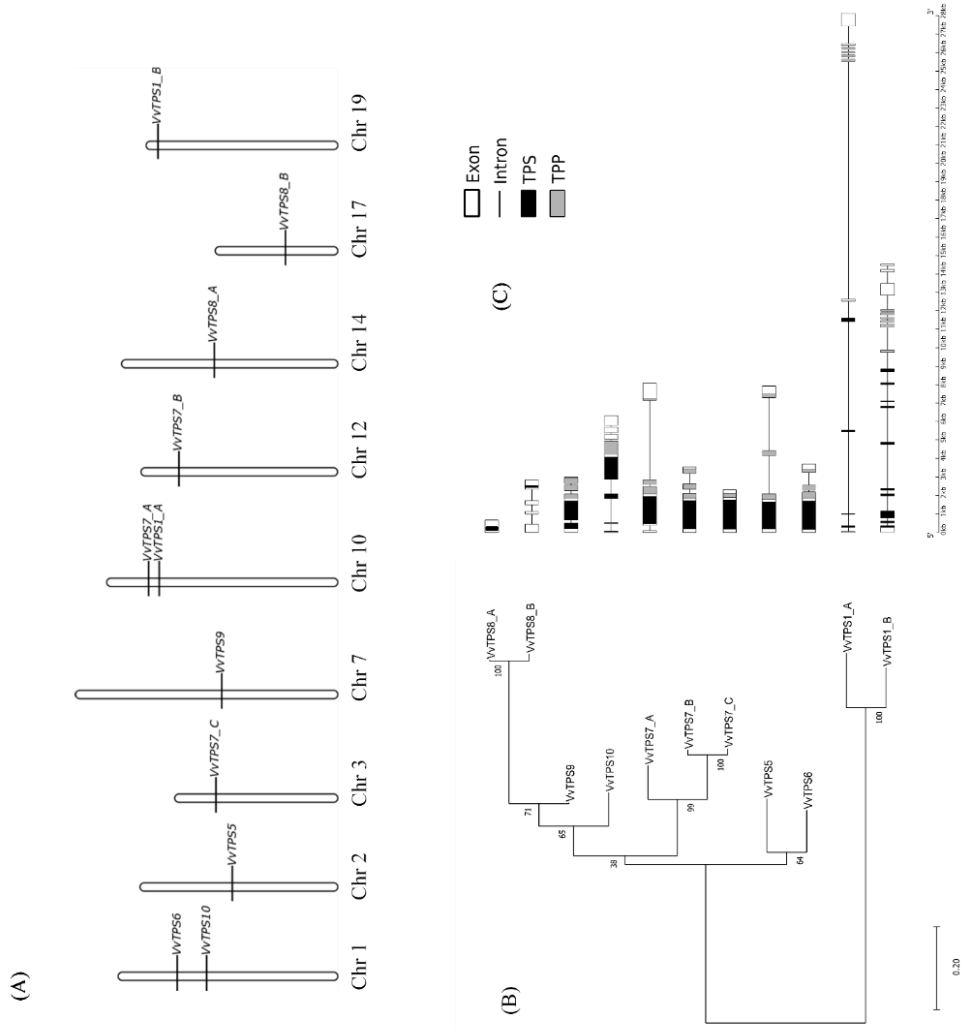

Fig. 1 – Chromosome distribution, phylogenetic tree, and gene structures of the *Vitis vinifera TPS* gene family (A). Gene mapping on chromosomes (B). Phylogenetic tree of the grapevine *TPS* family (C): boxes and lines represent exons and introns, respectively; the TPS and TPP domains are represented by respectively black and grey boxes.

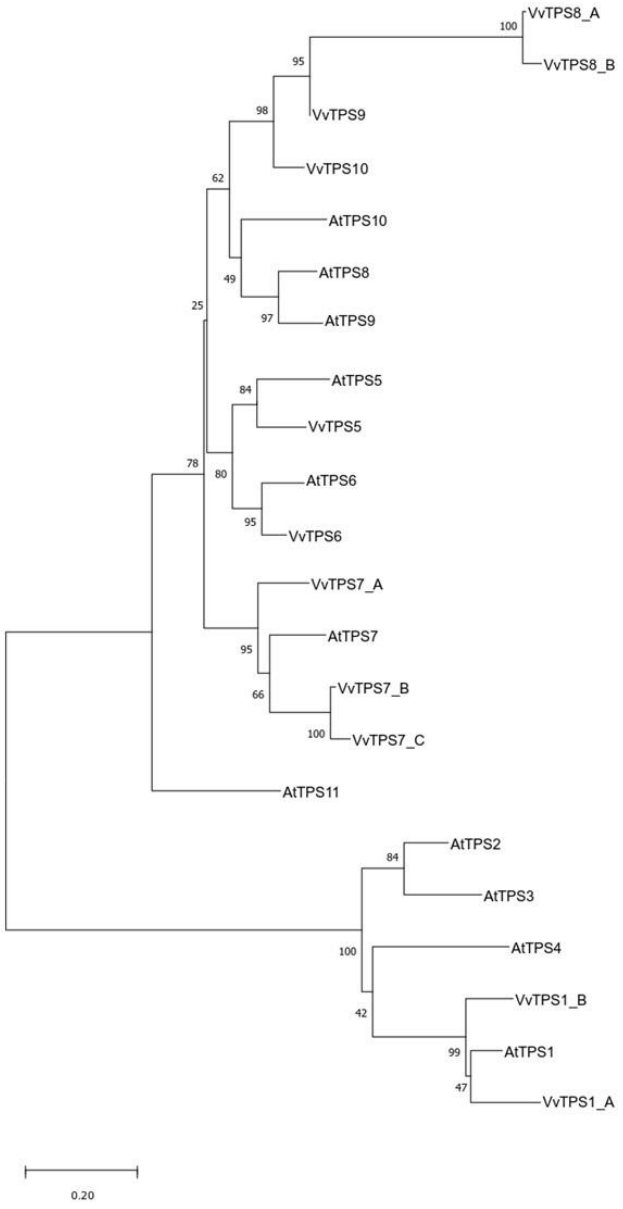

Fig. 2 – Phylogenetic analysis of *TPS* genes from grapevine (this study) and *Arabidopsis thaliana* (Vandesteene *et al*., 2010).

3.3. Alignment and analyses of conserved motifs

We assessed the similarity of protein sequences between *A. thaliana* and *V. vinifera* in pairwise sequence comparisons (Fig. 3). Class I proteins show a median percentage identity value of 42%, while Class II protein sequences show a median value of 60%. When the two different classes are compared, the median value drops down to 27%. *VvTPS8_A* and *VvTPS8_B* are represented as outliers in the graph and are respectively only 10% and 13% identical to the other Class II proteins and 5% and 10% identical to Class I protein sequences.

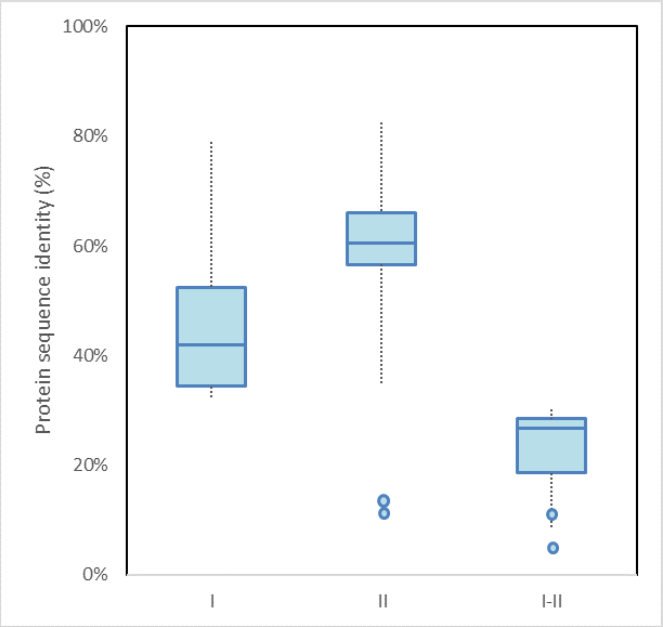

Fig. 3 – Pairwise sequence identity of TPS proteins of *V. vinifera* and *A. thaliana*. *I* and *II* represent pairwise sequence identities of respectively class I and II TPS proteins, *I-II* shows pairwise sequence identities between class I and II TPS proteins of each plant species. The boxplot displays the median (dark blue line), interquartile range (box), and maximum and minimum scores (whiskers) for each data set. Outliers (*VvTPS8_A* and *VvTPS8_B*) are represented in the graph as dots.

In Arabidopsis, *AtTPS1* (belonging to Class I) is considered the main biosynthetic TPS isoform. Alignment of the TPS domain of *AtTPS1* (corresponding to residues 91 to 559) with grapevine Class I TPS proteins shows that *VvTPS1_A* displays a deletion of the N-terminal 305 residues. Among seven residues considered important for glucose-6P binding and 12 for UDP-glucose binding by Du *et al*. (2012), respectively six and twelve are present in *VvTPS1_B*, while the *VvTPS1_A* sequence only contains seven conserved residues among those considered for UDP-glucose binding (Fig. 4).

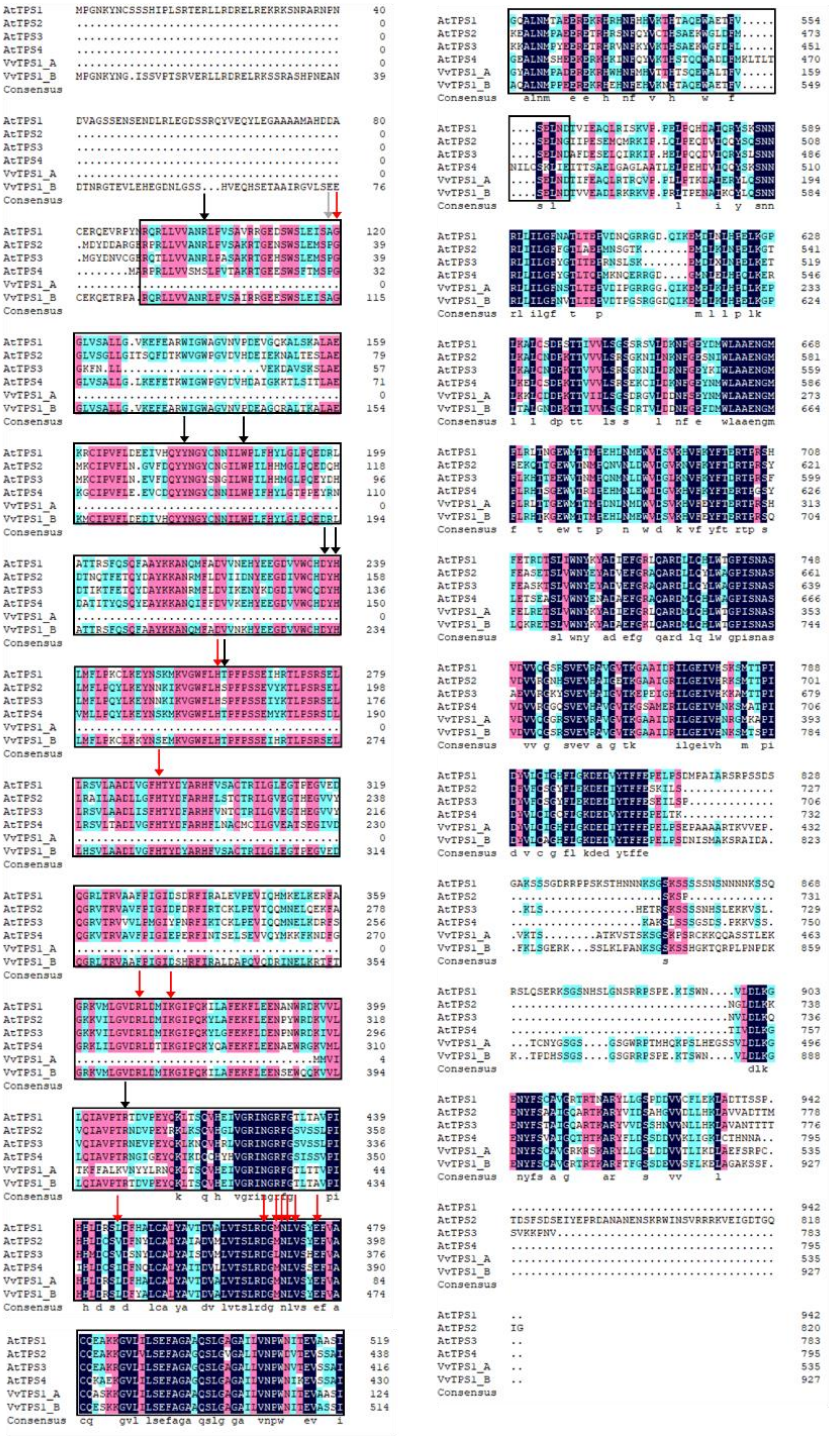

Fig. 4 – Amino acid sequence alignment of the TPS domains of grapevine TPS proteins and of *AtTPS1* as a reference. Overall conserved residues are depicted in white on black background; conserved residues are in black on pink background; similar residues are in black on light blue background. Black and red arrows show conserved residues important for G6P binding and UDP-Glc binding, respectively, according to Du *et al.* (2017). In Fernandez *et al.* (2017), another amino acid is annotated as important in substrate binding, here indicated by grey arrow.

3.4. Development- and organ-dependent expression of grapevine TPS genes

Real time qPCR assay was performed in order to analyse *VvTPS* gene expression patterns in different organs and during plant development. Expression of all genes was detectable. While the primer sequences were specific for almost all genes, it was not possible to discriminate the two isoforms of *VvTPS7* on chromosomes 3 and 12 (*VvTPS7_B* and *VvTPS7_C*, henceforth indicated collectively as *VvTPS7_BC*) and between the two isoforms of *VvTPS8*, due to high sequence similarity. The expression heatmap (Fig. 5) shows four gene expression clusters. *VvTPS7_BC* and *VvTPS5* are more expressed during flower development and fruit setting; *VvTPS1_A*, *VvTPS6* and *VvTPS8_AB* are mainly expressed in leaves and woody tissues; *VvTPS7* and *VvTPS9* are more expressed in unripe berries, mature leaves and shoots/tendrils; *VvTPS10* and *VvTPS1_B* are more expressed in berries in the pre-véraison phase. Genes belonging to Class 1, *VvTPS1_A* and *VvTPS1_B*, and thus putatively biosynthetic, are more expressed in leaf and berry respectively. The expression level normalized to the reference genes in mature leaf is one order of magnitude higher for *VvTPS1_A* than for *VvTPS1_B*. Transcripts from Class II genes *VvTPS5*, *VvTPS6*, and *VvTPS7_A* are more abundant and show relative expression levels in leaf in the same order of magnitude as Class I *VvTPS1_A*, while expression of *VvTPS7_BC*, *VvTPS8_AB*, *VvTPS9*, and *VvTPS_10* in leaf is very low or negligible (Fig. 6).

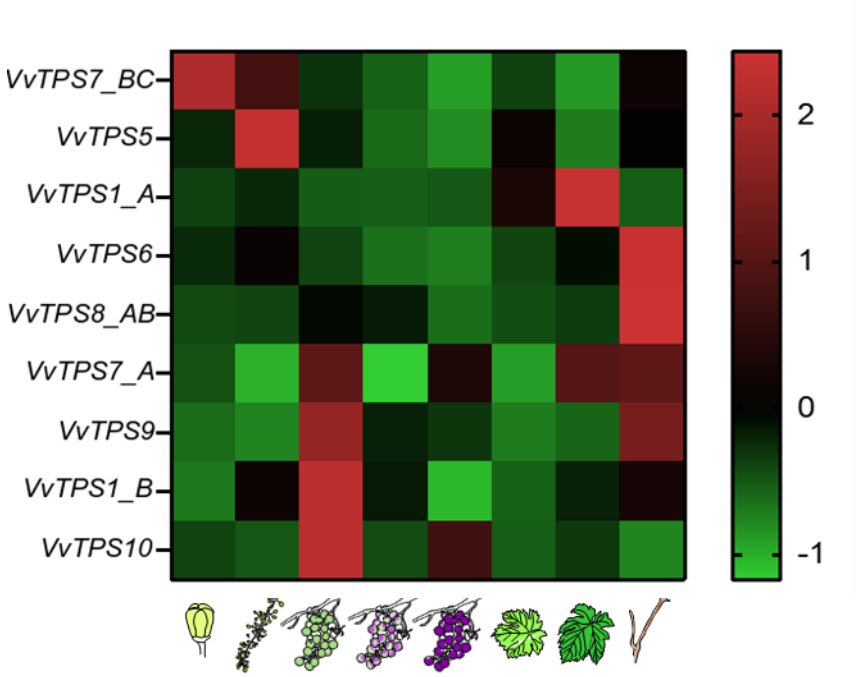

Fig. 5 – Heatmap of *VvTPS* gene expression in grape tissues and at different developmental stages (modified E-L system, revised from Coombe 1995). Left to right: flower buttons (E-L 20), fruit setting (E-L 29), green berry (E-L 33), berry at veraison (E-L 35), mature berry (E-L 38), young leaf (E-L 14), mature leaf (E-L 29) and lignified one-year-old shoot (E-L 43). The heatmap allows comparison between conditions within the same gene (i.e. within each row). Normalized expression data (delta Ct values) were used for standardization.

Fig. 6 – Analysis of *VvTPS* genes expression in grape tissues and at different developmental stages (modified E-L system, revised from Coombe 1995). Left to right: flower buttons (E-L 20), fruit setting (E-L 29), green berry (E-L 33), berry at veraison (E-L 35), mature berry (E-L 38), young leaf (E-L 14), mature leaf (E-L 29) and lignified one-year-old shoot (E-L 43). Expression data were normalized on housekeeping genes (*VvActin*, *VvUbiquitin*) expression.

3.5. Concentration of soluble sugars and expression of TPS genes following sucrose treatments

In non-treated plants, leaf sucrose concentration was about four times higher than glucose (Fig. 7A). Surprisingly, leaf sucrose concentration was negatively affected by sucrose treatment: concentrations it nearly halved after 1 hour from treatment and remained lower thereafter. Glucose content increased more than 50% after sucrose treatment, suggesting hydrolysis of sucrose (Fig.7A). Expression of cell wall invertase (*VvCWINV1*) progressively increased in sucrose-treated plants as shown by significant difference 24 hr after treatment. Expression of sucrose synthase (*VvSUSY2*) on the contrary followed an opposite trend. However, the expression level of cell wall invertase compared to reference genes was nearly one order of magnitude higher than sucrose synthase 24 hr after treatment (Fig. 7B).

Expression of *TPS* genes was affected by sucrose treatment. Class I *VvTPS_1A* and *VvTPS1_B* showed different trends, the first progressively decreasing expression in sucrose-treated leaves, the second being more expressed than in non-treated leaves. Among Class II genes, *VvTPS5* was significantly and progressively less expressed upon sucrose treatment (and sucrose depletion), while sucrose spraying induced a progressively higher expression of *VvTPS7_A* and *BC*, and of *VvTPS10* (Fig. 7C).

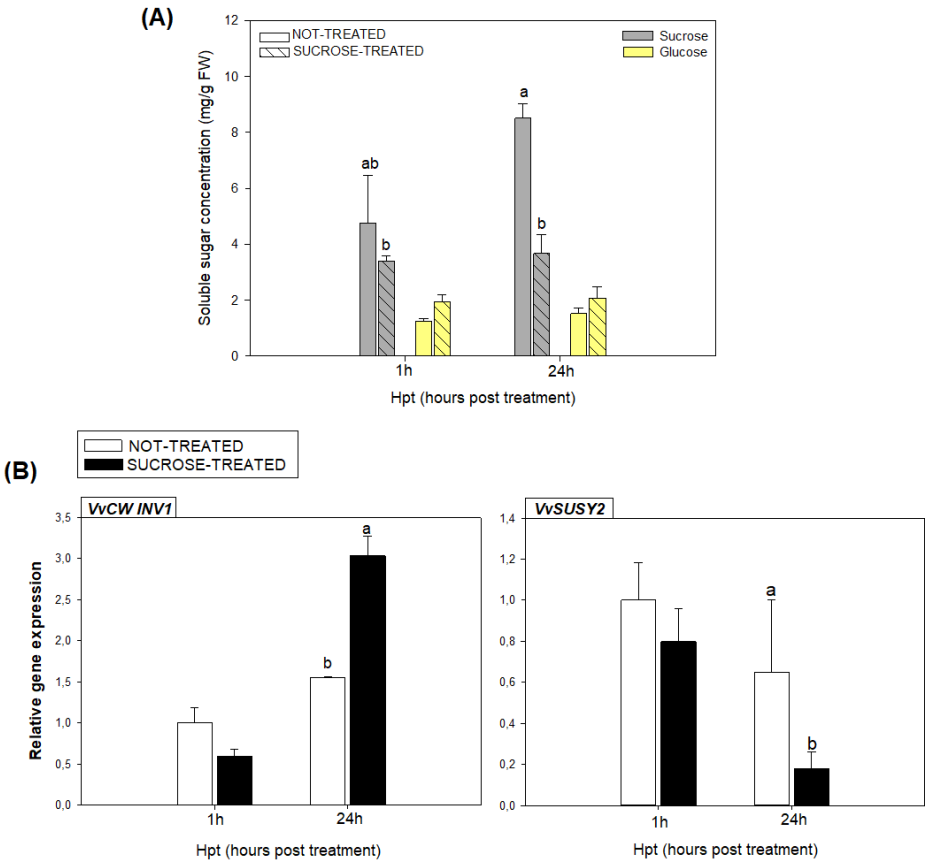

Fig. 7 – Effects of sucrose treatment on sucrose metabolism in grapevine leaves. A: sucrose and glucose concentration in leaves 1 and 24 hr after sucrose treatment. B: expression of genes encoding sucrose cleaving genes (cell wall invertase and sucrose synthase). Letters show statistical differences between treatments ($P < 0,05$) at each single time point, according to Student t-test.

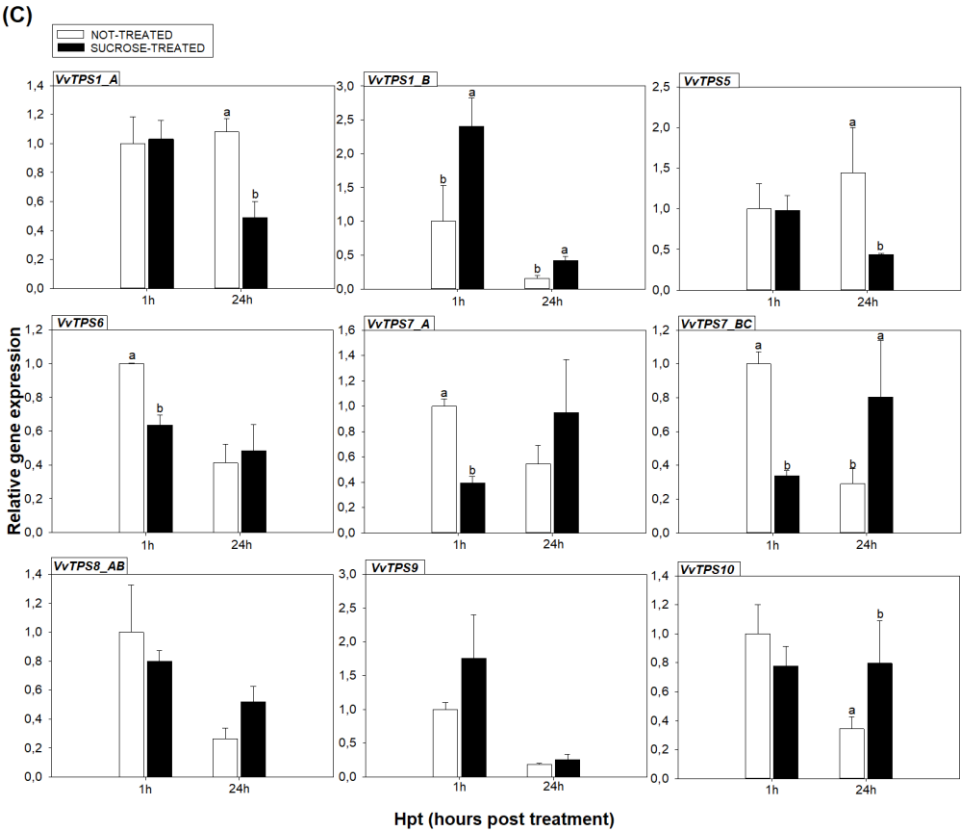

Fig. 7C – *VvTPS* gene expression following leaf sucrose treatment. Expression data were normalized to non-treated control at 1h after treatment. Letters denote statistical differences between treatments ($P < 0,05$) at each single time point, according to Student t-test.

3.6. Leaf gas exchange, stem water potential, soluble sugar concentration, and expression of VvTPS genes in drought-stressed and recovering plants

We exposed potted grapevines to water stress under glasshouse conditions. Interrupting irrigation caused a decrease in stem water potential (Ψ_w), resulting in a progressive loss of cell turgor. After 13 days with no irrigation, an average stem water potential of -1,93 MPa ± 0.07 was reached, and plants showed a strong wilting phenotype. Stomatal conductance (g_s) values progressively decreased in response to stress, indicating plants closed stomata to prevent tissue

desiccation. Simultaneously, drought caused a severe loss of net photosynthesis (A_N). After re-watering, stem water potential recovered within one day. However, 7 days of stress relief did not allow plants to fully accomplish stomatal recovery, and, accordingly, net photosynthetic activity was not completely restored within this time window (Tab. 3).

Tab. 3 – Stem water potential Ψ_w, stomatal conductance Gs, and net assimilation A_N, measured during the course of the drought and recovery experiment. Letters denote statistical differences between treatments ($P < 0,05$) according to Tukey test.

Treatment	Ψ_w (MPa)	Gs (mmol H_2O $m^{-2}s^{-1}$)	A_N (µmol CO_2 $m^{-2}s^{-1}$)
Control – day 0	-0,38 ± 0,01 *(ab)*	183 ± 14,53 *(a)*	8,90 ± 0,80 *(a)*
Control – day 5	-0,38 ± 0,04 *(abc)*	173 ± 6,67 *(a)*	9,62± 0,40 *(a)*
Control – day 13	-0,46 ± 0,03 *(bc)*	190 ± 0,00 *(a)*	9,19 ± 0,51 *(a)*
Control – day 20	-0,45 ± 0,04 *(bc)*	183 ± 12,01 *(a)*	9,71 ± 0,34 *(a)*
Drought stress – day 5	-0,71 ± 0,15 *(d)*	100 ± 30,55 *(b)*	5,64 ± 1,90 *(b)*
Drought stress – day 13	-1,93 ± 0,07 *(e)*	10 ± 0,00 *(c)*	0,06 ± 0,04 *(c)*
Recovery – day 1	-0,46 ± 0,27 *(bc)*	10 ± 0,00 *(c)*	0,46 ± 0,01 *(c)*
Recovery – day 3	-0,25 ± 0,04 *(a)*	30 ± 0,00 *(c)*	1,60 ± 0,36 *(c)*
Recovery – day 7	-0,56 ± 0,04 *(cd)*	113 ± 20,28 *(b)*	7,31 ± 1,26 *(ab)*

In irrigated control plants, sucrose concentration was again higher than glucose (Fig. 8A). Drought caused a significant and progressive decrease of sucrose concentration; following re-watering, sucrose concentration remained significantly lower than in irrigated control plants. Glucose concentration upon drought was comparable to irrigated control values, while at the last point of recovery was significantly higher, inversely related with the decrease in sucrose content (Fig. 8A).

Drought stress differently influenced *VvTPS* genes expression in mature leaves. Within class I, *VvTPS1_A* was downregulated during stress and its expression level remained stable upon recovery. Expression of *VvTPS1_B* was not significantly affected by drought stress. Genes from Class II follow three distinct

patterns. *VvTPS6, VvTPS8_AB, and VvTPS9* follow the same pattern as *VvTPS1_A*. The other three *VvTPS* members from Class II, *VvTPS7*, *VvTPS7_BC*, and *VvTPS10* are significantly and strongly overexpressed at the higher stress level while their expression decreases to control values following recovery. The third pattern is shown by *VvTPS5*, whose expression is not affected by drought stress, but drops during recovery (Fig. 8B).

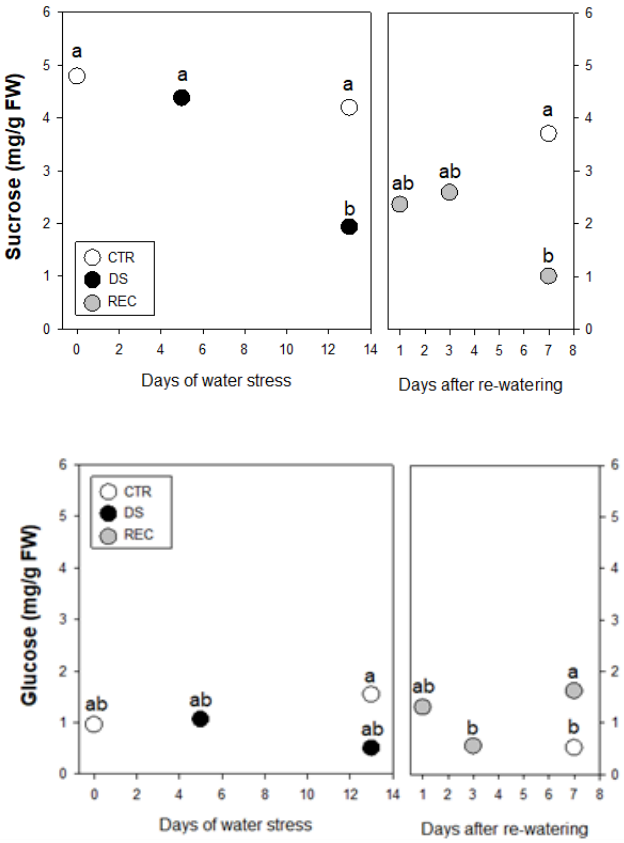

Fig 8A – Leaf sucrose and glucose content in mature leaves during the drought (DS) and recovery (REC) experiment. Letters show statistical differences among treatments (P < 0,05), according to Tukey test.

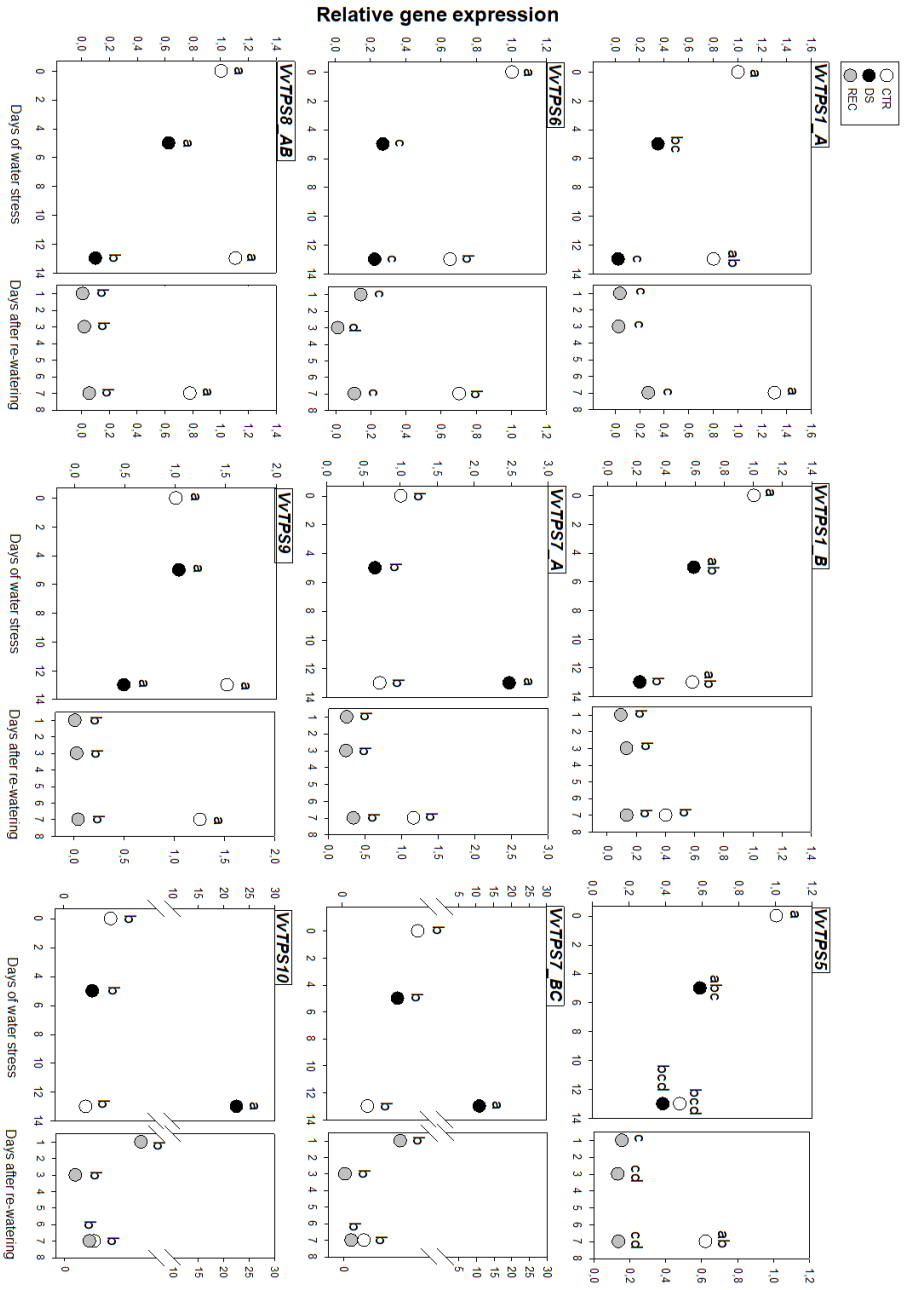

Fig 8B – Analysis of *VvTPS* genes expression in mature leaves. Expression data were normalized to the day 0 value. Letters show statistical differences among treatments ($P < 0,05$), according to Tukey test.

4. Discussion

TPS genes play pivotal roles in plant life and are involved in growth processes and in responses to abiotic stress. In this work, we identified 11 *V. vinifera TPS* gene sequences, confirming the seven genes identified by Fernandez *et al*. (2012) and broadening the family by four more genes. Phylogenetic analysis confirmed that these *VvTPS* genes are grouped into two main clusters, class I (two genes) and class II (nine genes). These groups are defined by different gene structures: *VvTPS1_A* and *VvTPS1_B*, belonging to Class I, have 11 and 19 introns respectively, while in grapevine genes from class II, the number of introns ranges from 0 to 6. Similar variability in the number of intronic sequences was shown in previous work in Arabidopsis, poplar, and rice (Yang *et al*., 2012) and apple (Du *et al*., 2017).

TPS activity has been demonstrated only for Class I genes: in Arabidopsis, *AtTPS1* is the main biosynthetic gene, although also *AtTPS2* and *AtTPS4* may encode functional TPS enzymes (Delorge *et al*., 2015; Vandesteene *et al*., 2012). AtTPS1 and the grapevine genes here identified as part of Class I, *VvTPS1_A* and *VvTPS1_B*, share sequence homology and similar residues at conserved positions in the TPS domain. *VvTPS1_B* corresponds to *VvTPS1* previously described in grapevine by Fernandez et al. (2012). Sucrose treatment induces an increase of T6P in Arabidopsis and other plants (Figueroa and Lunn, 2016). We treated grapevine leaves with sucrose, and we observed an early (after 1 hr) expression activation of *VvTPS1_B*, which is coherent with an activation of T6P biosynthesis. Although an increase in T6P concentration following sucrose treatment is well established, it is yet unclear whether this is due to activation of TPS or inactivation of TPP, and at which levels such processes are modulated. In the case of TPS, post-transcriptional regulation was proposed in Arabidopsis (Yadav *et al*., 2014), but also expression activation has been detected in apple (Du *et al*., 2017) as it was the case in this study. Previous reports show that T6P in turn induces a decrease in sucrose levels in leaves by diverting carbon fluxes

from sucrose to alternative biosynthetic pathways (Figueroa and Lunn, 2016). We correspondingly observed a progressive decrease in sucrose content and an increase in glucose concentration in sucrose-treated leaves. This suggests that in grapevine such a negative feedback of T6P on sucrose may be at least partly due to sucrose hydrolysis, and as a support of this hypothesis we detected a corresponding increase in cell wall invertase expression following sucrose treatment. The negative feedback effect of *VvTPS1_B* on sucrose concentration may be an even more relevant feature of this enzyme when it is considered that its preferential expression site is represented by developing fruit, a strong sink where controlling sucrose concentration may be essential in order to allow sustained phloem unloading.

Compared to *VvTPS1_B*, the yet undescribed *VvTPS1_A* shows an important N-terminal deletion, which includes the 80 nt N-terminal extension typical of several proven biosynthetic TPS1 genes (Fernandez *et al*., 2012). By testing TPS variants N-term truncated at the N term, van Dijck et al (2002) and Li *et al*. (2011) showed increased TPS activity and concluded that this N-terminal sequence may have a regulatory and autoinhibitory role. In Arabidopsis, the *AtTPS2* and *AtTPS4* proteins lack this N-terminal extension and were proven as functional biosynthetic enzymes (Delorge *et al*., 2015). In the case of *VvTPS1_A*, the N-terminal deletion includes not only this N-terminal extension, but also part (about 200 nt) of the TPS domain, and as a consequence this isoform lacks several of the conserved residues required for G6P binding described by Fernandez *et al*. (2012) and by Du *et al*. (2017). *VvTPS1_A* is the main Class I gene expressed in leaf, while *VvTPS1_B* is mostly expressed in immature fruit. Furthermore, *VvTPS1_A* expression is not activated by sucrose treatment. These observations suggest that *VvTPS1_A*, notwithstanding its deletion in the TPS domain, may represent a potentially active and not sucrose-regulated *TPS* biosynthetic gene expressed in leaves. A further hypothesis is that *VvTPS1_A* may cooperate with *VvTPS1_B*, possibly by contributing to binding of UDP-Glc, as several of the

residues required for binding this molecule (Du et al., 2017) are retained in its TPS domain. Additional analyses will be necessary to the confirm TPS activity and the possible interactions of these two putative biosynthetic grapevine proteins.

Several studies have shown that overexpression of plant (Avonce *et al*., 2004; Li *et al*., 2011) or yeast (Lee *et al*., 2003; Kondrák *et al*., 2012; Liu *et al*., 2015) *TPS* biosynthetic genes enhances drought stress tolerance in plants. The molecular mechanisms underlying this effect are however still debated. Accumulation of trehalose, which has an osmoprotective role in yeast, is very limited in plants overexpressing nuclear *TPS*, ruling out such a function (Lee *et al*., 2003; Avonce *et al*., 2004). An alternative hypothesis is that *TPS* overexpression may induce downstream effects through a modulation of T6P concentration, which has well known regulatory effects on cell metabolism (Avonce *et al*., 2004). A light-activated analogue of T6P (Griffiths *et al*., 2016), which proved effective not only in enhancing carbon allocation to wheat seed, but also in helping recovery from drought, supports this hypothesis. However, Arabidopsis lines with altered expression levels of trehalase do not show a consistent relationship between dehydration tolerance and T6P concentration (van Houtte *et al*., 2013), suggesting that TPS may affect drought stress tolerance by other, still unknown mechanisms, possibly involving modified ABA sensitivity (Avonce *et al*., 2004).

In this work, we exposed grapevine plants to progressive drought stress followed by recovery. Leaf sucrose content decreased with increasing stress confirming previous data (Cramer *et al*., 2007), and its concentration remained low also during relief from stress (recovery), suggesting plants used sucrose to help recovering by metabolizing through sucrose synthase and invertase. Concentrations of glucose however were littler affected and even increased at the end of the recovery period reflecting a balance of sucrose hydrolysis and continuous drain for metabolic purposes.

In our experiment, *VvTPSs* from Class I are differently regulated during stress and recovery. Expression of the sucrose-independent *VvTPS1_A* is reduced under stress and recovery. Down-regulation of this T6P biosynthetic enzyme, preferentially expressed in leaves, may help avoiding excessive sucrose metabolism and maintaining sucrose available for phloem loading in source leaves. Trehalose-mediated tolerance to drought stress, if any in grapevine, would in this case be controlled by downstream genes such as TPP or trehalase. On the contrary, the preferentially sink-expressed *VvTPSI_B* is not affected by drought stress, and this would avoid SnRK1-mediated alterations of fruit growth under drought stress. Such a scenario, where leaves would direct as much available sucrose to phloem loading as possible while sink growth would not be affected, well fits with the established positive effects of moderate drought stress on fruit development, ripening, and secondary metabolite accumulation in grapevine, which take place while at the same time vegetative growth is limited (Castellarin *et al*, 2007).

The function of Class II genes has not been completely elucidated yet. In *A. thaliana*, Class II *TPS* genes are differentially expressed in tissues during plant development, and in grapevine, we observed also time and tissue specific expression: flower development and fruit set show highest expression of *VvTPS5* and *VvTPS7_BC*, whilst *VvTPS7A*, *VvTPS9* and *VvTPS10* appear to be involved in berry development. *AtTPS5* positively influences thermotolerance in *A. thaliana* (Suzuki *et al*., 2008), thus its involvement during flower-fruit transition becomes even more important in this delicate phase. *VvTPS6* and *VvTPS8_AB* expression is particularly high in stem tissue. The homologous gene in Arabidopsis, *AtTPS6*, regulates plant architecture and cellular morphogenesis (Chary *et al*., 2008). We also observed some functional conservation between homologous Arabidopsis and grapevine genes under sucrose treatment, notably a positive correlation with sucrose concentration for *VvTPS5*, and a negative one for *VvTPS_10* (Ramon *et al*., 2009). Molecular networks may link the proteins

from the two classes. In Arabidopsis and in rice, researchers confirmed that both *AtTPS1* and *OsTPS1* are predominantly present in protein complexes (Geelen *et al*., 2007; Zang *et al*., 2011) which include TPS II proteins. In rice, for example, *OsTPS5* and *OsTPS8* directly interact with *OsTPS1*, suggesting for genes of Class II a role in T6P biosynthesis modulation. Co-expression patterns are also visible in our data set: for example, in both sucrose and drought treatment, *VvTPS1_A* and *VvTPS_5* followed a common expression pattern, always positively correlated with sucrose concentration. The other *TPS* II genes follow expression patterns not consistently linked to any putative T6P biosynthetic gene and could play other regulatory roles.

The Class II genes follow different expression patterns under water stress and recovery. The sucrose-dependent *VvTPS5* is down-regulated during the recovery. All the other Class II genes can be divided into two groups, based on their expression patterns. *VvTPS6, VvTPS9* and *VvTPS8_AB* respond to drought as *VvTPS5*, so under stress they could support *VvTPS1* activity. Other three Class II genes, *VvTPS7_A, VvTPS7_BC* and *VvTPS10,* are on the contrary significantly overexpressed after 13 days of water stress but not under recovery. Such a behaviour of *VvTPS_10* was observed in previous RNA-seq analyses conducted in two grapevine differently cultivars *VvTPS10* (Dal Santo *et al*., 2016) and agrees with the negative effect of sucrose levels on its expression.

5. Conclusions

Our results demonstrate the involvement of *TPS* genes at different stages of development in grapevine, as previously documented for other plant species. Since our data suggest *TPSs* play a crucial role in tissue differentiation, studying their activity as development regulators is worthy further investigation.

We show that drought and following recovery modulated *TPS* gene transcription. Biosynthetic Class I *TPS* genes are thus candidates for driving

responses to drought stress. Moreover, our results strengthen the hypothesis that Class II genes are involved in responses to drought, by co-operating or interacting with biosynthetic genes. Given the established connection between TPS activity and regulation of soluble carbohydrate metabolism, these results suggest that TPS proteins cross-link plant metabolism and stress signaling, acting as powerful regulator genes.

This work provides novel tools for further exploring the role of *TPS* gene family in stress responses, and for better understanding the role of Class II *TPS* genes.

References

Avonce, N., Leyman, B., Mascorro-Gallardo, J.O., van Dijck, P., Thevelein, J.M., Iturriaga, G., 2004. The Arabidopsis Trehalose-6-P Synthase *AtTPS1* Gene Is a Regulator of Glucose, Abscisic Acid, and Stress Signaling. Plant Physiology **136**. https://doi.org/10.1104/pp.104.052084

Blázquez, M.A., Santos, E., Flores, C., Martínez-Zapater, J.M., Salinas, J., Gancedo, C., 1998. Isolation and molecular characterization of the *Arabidopsis TPS1* gene, encoding trehalose-6-phosphate synthase. The Plant Journal **13**. https://doi.org/10.1046/j.1365-313X.1998.00063.x

Brumfield G, 2004. Cell Biology: just add water. Nature **428**, 14–15.

Carra, A., Gambino, G., Schubert, A., 2007. A cetyltrimethylammonium bromide based method to extract low-molecular-weight RNA from polysaccharide-rich plant tissues. Analytical Biochemistry **360**. https://doi.org/10.1016/j.ab.2006.09.022

Castellarin S, Pfeiffer A., Sivilotti P., Degan M, Peterlunger E, Di Gaspero G, 2007. Transcriptional regulation of anthocyanin biosynthesis in ripening fruits of grapevine under seasonal water deficit. Plant, Cell, and Environment **30**:1381-1399. doi: 10.1111/j.1365-3040.2007.01716.x

Chary, S.N., Hicks, G.R., Choi, Y.G., Carter, D., Raikhel, N. v., 2008. Trehalose-6-Phosphate Synthase/Phosphatase Regulates Cell Shape and Plant Architecture in Arabidopsis. Plant Physiology **146**. https://doi.org/10.1104/pp.107.107441

Cramer, G.R., Ergül, A., Grimplet, J., Tillett, R.L., Tattersall, E.A.R., Bohlman, M.C., Vincent, D., Sonderegger, J., Evans, J., Osborne, C., Quilici, D., Schlauch, K.A., Schooley, D.A., Cushman, J.C., 2007. Water and salinity stress in grapevines: early and late changes in transcript and metabolite profiles. Functional & Integrative Genomics**7**. https://doi.org/10.1007/s10142-006-0039-y

Dai, Z.W., Léon, C., Feil, R., Lunn, J.E., Delrot, S., Gomès, E., 2013. Metabolic profiling reveals coordinated switches in primary carbohydrate metabolism in grape berry (*Vitis vinifera* L.), a non-climacteric fleshy fruit. Journal of Experimental Botany 64. https://doi.org/10.1093/jxb/ers396

Dal Santo, S., Palliotti, A., Zenoni, S., Tornielli, G.B., Fasoli, M., Paci, P., Tombesi, S., Frioni, T., Silvestroni, O., Bellincontro, A., d'Onofrio, C., Matarese, F., Gatti, M., Poni, S., Pezzotti, M., 2016. Distinct transcriptome responses to water limitation in isohydric and anisohydric grapevine cultivars. BMC Genomics **17**. https://doi.org/10.1186/s12864-016-3136-x

Delatte, T.L., Sedijani, P., Kondou, Y., Matsui, M., de Jong, G.J., Somsen, G.W., Wiese-Klinkenberg, A., Primavesi, L.F., Paul, M.J., Schluepmann, H., 2011. Growth Arrest by Trehalose-6-Phosphate: An Astonishing Case of Primary Metabolite Control over Growth by Way of the SnRK1 Signaling Pathway. Plant Physiology **157**. https://doi.org/10.1104/pp.111.180422

Delorge, I., Figueroa, C.M., Feil, R., Lunn, J.E., van Dijck, P., 2015. Trehalose-6-phosphate synthase 1 is not the only active TPS in Arabidopsis thaliana. Biochemical Journal **466**. https://doi.org/10.1042/BJ20141322

Du, L., Qi, S., Ma, J., Xing, L., Fan, S., Zhang, S., Li, Y., Shen, Y., Zhang, D., Han, M., 2017. Identification of TPS family members in apple (Malus x domestica Borkh.) and the effect of sucrose sprays on TPS expression and floral induction. Plant Physiology and Biochemistry **120**. https://doi.org/10.1016/j.plaphy.2017.09.015

Fernandez, O., Vandesteene, L., Feil, R., Baillieul, F., Lunn, J.E., Clément, C., 2012. Trehalose metabolism is activated upon chilling in grapevine and might participate in *Burkholderia phytofirmans* induced chilling tolerance. Planta **236**. https://doi.org/10.1007/s00425-012-1611-4

Figueroa, C.M., Lunn, J.E., 2016. A Tale of Two Sugars: Trehalose 6-Phosphate and Sucrose. Plant Physiology **172**. https://doi.org/10.1104/pp.16.00417

Geelen, D., Royackers, K., Vanstraelen, M., de Bus, M., Inzé, D., van Dijck, P., Thevelein, J.M., Leyman, B., 2007. Trehalose-6-P synthase *AtTPS1* high molecular weight complexes in yeast and Arabidopsis. Plant Science **173**. https://doi.org/10.1016/j.plantsci.2007.07.002

Goddijn, O., van Dun, K., 1999. Trehalose metabolism in plants. Trends in Plant Science **4**. https://doi.org/10.1016/S1360-1385(99)01446-6

Griffiths, C.A., Sagar, R., Geng, Y., Primavesi, L.F., Patel, M.K., Passarelli, M.K., Gilmore, I.S., Steven, R.T., Bunch, J., Paul, M.J., Davis, B.G., 2016.

Chemical intervention in plant sugar signalling increases yield and resilience. Nature **540**. https://doi.org/10.1038/nature20591

Hochberg, U., Degu, A., Toubiana, D., Gendler, T., Nikoloski, Z., Rachmilevitch, S., Fait, A., 2013. Metabolite profiling and network analysis reveal coordinated changes in grapevine water stress response. BMC Plant Biology **13**. https://doi.org/10.1186/1471-2229-13-184

Jang, I.-C., Oh, S.-J., Seo, J.-S., Choi, W.-B., Song, S.I., Kim, C.H., Kim, Y.S., Seo, H.-S., Choi, Y. do, Nahm, B.H., Kim, J.-K., 2003. Expression of a Bifunctional Fusion of the *Escherichia coli* Genes for Trehalose-6-Phosphate Synthase and Trehalose-6-Phosphate Phosphatase in Transgenic Rice Plants Increases Trehalose Accumulation and Abiotic Stress Tolerance without Stunting Growth. Plant Physiology **131**. https://doi.org/10.1104/pp.007237

Kondrák, M., Marincs, F., Antal, F., Juhász, Z., Bánfalvi, Z., 2012. Effects of yeast trehalose-6-phosphate synthase 1 on gene expression and carbohydrate contents of potato leaves under drought stress conditions. BMC Plant Biology **12**. https://doi.org/10.1186/1471-2229-12-74

Kumar, S., Stecher, G., Li, M., Knyaz, C., Tamura, K., 2018. MEGA X: Molecular Evolutionary Genetics Analysis across Computing Platforms. Molecular Biology and Evolution **35**. https://doi.org/10.1093/molbev/msy096

Lee, S.-B., Kwon, H.-B., Kwon, S.-J., Park, S.-C., Jeong, M.-J., Han, S.-E., Byun, M.-O., Daniell, H., 2003. Accumulation of trehalose within transgenic chloroplasts confers drought tolerance. Molecular Breeding **11**. https://doi.org/10.1023/A:1022100404542

Li, H.-W., Zang, B.-S., Deng, X.-W., Wang, X.-P., 2011. Overexpression of the trehalose-6-phosphate synthase gene *OsTPS1* enhances abiotic stress tolerance in rice. Planta **234**. https://doi.org/10.1007/s00425-011-1458-0

Liu, Y., Han, L., Qin, L., Zhao, D., 2015. Saccharomyces cerevisiae gene TPS1 improves drought tolerance in *Zea mays* L. by increasing the expression of SDD1 and reducing stomatal density. Plant Cell, Tissue and Organ Culture (PCTOC) **120**. https://doi.org/10.1007/s11240-014-0647-5

Lunn, J.E., 2007. Gene families and evolution of trehalose metabolism in plants. Functional Plant Biology **34**. https://doi.org/10.1071/FP06315

Ma, J., Hanssen, M., Lundgren, K., Hernández, L., Delatte, T., Ehlert, A., Liu, C. M., Schluepmann, H., Dröge-Laser, W., Moritz, T., Smeekens, S., Hanson, J., 2011. The sucrose-regulated Arabidopsis transcription factor bZIP11 reprograms metabolism and regulates trehalose metabolism. New Phytologist **191**. https://doi.org/10.1111/j.1469-8137.2011.03735.x

Mu, M., Lu, X.-K., Wang, J.-J., Wang, D.-L., Yin, Z.-J., Wang, S., Fan, W.-L., Ye, W.-W., 2016. Genome-wide Identification and analysis of the stress-resistance function of the TPS (Trehalose-6-Phosphate Synthase) gene family in cotton. BMC Genetics 17. https://doi.org/10.1186/s12863-016-0360-y

Nietzsche, M., Landgraf, R., Tohge, T., Börnke, F., 2016. A protein–protein interaction network linking the energy-sensor kinase SnRK1 to multiple signaling pathways in *Arabidopsis thaliana*. Current Plant Biology 5. https://doi.org/10.1016/j.cpb.2015.10.004

Ramon, M., De Smet, I., Vandesteene, L., Naudts, M., Leyman, B., Van Dijck, P., Rolland, F., Beeckman, T., Thevelein, J.M., 2009. Extensive expression regulation and lack of heterologous enzymatic activity of the Class II trehalose metabolism proteins from *Arabidopsis thaliana*. Plant, Cell & Environment **32**. https://doi.org/10.1111/j.1365-3040.2009.01985.x

Schubert, A., Wyss, P., Wiemken, A., 1992. Occurrence of trehalose in vesicular arbuscular mycorrhizal fungi and in mycorrhizal roots. Journal of Plant Physiology **140**. https://doi.org/10.1016/S0176-1617(11)81054-0

Suzuki, N., Bajad, S., Shuman, J., Shulaev, V., Mittler, R., 2008. The Transcriptional Co-activator MBF1c Is a Key Regulator of Thermotolerance in *Arabidopsis thaliana*. Journal of Biological Chemistry **283**. https://doi.org/10.1074/jbc.M709187200

Vandesteene, L., López-Galvis, L., Vanneste, K., Feil, R., Maere, S., Lammens, W., Rolland, F., Lunn, J.E., Avonce, N., Beeckman, T., van Dijck, P., 2012. Expansive Evolution of the TREHALOSE-6-PHOSPHATE PHOSPHATASE Gene Family in Arabidopsis. Plant Physiology **160**. https://doi.org/10.1104/pp.112.201400

Vandesteene, L., Ramon, M., le Roy, K., van Dijck, P., Rolland, F., 2010. A Single Active Trehalose-6-P Synthase (TPS) and a Family of Putative Regulatory TPS Like Proteins in Arabidopsis. Molecular Plant **3**. https://doi.org/10.1093/mp/ssp114

Van Dijck, P., Mascorro-Gallardo, J. O., De Bus, M., Royackers, K., Iturriaga, G., & Thevelein, J. M. (2002). Truncation of Arabidopsis thaliana and *Selaginella lepidophylla* trehalose-6-phosphate synthase unlocks high catalytic activity and supports high trehalose levels on expression in yeast. The Biochemical journal, **366**(Pt 1), 63–71. https://doi.org/10.1042/BJ20020517

Van Houtte, H., Vandesteene, L., López-Galvis, L., Lemmens, L., Kissel, E., Carpentier, S., Feil, R., Avonce, N., Beeckman, T., Lunn, J.E., van Dijck, P., 2013. Overexpression of the Trehalase Gene *AtTRE1* Leads to Increased Drought Stress Tolerance in Arabidopsis and Is Involved in Abscisic Acid Induced Stomatal Closure. Plant Physiology **161**. https://doi.org/10.1104/pp.112.211391

Xie, D.W., Wang, X.N., Fu, L.S., Sun, J., Zheng, W., Li, Z.F., 2015. Identification of the trehalose-6-phosphate synthase gene family in winter wheat and expression analysis under conditions of freezing stress. Journal of Genetics **94**. https://doi.org/10.1007/s12041-015-0495-z

Yadav, U.P., Ivakov, A., Feil, R., Duan, G.Y., Walther, D., Giavalisco, P., Piques, M., Carillo, P., Hubberten, H.-M., Stitt, M., Lunn, J.E., 2014. The sucrose trehalose-6-phosphate (Tre6P) nexus: specificity and mechanisms of sucrose signalling by Tre6P. Journal of Experimental Botany **65**. https://doi.org/10.1093/jxb/ert457

Yang, H.-L., Liu, Y.-J., Wang, C.-L., Zeng, Q.-Y., 2012. Molecular Evolution of Trehalose-6-Phosphate Synthase (TPS) Gene Family in Populus, Arabidopsis and Rice. PLoS ONE **7**. https://doi.org/10.1371/journal.pone.0042438

Zang, B., Li, H., Li, W., Deng, X.W., Wang, X., 2011. Analysis of trehalose-6 phosphate synthase (TPS) gene family suggests the formation of TPS complexes in rice. Plant Molecular Biology **76**. https://doi.org/10.1007/s11103-011-9781-1

Zhang, Y., Primavesi, L.F., Jhurreea, D., Andralojc, P.J., Mitchell, R.A.C., Powers, S.J., Schluepmann, H., Delatte, T., Wingler, A., Paul, M.J., 2009. Inhibition of SNF1-Related Protein Kinase1 Activity and Regulation of Metabolic Pathways by Trehalose-6-Phosphate. Plant Physiology **149**. https://doi.org/10.1104/pp.108.133934

CHAPTER III

Flavescence dorée phytoplasma-grapevine interaction: novel insights on sucrose metabolism and signalling involvement

Cristina Morabito

Thomas Roitsch, Andrea Schubert

Summary

Flavescence dorée, an epidemic disease caused by FD phytoplasma (FDp) infection, is one of the main causes of yield losses in European viticulture. Knowledge on molecular mechanisms influencing the FDp-grapevine interaction is still highly limited and debated.

Aim of this work was to investigate the role of sucrose metabolism and signalling in potentially conferring tolerant behaviours against FDp, through two parallel strategies. Direct involvement of sucrose was assessed by exposing field-grown grapevines to exogenous applications of sucrose solution. We performed foliar spray and trunk infusion treatments on both FDp-infected and healthy plants. On the other side, three FDp-tolerant *Vitis vinifera* varieties (Merlot, Brachetto and Moscato) were analysed in comparison to the highly susceptible cultivar Barbera. Carbohydrate-related enzyme and gene activities were measured and evaluated in both experiments, confirming the crucial role carbohydrate metabolism and signalling in FDp-grapevine interaction. Obtained results revealed that in FDp-infected plants treated with sucrose infusion and in tolerant varieties, trehalose-6-phosphate (T6P) metabolism and signaling was enhanced, together with cell wall invertase activation. Considering that both T6P and cell wall invertase have a documented role in helping plants overcoming stresses, future work will be useful to further elucidate involvement of these pathways.

1. Introduction

Flavescence dorée is an epidemic disease, caused by FD phytoplasma (FDp) infection, which widely affects European viticulture yields in terms of quantity and quality (EFSA Panel on Plant Health, 2014). The leafhopper *Scaphoideus titanus* Ball (Schvester *et al*., 1963) is renowned to be the principal vector for grapevine (Chuche and Thiéry, 2014). FDp is a quarantine pathogen in Europe (EPPO list A2) and, at the current moment, only indirect approaches are available to limit its spread (use of certified phytoplasma-free propagation material, removal of infected plants from the vineyard and management of insect vectors). Phytoplasma colonization of sieve elements causes a wide range of alterations in terms of vine physiology (Vitali *et al*., 2013) and metabolism (Gambino *et al*., 2013; Pagliarani *et al*., 2020). Symptoms, such as leaf vein reddening, floral abortion and lack of shoot lignification, occur and worsen along the vegetative season, causing yield reduction or even plant death. Nevertheless, FDp-infected plants can undergo recovery (Caudwell A., 1961; Morone *et al*., 2007), a natural symptom regression connected to a decreasing phytoplasma titre. Recovery in grapevine appears to be linked to different geographical localization (Morone *et al*., 2007), and to be cultivar-dependent. Based on existing literature, all varieties are susceptible to infection, albeit showing different grade of severity (Eveillard *et al*., 2016; Kuzmanovic *et al*., 2008). A recent study conducted on a large group of grapevine genotypes representative of Piedmontese region designated Brachetto and Moscato as the two more tolerant cultivars, while Barbera 84 was confirmed to be the most susceptible one (Ripamonti *et al*., 2020) Diverse genotype susceptibility is also positively correlated to different FDp loads (Galetto *et al*., 2014; Roggia *et al*., 2014). Field observations integrated by molecular diagnostic analyses lead to the assumption that highly susceptible cultivars are more prone to recover from infection (Pagliarani *et al*., 2020). Still, it should be also underlined that recovered plants could be subjected to re-infection phenomena (Pegoraro *et al*., 2017).

FDp infection is responsible for an extensive reprogramming of the entire plant machinery, on a physiological (Vitali *et al*., 2013) and metabolic point of view. Pathogen infections are commonly linked to alterations of soluble carbohydrate (SC) concentrations. Studies on FDp colonization confirmed this rule. Indeed, phytoplasmas utilize plant phosphorylated hexoses as main source of energy (Prezelj *et al*., 2016). Previous studies, mainly conducted on *Bois Noir*, a similar grapevine phytoplasma disease, showed how phytoplasmas are able to alter carbohydrate enzymatic activity, with particular reference to enzymes involved in interconversions among phosphorylated sugar forms (phosphoglucomutase, phosphoglucoisomerase, phosphofructokinase, fructokinase) and in sucrose cleavage (sucrose synthase and invertase). On the plant side, changes of primary metabolism may represent a signal inducing immunity (Delaney, 1997; Yoshida *et al*., 2002). Specific knowledge of the role of soluble sugars on FDp infection and recovery-associated molecular mechanisms is still limited and worthy further investigation.

In this work, we focused on the connection between SC concentration and metabolism, and the tolerance of grapevine towards FD. To this aim, we first analysed the carbohydrate status and the expression and activity of enzymes involved in SC metabolism in leaves of grapevine cultivars showing different degrees of tolerance to FD. We show that the tolerant Brachetto, Moscato (Pegoraro *et al*., 2020), and Merlot (Eveillard *et al*., 2016) have higher content of sucrose than the sensitive Barbera, and that they show increased activity and expression of enzymes linked to soluble carbohydrate metabolism.

Second, we exposed vineyard-grown FDp-infected and healthy grapevines to exogenous sucrose treatments (foliar spraying and trunk injection). Results suggest that sucrose application was effective in enhancing SC-related enzyme activity and expression, particularly on diseased plants. The two treatments however influenced SC metabolism in an opposite and complementary way, probably due to the difference in sucrose uptake pathways and localization

in the plant and its consequent availability to the pathogen. Finally, we discuss the potential role of SC in triggering tolerance against the pathogen.

2. Materials and methods

2.1 Experimental set up: plant material and sample collection

In order to assess molecular and biochemical aspects putatively involved in conferring a different level of tolerance against *Flavescence dorée*, *Vitis vinifera* cuttings belonging to the cultivars Barbera (susceptible), Merlot, Brachetto and Moscato (tolerant) were grafted onto Kober 5BB rootstocks and grown in 30L pots in a screenhouse in order to avoid FDp infection. Pooled leaf samples (six fully expanded leaves) were collected on the 30th of August 2019 from five plants per genotype (Fig. 1).

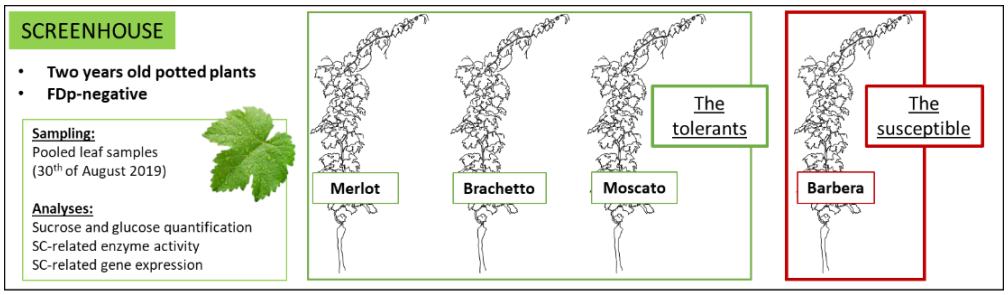

Fig. 1 – Varietal screening experiment setup.

In order to assess the effect of treatment with exogenous sucrose, negative control and FDp-positive grapevines cv Barbera grown in the experimental vineyard (Istituto "Giovanni Penna") located in Asti (44°55'18.33"N – 8°11'44.05"E) and selected based on diagnostic analysis performed on 1st July, were exposed to two different types of sucrose treatment in two separated experiments, respectively based on i) trunk infusion, and ii) leaf

spraying. Each type of treatment was applied twice (spaced two weeks) with the aim of strengthening the effect, and sampling was performed after the second application.

In the infusion treatment, performed on the 15th and on the 31st of July 2019, a 5% sucrose solution was directly injected into the xylem of both heathy and FDp-infected plants by using a manual, drill-free instrument recently developed by the University of Padua in Italy (Bite® - Blade for Infusion in TrEes; https://drp.bio/en/what-we-do/tree-care-en/bite-tree-care/; Fig. 2 and 3). A small lenticular shaped perforated blade enters the trunk by simply separating wood fibres (fig. 2), reducing the perforation damage. The solution uptake works through regular plant transpiration, avoiding cavitation problems due to traditional pressure injection. Ten FDp-positive and ten FDp-negative plants were used.

Fig. 2 – A representation of the lenticular shaped perforated blade on the left. On the right, the infusion treatment in progress.

The leaf spraying treatment was performed on a different group of plants on 1 and 14 August 2019. A 1% sucrose solution was sprayed on the canopy of six FDp-infected plants and six healthy plants respectively. One hour after treatment, excess sucrose was removed by spraying and rinsing leaves with distilled water.

Six fully expanded, sun-exposed leaves were randomly collected from different points of the canopy of each plant included in the experiments after one and 24 hours from sucrose spraying, and 24 hours and five days after endotherapic infusion. All leaf samples were ground in liquid nitrogen and stored at -80°C in order to perform SC quantification, and SC-related gene expression and enzyme activity analysis.

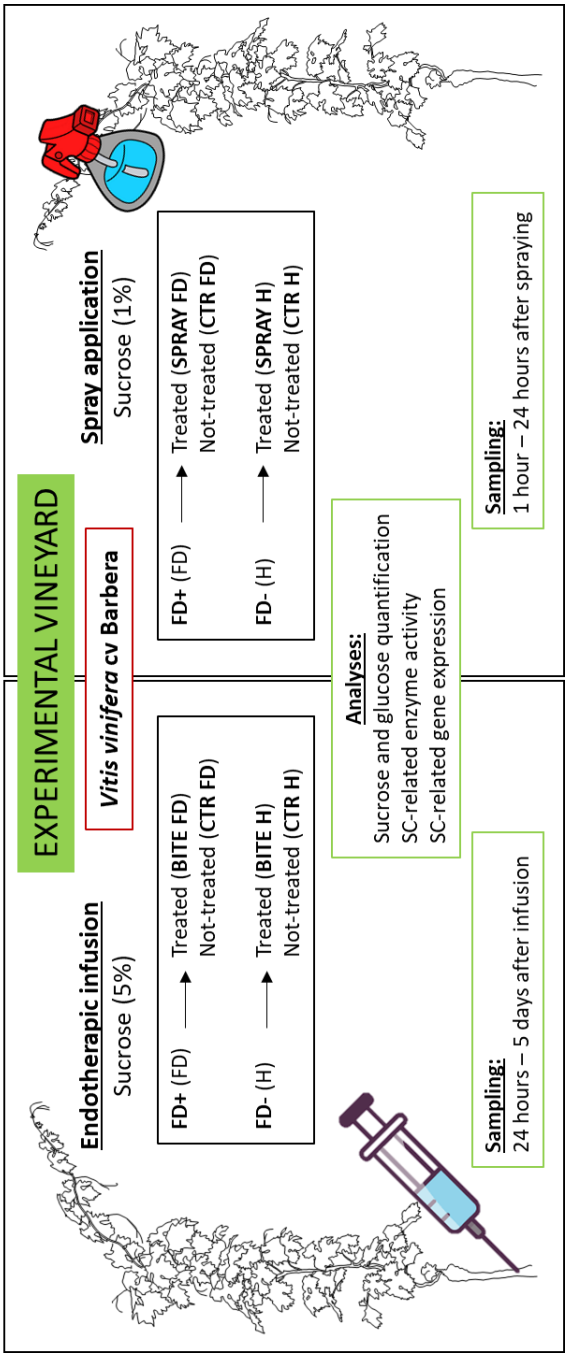

Fig. 3 – Exogenous sucrose application experiments setup.

2.2 Diagnostic analyses

Potted grapevines belonging to the cultivars Barbera, Brachetto, Moscato and Merlot, cultivated under partially controlled conditions (screenhouse) were tested for FDp and *Bois Noir* phytoplasma absence.

In order to assess the presence of FDp, leaves were collected from Barbera grapevines grown in the experimental vineyard (Istituto "Giovanni Penna") located in Asti (44°55'18.33"N – 8°11'44.05"E) on 1st July 2019, before the beginning of the experiment. Symptomatic leaves were preferably chosen. Control plants were also tested to confirm their negativity to FD.

Total DNA was extracted according to Pelletier *et al*. (2009) from 200 mg-aliquots of mid-ribs from five leaves randomly collected from the canopy of each plant. Mid-ribs were collected from fresh leaves and ground in liquid nitrogen. Samples for diagnostic analyses were stored at -80°C until DNA extraction was performed.

The molecular diagnosis was performed using a commercial kit (Detection kit *Flavescence dorée* and *Bois Noir*, Multiplex Real-time PCR system, IPADLAB), through a Real-Time PCR-based assay. A Taq Internal Positive Control IPC (TaqMan® Exogenous Internal Positive Control, Applied Biosystems) was added to the reaction mix, in order to confirm absence of contaminations inhibiting the amplification process.

2.3 Analysis of soluble sugar concentration

25 mg-aliquots of ground leaf tissue were extracted with deionized water for 15 min at 70°C and then centrifuged at 10000 g for 20 min. Glucose concentration was assessed on a fraction of the supernatant using the glucose-oxidase Glucose Assay kit (GAGO-20, Sigma-Aldrich), reading absorbance at 540 nm. Another fraction of the supernatant was used for determination of sucrose concentration, after digesting with 15 units of invertase (I4504, Sigma-Aldrich) and assessing glucose concentration as described above.

2.4 Protein extraction and analysis of SC-related enzyme activity

Protein extraction and purification and SC-related enzymes activity assays were performed following partially modified protocols from Jammer *et al*. (2015) and Covington *et al*. (2016).

Aliquots of 180 mg of ground leaf samples were used to perform protein extraction. In order to reduce phenols and polyphenols contamination, 25% p/p of polyvinylpolypyrrolidone (PVPP) and 25% p/p of Amberlite® XAD4 (Merck/Sigma-Aldrich) were added to each aliquot. The extraction buffer (100 mM KPO_4, 7.5 mM $MgCl_2$, 20 mM $MnCl_2$, 10% glycerol, 1% polyvinylpyrrolidone, 5 mM DTT, 5 mM ascorbate, 5 mM sodium bisulfite) developed by LaFever et al. (1994) for protein extraction in conifers was selected as the most suitable for our purpose and slightly modified.

1,5 ml of extraction buffer was added to each sample, then incubated at 4°C for 40 minutes in continuous shaking. Following centrifugation allowed liquid fraction and pellet separation. Liquid supernatant was pipetted into dialysis tubes and dialysed against 20 mM potassium phosphate buffer (pH 7.4) at 4°C. Dialysis against the same buffer was repeated twice (after two and three hours, the latter continued overnight). The dialyzed supernatant (D-extract) was then collected and stored at -20°C. The pellet was washed with deionized water three times and then re-suspended in 1 ml of high salt buffer (40 mM Tris-HCl pH 7.6, 3 mM $MgCl_2$, 15 Mm EDTA, 1 M NaCl). The mixture was incubated overnight in continuous shaking; the remaining pellet was centrifuged and the resulting supernatant was subjected to dialysis following the same protocol as above. The obtained dialyzed extract (Z-extract) was collected and stored at -20°C.

Protein concentration in the extracts was determined through the Bradford staining method. A flat bottomed 96-well microtitre plate (Sartsted, Germany) was used to perform the assay. D-extracts and Z-extracts were diluted 1:25 and 1:50 respectively, in a final volume of 100 µl. The analysis was

performed in four technical replicates. A bovine serum albumin (BSA, Sigma-Aldrich) standard curve was used for protein quantification. 150 µl of Bradford staining solution was added to each replicate and to the standard curve in the microtitre plate, then incubated for 20 minutes at room temperature. Absorbance of the samples was read at 630 nm at room temperature using a plate reader (Bio Tek).

Cell-wall, cytosolic and vacuolar invertase activity

20 µl of Z–extract and 20 µl of D-extract were respectively used to assess cell-wall (CWInv) and cytosolic and vacuolar invertase (CytInv, VacInv) activity in leaf, through an end-point measurement. The reaction was performed by adding 5 µl of reaction buffer pH 4.5 (454 mM Na_2HPO_4/273 mM citric acid) for cell-wall and vacuolar invertase and pH 6.8 (772 mM Na_2HPO_4/114 mM citric acid) for cytosolic invertase, 5 µl of sucrose 0.1 M and 20 µl of deionized water in a final reaction volume of 50 ul. Each sample was pipetted in three technical replicates in a 96-well plate (Sartsted, Germany) and one control replicate lacking substrate (sucrose). A glucose standard curve (0-50 nmol) was used to estimate enzymatic activity. The reaction mix was incubated at 37°C for 30 minutes and then cooled down on ice for 5 minutes. 200 µl of GOD-POD solution (10 U ml^{-1} GOD, 0,8 U ml-1 POD, 0,8 mg ml^{-1} ABTS in 0.1 M potassium phosphate buffer, pH 7.0) were added to each well (including the standard curve). After 20 minutes of incubation at room temperature, absorbance was measured at a wavelength of 405 nm. Specific enzymatic activity was expressed as nkat mg $protein^{-1}$.

Sucrose synthase activity

Sucrose synthase (Susy) activity was measured through a two reaction -based protocol. In the first reaction, 1 mM UDP was included in order to detect both Susy and cytInv background activity, while the second reaction, performed

without 1 mM UDP, detected only the cytInv background activity. Final Susy activity was estimated by subtracting cytInv background activity from total activity, measured in the first reaction. 20 µl-aliquots of D-extract were added to 160 µl of reaction buffer (1 mM EDTA, 2 mM $MgCl_2$, 5mM DTT, 250 mM sucrose, 1 mM UDP -exclusively in the first reaction mix-, 1.3 mM ATP, 0.5 mM NAD, 0.672 U of hexokinase, 0.56 U of phosphoglucoisomerase, 0.32 U of glucose 6-phosphate dehydrogenase in 50 mM HEPES/NaOH at pH 7.0) in both reactions. The analyses was performed in three technical replicates and sucrose was omitted in control reactions. 96-well flat-bottomed UV-Star microtitre plates (Greiner Bio One, Austria) were used for these assays.

The reaction was carried out at 50°C and the increase in absorbance at 340 nm due to conversion of NAD to NADH was monitored every 30 s throughout the incubation using a plate reader (Bio Tek). Specific enzymatic activity was expressed as nkat mg $protein^{-1}$.

Phosphoglucomutase activity

In order to determine phosphoglucomutase (PGM) activity, 5 µl of D-extract from each sample were incubated with 10 mM $MgCl_2$, 4 mM DTT, 0.1 mM glucose1,6-bisphosphate (G1,6bisP), 1 mM glucose 1-phosphate (G1P), 0.25 U NADP, 0.64 U G6PDH in 20 mM Tris-HCl at pH 8.0. The analyses was performed in three technical replicates and the substrate, G1P, was omitted in control reactions. 96-well flat-bottomed UV-Star microtitre plates (Greiner Bio One, Austria) were used for these assays. The reaction was carried out at 50°C and the increase in absorbance at 340 nm due to conversion of NAD to NADH was monitored every 30 s throughout the incubation using a plate reader (Bio Tek). Specific enzymatic activity was expressed as nkat mg $protein^{-1}$.

Phosphoglucoisomerase activity

For phosphoglucoisomerase (PGI) activity measurement the reagent buffer modified from Zhou and Cheng (2008) (4 mM $MgCl_2$, 4 mM DTT, 2mM fructose-6-phosphate (F6P), 0.25 mM NAD, 0.32 mM G6PDH in 100 mM Tris-HCl at pH 8.0) was added to 5 µl of D-extract. F6P was omitted in control reactions. 96-well flat-bottomed UV-Star microtitre plates (Greiner Bio One, Austria) were used for these assays. The reaction was carried out at 50°C and the increase in absorbance at 340 nm due to conversion of NAD to NADH was monitored every 30 s throughout the incubation using a plate reader (Bio Tek). Specific enzymatic activity was expressed as nkat mg $protein^{-1}$.

Hexokinase activity

Hexokinase (HXK) activity was estimated incubating 20 µl of D-extract with 5 mM $MgCl_2$, 5 mM glucose (omitted in control reactions), 2.5 mM ATP, 1 mM NAD, 0,8 U of G6PDH in 50 mM BisTris at pH 8.0. 96-well flat-bottomed UV-Star microtitre plates (Greiner Bio One, Austria) were used for these assays. The reaction was carried out at 50°C and the increase in absorbance at 340 nm due to conversion of NAD to NADH was monitored every 30 s throughout the incubation using a plate reader (Bio Tek). Specific enzymatic activity was expressed as nkat mg $protein^{-1}$.

Glucose 6-phosphate dehydrogenase activity

For determination of glucose 6-phosphate dehydrogenase (G6PDH) activity, 20 µl of D-extract were incubated with 5 mM $MgCl_2$, 1 mM G6P, 0.4 mM NADP in 100 mM Tris-HCl at pH 7.6. G6P was omitted in control reactions. 96-well flat-bottomed UV-Star microtitre plates (Greiner Bio One, Austria) were used for these assays. The reaction was carried out at 50°C and the increase in absorbance at 340 nm due to conversion of NAD to NADH was

monitored every 30 s throughout the incubation using a plate reader (Bio Tek). Specific enzymatic activity was expressed as nkat mg protein^{-1}.

ADP-glucose pyrophosphorylase activity

20 µl-aliquots of D-extract were incubated with 0.44 mM EDTA, 5 mM $MgCl_2$, 0.1% BSA, 2 mM ADP-glucose (not included in control reactions), 1.5 mM PPi, 1 mM NADP, 2 mM 3-PG, 0.432 U of PGM and 1.28 U of G6PDH in 100 mM Tris-HCl at pH 8.0 to evaluate ADP-glucose pyrophosphorylase (AGPase) activity. 96-well flat-bottomed UV-Star microtitre plates (Greiner Bio One, Austria) were used for these assays. The reaction was carried out at 50°C and the increase in absorbance at 340 nm due to conversion of NADP to NADPH was monitored every 30 s throughout the incubation using a plate reader (Bio Tek). Specific enzymatic activity was expressed as nkat mg protein^{-1}.

Aldolase activity

Aldolase (Ald) activity was measured adding 10 µl of D-extract to a reaction buffer composed by 1 mM EDTA, 5 mM $MgCl_2$, 1 mM F1,6bisP, 0.15 mM NADH, 0.48 U of TPI, 0.8 U of GPDH in 50 mM Tris-HCl at pH 8.0. The substrate, F1,6bisP, was not included in the mix for control reactions. 96-well flat-bottomed UV-Star microtitre plates (Greiner Bio One, Austria) were used for these assays. The reaction was carried out at 50°C and the decrease in absorbance at 340 nm due to conversion of NADH to NAD was monitored every 30 s throughout the incubation using a plate reader (Bio Tek). Specific enzymatic activity was expressed as nkat mg protein^{-1}.

Fructokinase activity

Incubation of 20 µl of D-extract with a reaction buffer prepared in 50 mM BisTris at pH 8.0 (5 mM $MgCl_2$, 5 mM fructose, 2.5 mM ATP, 1 mM NAD, 0.8

U of PGI and 0.8 U of G6PDH) allowed the determination of fructokinase (FK) activity. Fructose was omitted for control reactions. 96-well flat-bottomed UV-Star microtitre plates (Greiner Bio One, Austria) were used for these assays. The reaction was carried out at 50°C and the increase in absorbance at 340 nm due to conversion of NAD to NADH was monitored every 30 s throughout the incubation using a plate reader (Bio Tek). Specific enzymatic activity was expressed as nkat mg protein^{-1}.

Phosphofructokinase activity

Phosphofructokinase (PFK) activity was estimated by incubating 10 µl of D-extract with 1 mM EDTA, 5 mM MgCl2, 1 mM fructose 6-phosphate, 0.15 mM NADH, 0.2 mM ATP, 0.16 U aldolase, 0.8 U glycerol 3-phosphate dehydrogenase, 0.48 U TPI in 50 mM Tris-HCl at pH 8.0. Fructose 6-phosphate was omitted in control reactions. 96-well flat-bottomed UV-Star microtitre plates (Greiner Bio One, Austria) were used for these assays. The reaction was carried out at 50°C and the decrease in absorbance at 340 nm due to conversion of NADH to NAD was monitored every 30 s throughout the incubation using a plate reader (Bio Tek). Specific enzymatic activity was expressed as nkat mg protein^{-1}.

UDP-glucose pyrophosphorylase activity

In order to determine UDP-glucose pyrophosphorylase (UGPase) activity, 20 µl of D-extract were added to a reaction buffer in 100 mM Tris-HCl at pH 8.0 (0.44 mMEDTA, 5 mM $MgCl_2$, 0.1% BSA, 2 mM UDP-glucose, 1.5 mM PPi, 1 mM NADP, 2 mM 3-PG, 0.432 U of PGM, 1.28 U of G6PDH). For control reactions, UDP-glucose was omitted. 96-well flat-bottomed UV-Star microtitre plates (Greiner Bio One, Austria) were used for these assays. The reaction was carried out at 50°C and the increase in absorbance at 340 nm due to conversion of NADP to NADPH was monitored every 30 s throughout the

incubation using a plate reader (Bio Tek). Specific enzymatic activity was expressed as nkat mg protein^{-1}.

Trehalose 6-phosphate phosphatase activity

Trehalose 6-phosphate phosphatase (T6PP) activity was assessed slightly modifying the protocol described in Farelli *et al*. 2014. 10 µl of D-extract were added to a reaction mix with 5 mM $MgCl_2$, 1 mM DTT, 50 mM NaCl, 2 mM trehalose 6-phosphate dipotassium salt in 25 mM Tris-HCl at pH 7.5. Trehalose 6-phosphate dipotassium salt was omitted in the control mix. A phosphate standard curve was included in the assay to estimated enzymatic activity. The mixture was incubated at 38°C for 45 minutes. After incubation, 100 µl of the staining solution BIOMOL® Green (Enzo Life Sciences) used for colorimetric phosphate quantitation were pipetted in each well of the 96-wells plate (Sartsted, Germany). Absorbance was measured at 620 nm with a plate reader (Bio Tek). Specific enzymatic activity was expressed as nkat mg protein^{-1}.

Trehalase activity

The protocol used to measure trehalase (Tre) activity was set up following the protocol structure utilized for invertase activity determination. Aliquots of 10 µl of Z-extract were incubated at 38°C for 30 minutes with 10X reaction buffer at pH 4.5 (454 mM Na_2HPO_4/273 mM citric acid), also used to perform cell-wall invertase activity assay, and 10 mM trehalose as the substrate (omitted in control reactions). A glucose standard curve (0-50 nmol) was used to estimate enzymatic activity. 200 µl of GOD-POD solution (10 U ml-1 GOD, 0,8 U ml-1 POD, 0,8 mg ml^{-1} ABTS in 0.1 M potassium phosphate buffer, pH 7.0) were added to each well (including the standard curve). After 20 minutes of incubation at room temperature, absorbance was measured at a wavelength of 405 nm. Specific enzymatic activity was expressed as nkat mg protein^{-1}.

2.5 Measurement of gene expression

Total RNA was extracted from 160 mg of ground leaf sample, using a CTAB-based protocol adapted to grapevine tissues (Carra *et al*., 2007). RNA quantification and quality evaluation were performed using a NanoDrop™ 2000 spectrophotometer (ThermoFisher Scientific). RNA samples integrity was further checked through electrophoresis on a 1% agarose gel.

In order to avoid genomic DNA contamination, total RNA was treated with RNase-free DNase (DNase I, Amplification Grade Invitrogen, ThermoFisher Scientific). Then, 500 ng of DNase I-treated RNA was reverse-transcribed into cDNA using the High Capacity cDNA Reverse Transcription Kit (Applied Biosystems).

Gene-specific primers were designed with Primer3 (http://primer3.ut.ee/) (Tab. 1). Annealing temperatures, GC content (%) and absence of primer dimers or not specific secondary structures were confirmed through Oligo Evaluator (SIGMA-Aldrich; http://www.oligoevaluator.com/).The geometric average of *VvUbiquitin* and *VvActin e*xpression was used as reference in order to normalise gene expression data. Primer specificity and efficiency were assayed to ensure measurement accuracy.

RT-qPCR analyses were performed in a StepOnePlus™ Real-time PCR detection system (Applied Biosystems), supported by the StepOne software, version 2.3. Reactions were carried out in a final volume of 10 µl, consisting of 1 µl diluted cDNA, 1 µl of primer mix (10 µM), 5 µl Luna® Universal qPCR Master Mix (BioLabs Inc.) and 3 µl DEPC-treated ultrapure water. The PCR program was set as follows: 95°C for 10 min (initial holding stage); 45 cycles of 95°C for 15 sec, 63°C for 1 min. For melting curve analysis, the temperature was set at 95°C for 15 sec and at 63°C for 1 min. The ΔCt method was used to calculate normalized gene expression levels for the genotype tolerance study, while gene expression results from drought experiment were normalized on control samples. Analyses were performed in three technical replicates.

Tab. 1 – Specific primers sequence list.

Gene name	Gene ID (CRIBI)	Primer name	Forward primer sequence	Reverse primer sequence	Amplicon size (bp)
VvTPS1_A *(T6P synthase 1)*	VIT_10s0003g02160	***VvTPS1_A***	CTCACAAGCCAGGTTCATGA	GGCCACAAACTCATAGCTAACA	192
VvTPS5 *(T6P sythase 5)*	VIT_02s0012g01680	***VvTPS5***	GTGTTCTTGCCAATGAGCCA	TGCCGCATTGTTACAAGGAG	115
VvTPS7_A *(T6P synthase 7)*	VIT_10s0003g01680	***VvTPS7_A***	GGACAGAAACCAAGTAAAGCCA	GAGATGGGGAAGGGTCTGAA	100
VvTPS10 *(T6P synthase 10)*	VIT_01s0026g00280	***VvTPS10***	TTATGCTCGCCACTTCCTGT	CACAGTCCGACCCGAGTAAT	100
VvT6PP *(T6P phosphatase)*	VIT_16s0022g00660	***VvT6PP***	GCTGGTAGTCATGGGATGGA	AAAATTCACTCGCAGGCTGG	130
VvbZIP11 *(bZIP 11 transcrption factor)*	VIT_18s0001g13040	***VvbZIP11***	CCTCAATTACATGAACACAAGCA	TGATGATGACACGAAGGAGGA	160
VvCWINV1 *(cell-wall invertase 1)*	VIT_09s0002g02320	***VvCWINV1***	TCTATCAACAGCTCTACGGGT	TCTCACGGTTGTAGCTTCCA	124
VvSUSY2 *(sucrose synthase 2)*	VIT_07s0005g00750	***VvSUSY2***	GCCCTGCATGGTTCAATTGA	GTCAAGCCTTGCCATGGAAA	114
VvCAS2 *(callose synthase 2)*	VIT_06s0004g01270	***VvCAS2***	TTCACCCCAGTTGCATTTCT	CCGATCCTTCCTATGACCAC	129
VvAGPase *(ADP-glucose pyrophosphorylase)*	VIT_05s0020g02880	***VvAGPase***	CAGCATCACTCAACAGGCAT	TGGAGTTTGAGTGGCTGCTA	101
VvActin *(actin)*	VIT_04s0044g00580	***VvACT***	GCCCCTCGTCTGTGACAATG	CCTTGGCCGACCCACAATA	101
VvUbiquitin *(ubiquitin)*	VIT_16s0098g01190	***VvUBI***	TGAGGCTTCGTGGTGGTATT	GCGGCAGATCATTTTTGTCCT	80

2.6 Statistical analyses

In the sucrose treatment experiments, data were submitted to one-way analysis of variance (ANOVA) and means were compared using Fisher LSD post hoc test. Statistical significance was set at $P < 0.05$. When no statistical significance was detected comparing all the theses, a Student t-test ($P < 0.05$) was performed to evaluate statistical difference among treated and not-treated samples for each condition (healthy or FDp-infected) at every single time point. Three replicates were used. Sigma Plot® software (Systat Software Inc.) was used to perform statistical analyses and to create figures.

The heatmaps summarizing the SC-enzymes key signatures and the gene expression results were realized with Python (version 3.9.2; Jupyter notebook) on a z-score normalized data matrix (mean-centered data, normalized on standard deviation). Euclidean distance was applied to accomplish cluster analysis. Graphical implementation of figures was carried out with python and Inkscape software version 0.92.4 (https://inkscape.org/).

3. Results

In this work, we focused the attention on SC-related metabolism and signalling. We measured changes in sucrose and glucose concentrations and SC-related enzyme activity and gene expression in leaves exposed to two exogenous sucrose applications and belonging to four different varieties characterized by a diverse susceptibility towards *Flavescence dorée*. Enzyme activity and gene expression results are described with heatmaps divided per metabolic pathway (sucrose metabolism, trehalose metabolism, hexose-P metabolism, starch and cell-wall related metabolism) as reported here in figure 4. Results were subjected to z-score transformation and organized following cluster analysis (Euclidean distance).

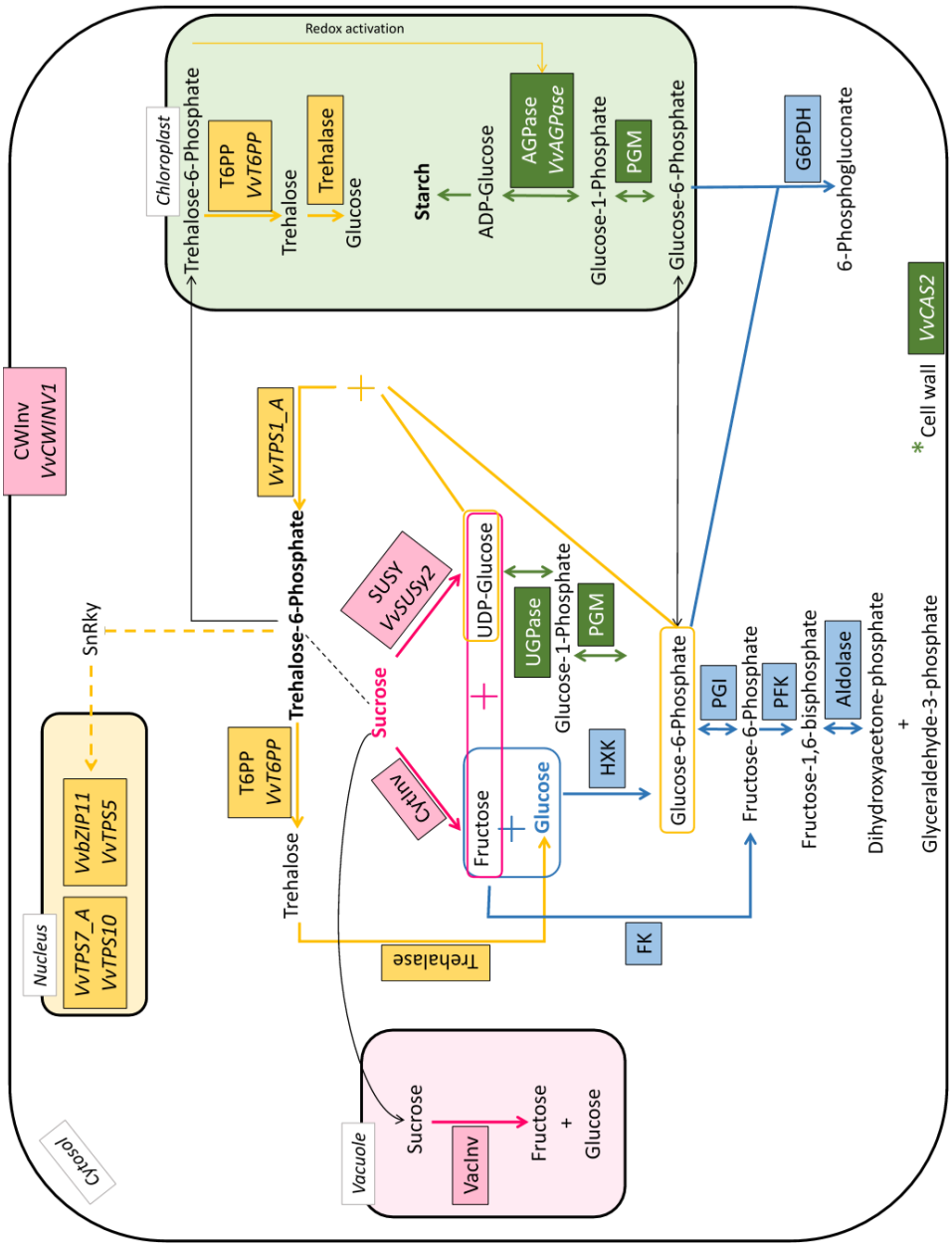

Fig. 4 – Scheme of SC-metabolism. Different colours were used to indicate each considered pathway: sucrose metabolism is represented in pink, trehalose metabolism in yellow, hexose-P metabolism in blue, starch and cell-wall related metabolism in green.

3.1 Varietal screening experiment

3.1.1 Sucrose and glucose concentrations

Carbohydrate concentration measurements (Fig. 5) in leaf revealed an average stable content of glucose among the varieties. Sucrose concentrations were significantly higher in Brachetto and Moscato.

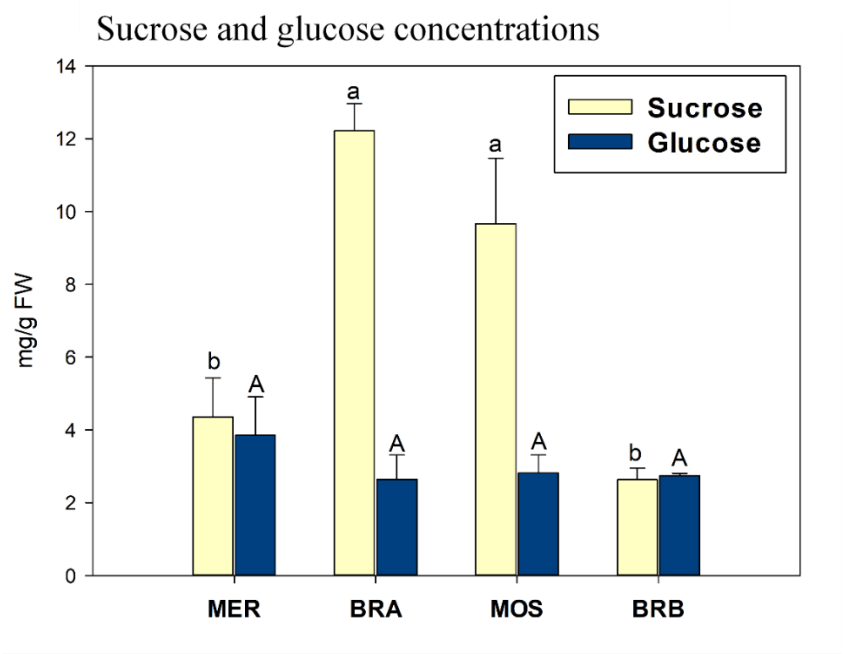

Fig. 5 – Sucrose and glucose amount in leaf tissues belonging to *V. vinifera* cv Merlot (MER), Brachetto (BRA), Moscato (MOS) and Barbera (BRB). Letters denote statistical differences among the varieties according to Fisher's LSD test.

3.1.2 SC-related enzyme activity and target gene expression

Protein concentration obtained from the extraction process was between 0,4 and 0,6 µg/µl for D-extract and between 0,15 and 0,25 µg/µl for Z-extract, trough Bradford staining assay. Enzyme activity was calculated based on protein content (nkat/mg protein) and values were normalized on untreated controls.

Target gene expression was evaluated by Real-Time qPCR analysis and normalized on housekeeping genes activity. The genes here presented were selected as the most representative for this study.

Enzymatic activity was generally higher in Merlot, respect to the other varieties, while gene expression appeared to be mainly activated in Brachetto and Moscato cultivars.

3.1.2 Sucrose metabolism

Activity of CWInv, on a transcriptomic (*VvCWINV1*) and protein level, was higher in Merlot, Brachetto and Moscato. The three tolerant cultivars showed a greater activity of Susy, while its encoding gene VvSUSY2 appeared activated only in Brachetto and Moscato. VacInv activity seemed to be relevant only for Moscato. On the other hand, CytInv was the only sucrose hydrolyzing enzyme to be strongly enhanced in susceptible Barbera.

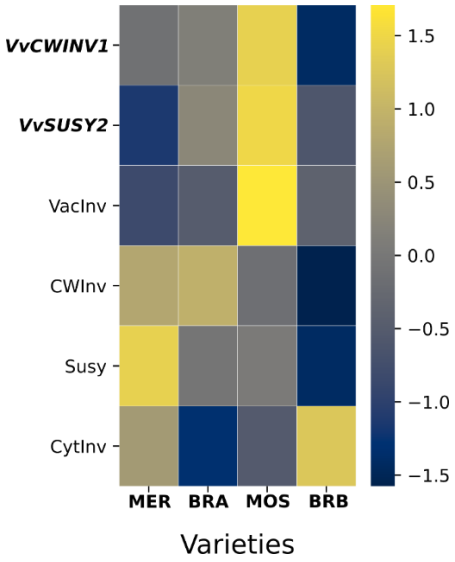

Fig. 6 – Sucrose-related gene expression and enzyme activity in leaf tissues belonging to *V. vinifera* cv Merlot (MER), Brachetto (BRA), Moscato (MOS) and Barbera (BRB).

3.1.2 Trehalose metabolism and T6P signaling

Trehalose metabolism and T6P signaling appeared to be more active in the tolerant Merlot, Brachetto, and Moscato, than in the susceptible Barbera. In Brachetto the transcript of the putative T6P biosynthetic gene *VvTPS1_A* was most elevated. The gene *VvTPS10* from Class 2 was mainly activated in Moscato, as it was shown for *VvT6PP* and the relative enzyme T6PP. In Barbera the low activity of T6PP, in comparison to the high transcription of the gene *VvT6PP* was probably due to post-transcriptional regulation. Trehalase activity was evident for Merlot and Brachetto.

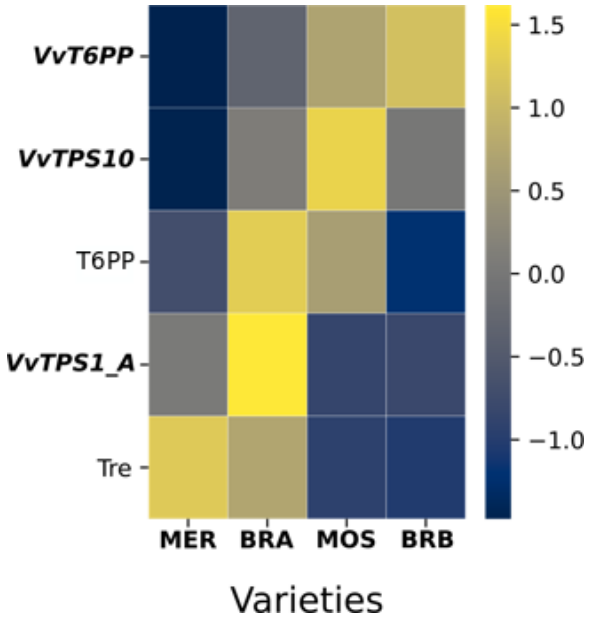

Fig. 7 – Trehalose-related gene expression and enzyme activity in leaf tissues belonging to *V. vinifera* cv Merlot (MER), Brachetto (BRA), Moscato (MOS) and Barbera (BRB).

3.1.2 Hexose phosphate metabolism

Enzymes involved in glycolysis and interconversion among the different hexose phosphate forms were remarkably active in Merlot and strongly reduced in Moscato. HXK, involved in signaling mechanism and responsible for G6P accumulation, was also present in Brachetto samples. Moreover, the enhanced activity of PGI suggests formation of F6P from G6P is also favored in this cultivar. In Barbera, the enzymes involved in the interconversion among the hexose phosphate forms (FK and PFK) and in their oxidation (G6PDH) were most active.

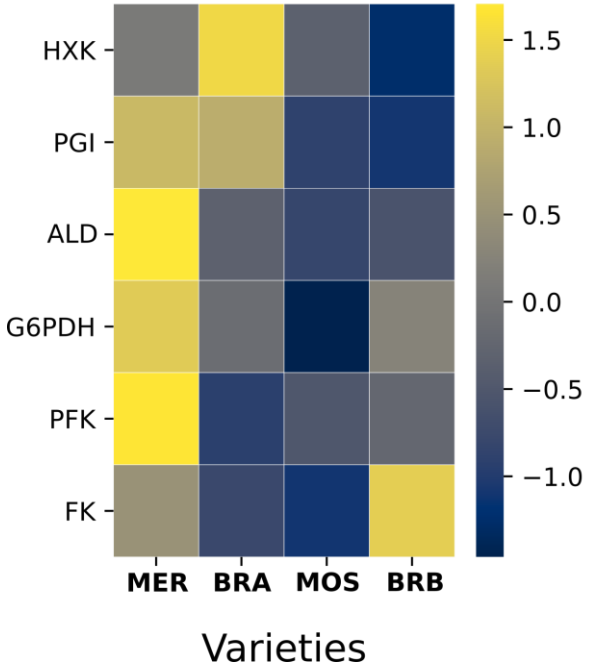

Fig. 8 – Hexose phosphate-related gene expression and enzyme activity in leaf tissues belonging to *V. vinifera* cv Merlot (MER), Brachetto (BRA), Moscato (MOS) and Barbera (BRB).

3.1.2 Starch and cell wall-related metabolism

Results obtained for PGM activity and *VvAGPase* transcription showed a similar trend. Nevertheless, the enzyme AGPase measurements revealed a remarkable activity only in Barbera. UGPase was instead activated peculiarly in Merlot.

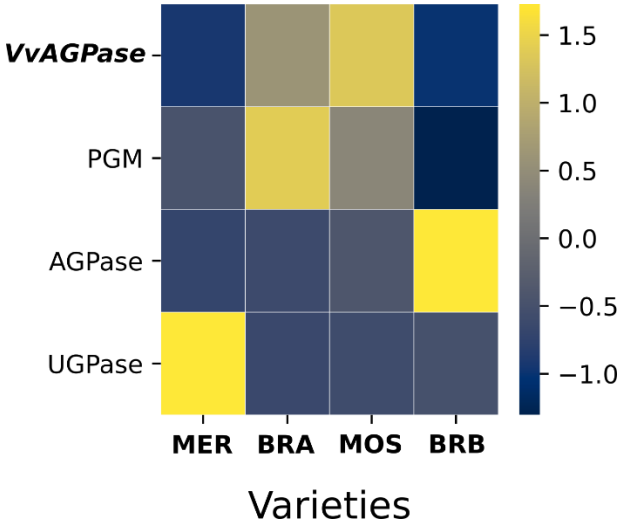

Fig. 9 – Starch and cell wall-related gene expression and enzyme activity in leaf tissues belonging to *V. vinifera* cv Merlot (MER), Brachetto (BRA), Moscato (MOS) and Barbera (BRB).

3.2 Exogenous sucrose application experiments

3.2.1 Diagnostic evaluation

The molecular diagnosis, performed using a commercial kit (Detection kit *Flavescence dorée* and *Bois Noir*, Multiplex Real-time PCR system, IPADLAB), confirmed the presence of the phytoplasma in all plants with symptomatic leaves, and its absence in all visually asymptomatic plants of the

experimental vineyard at the onset of the trial. Fungicide treatments were performed along the season on all the plants of the experimental vineyard.

3.2.2 Sucrose and glucose concentrations

Both sucrose infusion and spraying caused a mostly decreasing trend of sucrose concentration, which resulted generally more evident for FDp-infected plants, and significant in the healthy, infused plants, and in the FDp-infected, sprayed plants (Fig. 10a,b). Glucose concentration followed a reverse trend, with differences in favour of treated plants being significant for infused healthy plants and for sprayed FDp-infected plants above the respective controls (Fig. 10a,b).

The sucrose concentration of FDp-infected, not-treated grapevines of the spray experiment was 20-40% higher than in the respective treatment of the infusion experiment. This difference could be due to an increase of the phytoplasma load along the season. In fact, sampling in the spray treatment was performed 15 days later respect to the infusion probably in closer correspondence of the expected infection peak.

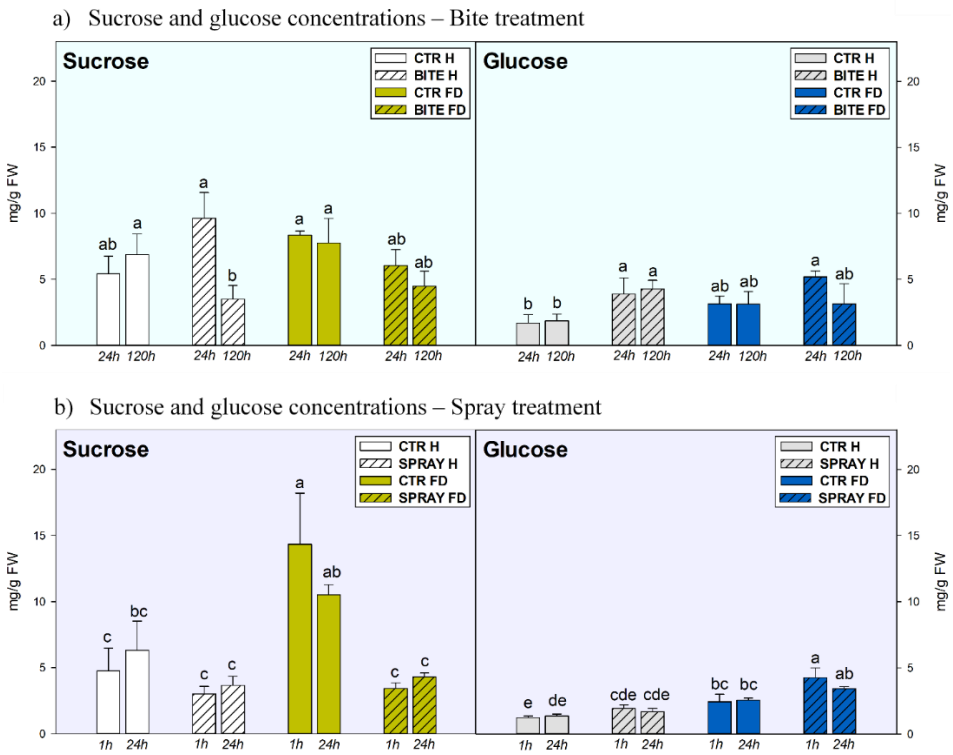

Fig. 10 – Sucrose and glucose quantification changes in healthy (H) and FDp-infected (FD) leaves in response to sucrose treatments. a) Sucrose and glucose quantification in leaves 24 and 120 hours after sucrose trunk infusion (BITE). Letters denote statistical difference (P<0,05) among sucrose-treated and non-treated plants according to Student t-test (no significant differences among treatments were detected with Fischer LSD test). b) Sucrose and glucose quantification in leaves 1 and 24 hours after sucrose spray treatment (SPRAY). Letters denote statistical differences (P<0,05) among treatments according to LSD Fisher test.

3.2.3 SC-related enzyme activity and target gene expression

Protein concentration obtained from the extraction process was between 0,4 and 0,6 µg/µl for D-extract and between 0,15 and 0,25 µg/µl for Z-extract,

trough Bradford staining assay. Enzyme activity was calculated based on protein content (nkat/mg protein) and values were normalized on untreated controls. Enzymes for which it was not possible to assess a reliable and repeatable measurement were not included in this analysis (VacInv, AGPase, FK, PFK and Ald).

Target gene expression was evaluated by Real-Time qPCR analysis and normalized on housekeeping gene activity.

Both sucrose treatments affected enzymatic activity and target gene expression.

3.2.3 Sucrose metabolism

Sucrose infusion induced an enhanced activity of the sucrose hydrolysing enzymes in both healthy and infected plants, with Susy activated more in healthy, and CytInv significantly more activated in FDp-infected plants. CWInv was significantly increased in both healthy and FDp-infected grapevines 120 hours after the treatment. Enzyme activation was reflected by significant increased expression of the *VvSUSY2* (encoding a Susy isoform) and *VvCWINV1* genes only in FDp-infected plants. The effect on FDp positive grapevines was in general more evident 120 hours after the treatment.

On the contrary, sucrose spraying mainly affected healthy plants causing a lower invertase activity, but significantly enhancing Susy activity. *VvCWINV1* and *VvSUSY2* expression changes were not in agreement with activity changes of the respective enzymes, suggesting post-transcriptional mechanisms of protein stability and enzymatic activity regulation.

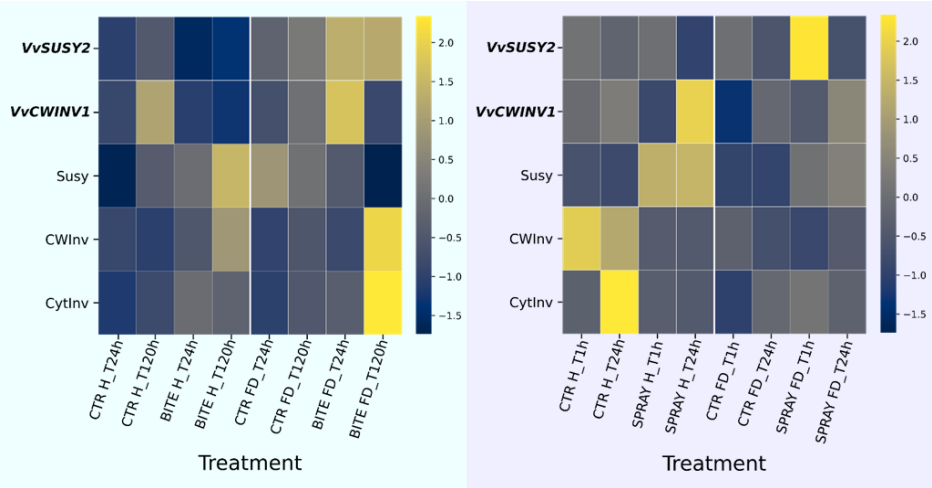

Fig. 11 – Sucrose-related gene expression and enzyme activity changes in healthy (H) and FDp-infected (FD) leaves in response to sucrose treatments. a) Sucrose-related gene expression and enzyme activity in leaves 24 (T24 h) and 120 (T120 h) hours after sucrose trunk infusion (BITE). b) Sucrose-related gene expression and enzyme activity in leaves 1 (T1 h) and 24 (T24 h) hours after sucrose spray treatment (SPRAY). Results were subjected to z-score transformation and organized following cluster analysis.

3.2.3 Trehalose metabolism and T6P signaling

Sucrose treatment induced a general acceleration of the trehalose metabolic branch. The potentially (see chapter II) biosynthetic, leaf-specific *TPS1_A* gene was significantly upregulated following both sucrose treatments in FD-infected plants. Both infusion and spray application were effective in promoting T6PP activity in both healthy and FDp-infected plants, although only in spraying the differences were statistically significant. Nevertheless, expression of *VvT6PP* was not affected. Trehalase activity was reduced by sucrose infusion, and significantly activated by spraying only at the T24 sampling (fig. 12b). Expression of the TPS Class 2 genes, whose role is not known yet, followed variable patterns of response. As already underlined in chapter II under different conditions, *VvTPS1_A* and *VvTPS5* as well as *VvTPS7_A* and *VvTPS10*

in both cases share the same trend. In FDp-infected plants, sucrose infusion induced a significant increase of the transcription of *VvTPS7_A* and *VvTPS10*, while spraying caused a significant reduction. Expression of *VvbZIP11*, which is involved in the T6P signal, was significantly activated by infusion in FDp-infected plants.

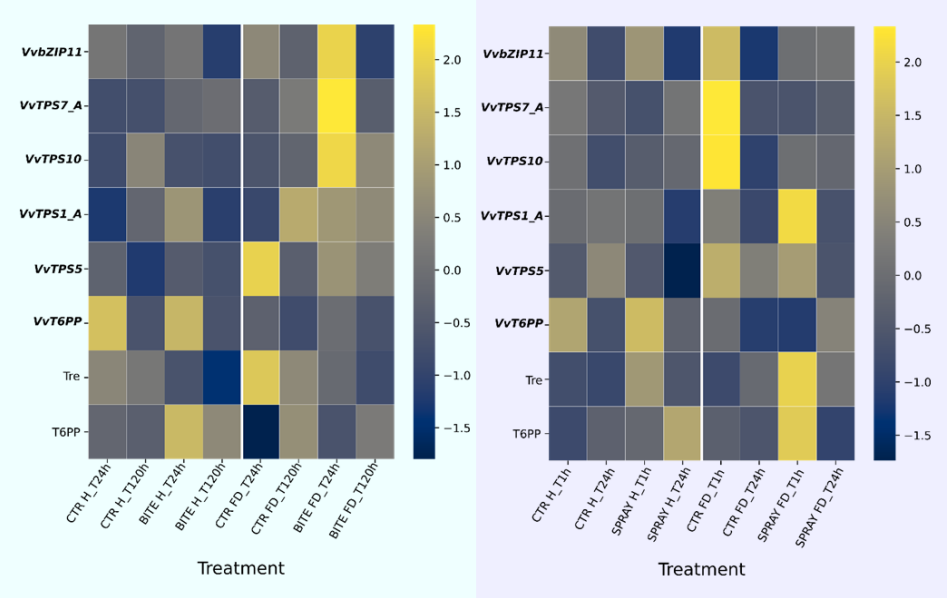

Fig. 12 – Trehalose-related genes expression and enzymes activity changes in healthy (H) and FDp-infected (FD) leaves in response to sucrose treatments. a) Trehalose-related gene expression and enzyme activity in leaves 24 (T24 h) and 120 (T120 h) hours after sucrose trunk infusion (BITE). b) Sucrose-related gene expression and enzyme activity in leaves 1 (T1 h) and 24 (T24 h) hours after sucrose spray treatment (SPRAY). Results were subjected to z-score transformation and organized following cluster analysis.

3.2.3 Hexose phosphate metabolism

Sucrose infusion was effective in encouraging sucrose hydrolysis, and consequently, glucose accumulation, mainly in infected grapevines, whilst interconversion to hexose phosphates and G6P oxidation were enhanced in sucrose-infused healthy plants. On the other hand, glucose phosphate metabolism appeared to be strongly compromised by spray treatment, in particular in not-infected plants.

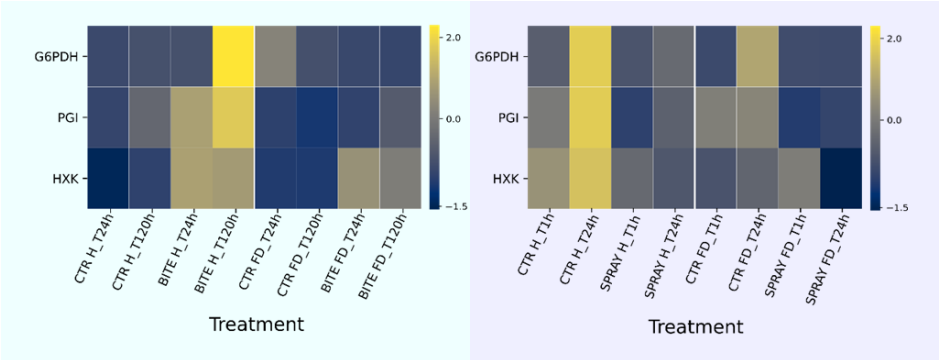

Fig. 13 –Hexose phosphate metabolism enzyme activity changes in healthy (H) and FDp-infected (FD) leaves in response to sucrose treatments. a) Hexose phosphate metabolism enzyme activity in leaves 24 (T24 h) and 120 (T120 h) hours after sucrose trunk infusion (BITE). b) Hexose phosphate metabolism enzyme activity in leaves 1 (T1 h) and 24 (T24 h) hours after sucrose spray treatment (SPRAY). Results were subjected to z-score transformation and organized following cluster analysis.

3.2.3 Starch and cell wall-related metabolism

The effect of sucrose infusion in the trunk is similar in healthy and diseased plants, but it is mainly evident in not-infected Barbera, where induced a significantly higher activity of PGM and UGPase and downregulation of

VvAGPase. Spraying displayed an opposite tendency: a statistically significant lower activity of PGM and UGPase is accompanied by an augmented *VvAGPase* transcription. Transcription of the gene encoding for the enzyme callose synthase, *VvCAS2* was significantly enhanced in FDp-infected, infused plants, while it was remarkably downregulated 24 hours after the foliar spray application.

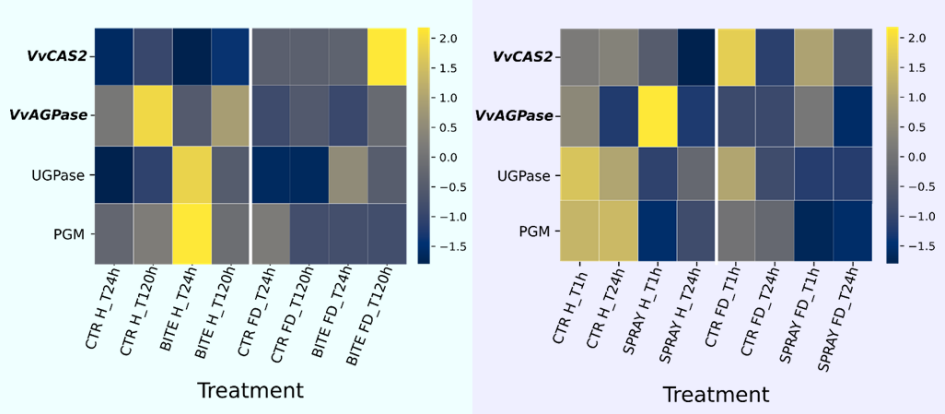

Fig. 14 – Starch and cell wall-related gene expression and enzyme activity changes in healthy (H) and FDp-infected (FD) leaves in response to sucrose treatments. a) Starch and cell wall-related gene expression and enzyme activity in leaves 24 (T24 h) and 120 (T120 h) hours after sucrose trunk infusion (BITE). b) Sucrose-related gene expression and enzyme activity in leaves 1 (T1 h) and 24 (T24 h) hours after sucrose spray treatment (SPRAY). Results were subjected to z-score transformation and organized following cluster analysis.

4. Discussion

Soluble carbohydrates have a renowned role in helping plants coping with stress of different origin. Modifications and rearrangements of primary metabolism are in fact the main consequences of physiological alterations occurring in presence of both biotic and abiotic stress.

Flavescence dorée is a disease caused by a phytoplasma, which colonizes grapevine sieve elements, deeply influencing plant metabolism and function. This pest severely affects vineyards all over Europe, causing a dramatic reduction of yields in terms of quantity and quality. At this moment, only two strategies to contain the pathogen spread can be applied: eradication of infected grapevines and control of vector population through insecticide treatments. Knowledge on phytoplasma-plant specific interaction is still very limited and mostly limited to other phytoplasmas such as the causing agent of *Bois Noir* (Rotter *et al*., 2017; Dermastia *et al*., 2021). Moreover, there is a lack of information about molecular and physiological basis of tolerance and recovery from the infection. Investigating the pathways involved would help finding new insights and improving tools for limiting pathogen spread and/or restraining negative effect of the symptoms. Previous studies underlined alterations of carbohydrate metabolism due to FDp infection, potentially linked to the distribution of sugars, sucrose in particular, among source and sink tissues (Prezelj *et al*., 2016; Pagliarani *et al*., 2020). Therefore, aiming to further explore the putative involvement of sugar metabolism in response to *Flavescence dorée* in grapevine, we exposed a group of plants to exogenous applications of sucrose in field. We compared two different types of application, trunk infusion and leaf spraying, measuring soluble carbohydrates content and related enzyme activity and gene expression. In parallel, we performed an evaluation of the carbohydrate metabolism of *Vitis vinifera* plants belonging to the varieties Merlot, Brachetto, Moscato and Barbera, which have been shown to display a different grade of tolerance against the pathogen.

Exogenous intake of sucrose resulted in a progressive reduction of sucrose content coupled with an increase in total glucose for both applications. The measured increase of sucrose synthase and invertases (cell wall and cytosolic) activity in response to the treatments confirms that added sucrose was promptly hydrolysed, explaining the lower content of sucrose in treated leaves.

The diverse mode of application of sucrose to the plant and its consequent availability to the pathogen influenced the final effect (Fig.15). Sucrose provided through the infusion treatment reached leaves by the xylem path, causing a high activation of the invertases, which promoted hexoses accumulation. On the other hand, sucrose sprayed on leaf surface was probably absorbed through leaf epidermal cells. In this case, Susy was the designated enzyme for sucrose cleavage. UGPase, highly activated in the infusion treatment, was down-regulated in sprayed leaves, in which UDP-glucose was already derived from Susy activity. In both FDp-infected and healthy plants, infusion enhanced activity of the enzymes responsible for hexose phosphate interconversion, while spraying caused a significant reduction of these processes.

Presence or absence of the pathogen clearly directed the SC-metabolism towards two different pathways: FDp-infected grapevines seemed to preferably promote regulatory mechanisms through trehalose metabolism activation, while in healthy plants, sucrose treatments drove the metabolism into starch direction. Interestingly, sucrose infused in the xylem was particularly effective in FD positive plants, hinting at a stronger pathogen-treatment interaction. In fact, exclusively in response to infusion treatment we assisted to a significant activation of T6P biosynthesis, by increased expression of *TPS* genes from Class I and Class II. Moreover, sucrose infusion significantly affected transcription of *VvCAS2*. The gene, responsible for the synthesis of callose, a cellulose derivative, already found to be upregulated in grapevines affected by FD (Pagliarani *et al*., 2020) and by *Bois Noir* (Santi *et al*., 2013a) was further enhanced in response to the treatment. Deposition of callose on sieve plates help the plant containing phytoplasma spread in the phloem (Santi *et al*., 2013b). Cell wall invertase was also significantly activated in response to BITE application in FDp-infected leaves. CWInv has a documented role in driving plant responses against pathogen attacks, enhancing overall tolerance (Proels and Huckelhoven, 2014).

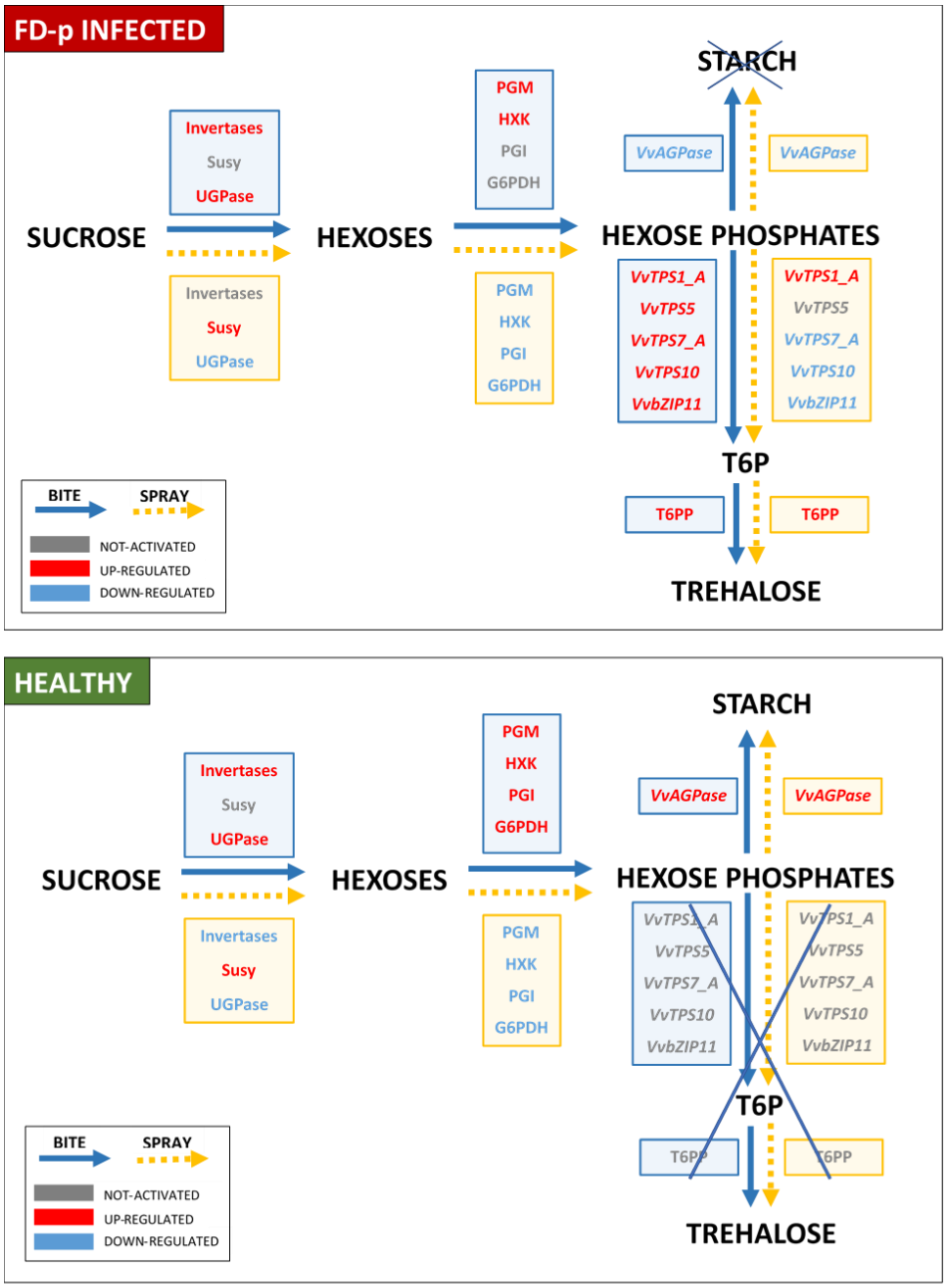

Fig. 15 – Schematic representation of the effects derived from the two different exogenous sucrose applications (BITE and SPRAY) on SC-metabolism in FDp-infected and healthy grapevine leaves.

In a recent study by Ripamonti *et al*. (2020), a large group of grapevine genotypes was assessed to evaluate their degree of tolerance against FDp. Brachetto and Moscato showed the lowest percentage of infection, apparently as a result of two different mechanisms of tolerance. Indeed, Moscato tolerance was mainly based on insect-plant interaction, because leafhoppers rarely fed on Moscato leaves and therefore they did not transmit the phytoplasma. On the other side, Brachetto leaves were very palatable for the vector; however, the rate of FDp transmission was incredibly low, suggesting the activation of a specific plant responsive mechanism.

With the aim of individuating molecular and biochemical aspects conferring tolerance towards FD, we investigated soluble sugar concentration and metabolism in the tolerant Merlot, Brachetto and Moscato, and in the susceptible Barbera. This approach allowed us to identify enzymes and genes putatively link to tolerant behaviour.

First, Brachetto and Moscato had a significantly higher content of sucrose in leaf, respect to Barbera, suggesting that sucrose-related metabolism is probably involved in conferring tolerance traits. Merlot and Brachetto tolerance seems to be based on a plant-pathogen interaction level. These two cultivars showed a high enzymatic activity, with particular reference to pathways related to sucrose hydrolysis, glucose phosphorylation and sugar signaling. Merlot and Brachetto share also great levels of *VvTPS1_A* transcription and downregulation of *VvT6PP*, underlying again a putative involvement of T6P in responses to the pathogen. Moscato did not exhibit remarkable SC-enzymes activation, except for vacuolar invertase; nevertheless, transcription of the evaluated carbohydrate-related genes was the highest among the four varieties. Elevated gene expression could be a reasonable explanation of the tolerance strategy of Moscato. On the contrary, enzymatic activity in Barbera was principally focused on cytosolic invertase, phosphofructokinase, fructokinase, glucose-6-phosphate dehydrogenase and AGPase (Fig. 14). PFK, FK and G6PDH are all enzymes

involved in fructose metabolism, which are known to be activated in presence of other phytoplasmas as Bois Noir, as well as invertases. Therefore, the high activity of these enzymes in Barbera could be linked to a stronger susceptibility exhibited by this cultivar. In conclusion, our results suggest an increased activity of the T6P and trehalose-related metabolism and signaling in tolerant varieties and a predominant starch-directed metabolism for the susceptible one (Fig. 16).

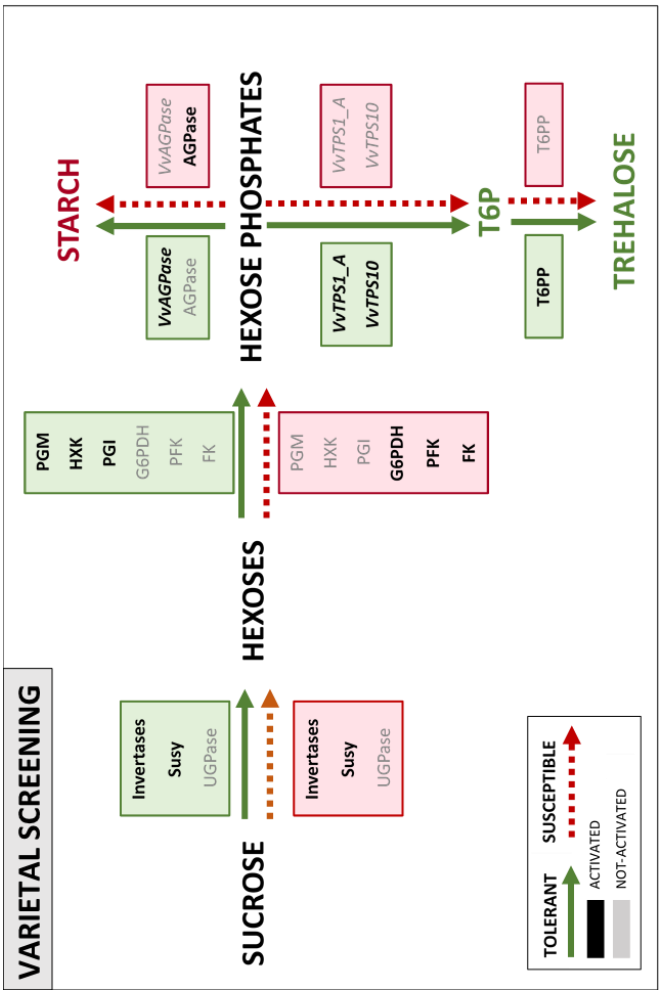

Fig. 16 – Schematic representation of the SC-related enzymes and genes activation in tolerant and susceptible varieties.

5. Conclusions

Interestingly, effects derived from sucrose infusion treatment on FDp-infected plants and analyses carried on tolerant varieties showed common results. In fact, T6P metabolism resulted to be activated specifically in FD-infected, treated grapevines and in the tolerant varieties Merlot and Barbera. Cell wall invertase, both at the enzymatic and at the gene level, was highly induced in treated samples and appeared to be a feature shared among the three tolerant varieties. These results suggest that applying exogenous doses of sucrose in the trunk to enhance tolerant behaviour against FDp could be a valuable strategy, which should be further investigated. Besides, the current study confirmed the pivotal role of carbohydrate metabolism and signalling in FDp-grapevine interaction.

Tab. 2 – Raw values of enzyme activity and gene expression in response to BITE and SPRAY treatments. Letters denote statistical differences (P < 0,05) according to LSD Fisher test.

	nkat/mg protein								normalized expression			
BITE	**CTR H_T24 h**		**CTR H_T120 h**		**BITE H_T24 h**		**BITE H_T120 h**		**CTR FD_T24 h**		**CTR FD_T120 h**		**BITE FD_T24 h**		**BITE FD_T120 h**	
CWInv	0,04	**c**	0,03	**c**	0,06	**bc**	0,17	**ab**	0,03	**c**	0,06	**bc**	0,04	**c**	0,26	**a**
CytInv	0,00	**b**	0,01	**b**	0,02	**b**	0,02	**b**	0,01	**b**	0,01	**b**	0,02	**b**	0,06	**a**
Susy	0,09	-	0,13	-	0,15	-	0,20	-	0,18	-	0,15	-	0,13	-	0,08	-
PGM	0,27	**b**	0,38	**b**	0,84	**a**	0,31	**b**	0,37	**b**	0,15	**b**	0,15	**b**	0,14	**b**
PGI	0,24	**c**	0,74	**b**	1,53	**ab**	2,03	**a**	0,18	**c**	0,02	**c**	0,21	**c**	0,57	**b**
T6PP	3,49E-05	-	3,17E-05	-	6,78E-05	-	4,95E-05	-	4,55E-06	-	5,21E-05	-	2,64E-05	-	4,36E-05	-
Tre	0,10	-	0,09	-	0,04	-	0,00	-	0,17	-	0,11	-	0,07	-	0,03	-
HXK	0,00	-	0,01	-	0,03	-	0,03	-	0,01	-	0,01	-	0,03	-	0,02	-
G6PDH	0,04	-	0,06	-	0,06	-	0,43	-	0,20	-	0,06	-	0,03	-	0,03	-
UGPase	0,33	**c**	1,23	**b**	4,95	**a**	1,95	**b**	0,52	**b**	0,49	**b**	3,24	**ab**	1,99	**b**
VvTPS1_A	0,05	**c**	0,10	**abc**	0,06	**c**	0,15	**a**	0,07	**bc**	0,17	**a**	0,14	**ab**	0,15	**a**
VvTPS5	0,01	**c**	0,00	**d**	0,01	**cd**	0,01	**d**	0,03	**a**	0,01	**cd**	0,02	**b**	0,02	**bc**
VvTPS7_A	0,13	**b**	0,14	**b**	0,20	**b**	0,22	**b**	0,17	**b**	0,25	**b**	0,50	**a**	0,18	**b**
VvTPS10	0,04	**bc**	0,08	**b**	0,04	**bc**	0,04	**c**	0,04	**bc**	0,05	**bc**	0,13	**a**	0,08	**b**
VvT6PP	1,47	**a**	0,19	**b**	1,36	**a**	0,19	**b**	0,37	**b**	0,10	**b**	0,52	**b**	0,17	**b**
VvbZIP11	0,10	**bc**	0,08	**b**	0,10	**b**	0,04	**c**	0,13	**bc**	0,08	**bc**	0,20	**a**	0,04	**c**
VvSUSY2	0,30	**c**	0,42	**c**	0,18	**cd**	0,23	**cd**	0,47	**bc**	0,58	**ab**	0,82	**ab**	0,80	**a**
VvCWINV1	0,07	**b**	0,08	**b**	0,06	**b**	0,04	**b**	0,09	**b**	0,16	**b**	0,43	**a**	0,08	**b**
VvCAS2	0,02	**e**	0,04	**cde**	0,02	**e**	0,03	**de**	0,06	**bcd**	0,06	**bc**	0,06	**b**	0,14	**a**
VvAGPase	0,21	**ab**	0,52	**ab**	0,11	**bc**	0,34	**a**	0,05	**bc**	0,10	**bc**	0,04	**c**	0,17	**ab**

	nkat/mg protein												normalized expression									
SPRAY	**CTR H_T1 h**		**CTR H_T24 h**		**SPRAY H_T1 h**		**SPRAY H_T24 h**		**CTR FD_T1 h**		**CTR FD_T24 h**		**SPRAY FD_T1 h**		**SPRAY FD_T24 h**							
CWInv	0,95	-	0,72	-	0,17	-	0,15	-	0,21	-	0,07	-	0,01	-	0,16	-						
CytInv	0,00	**bc**	0,02	**a**	0,00	**bc**	0,00	**c**	0,00	**bc**	0,00	**d**	0,01	**b**	0,00	**bc**						
Susy	0,09	**b**	0,05	**b**	0,54	**a**	0,56	**a**	0,03	**b**	0,02	**b**	0,25	**ab**	0,33	**ab**						
PGM	3,82	**a**	3,93	**a**	0,41	**c**	1,22	**bc**	2,23	**b**	1,96	**b**	0,22	**c**	0,40	**c**						
PGI	1,46	-	2,71	-	0,47	-	1,02	-	1,54	-	1,64	-	0,39	-	0,53	-						
T6PP	0,00	**c**	0,00	**c**	0,00	**bc**	0,00	**ab**	0,00	**c**	0,00	**c**	0,00	**a**	0,00	**c**						
Tre	0,07	**bc**	0,04	**c**	0,44	**ab**	0,12	**bc**	0,05	**bc**	0,22	**bc**	0,69	**a**	0,28	**bc**						
HXK	0,05	-	0,07	-	0,03	-	0,03	-	0,03	-	0,03	-	0,04	-	0,01	-						
G6PDH	0,03	**b**	0,15	**a**	0,02	**b**	0,05	**b**	0,01	**b**	0,11	**a**	0,01	**b**	0,01	**b**						
UGPase	2,21	**a**	1,84	**a**	0,53	**b**	1,06	**b**	1,86	**a**	0,66	**b**	0,47	**b**	0,46	**b**						
VvTPS1_A	0,10	**bcd**	0,11	**bc**	0,11	**bc**	0,05	**d**	0,12	**bc**	0,06	**cd**	0,21	**a**	0,07	**bcd**						
VvTPS5	0,02	-	0,03	-	0,02	-	0,01	-	0,03	-	0,03	-	0,03	-	0,02	-						
VvTPS7_A	0,32	**b**	0,18	**b**	0,13	**b**	0,31	**b**	0,80	**a**	0,14	**b**	0,14	**b**	0,19	**b**						
VvTPS10	0,09	**b**	0,03	**b**	0,06	**b**	0,08	**b**	0,26	**a**	0,01	**b**	0,09	**b**	0,08	**b**						
VvT6PP	0,54	**ab**	0,14	**cd**	0,63	**a**	0,23	**bcd**	0,28	**bc**	0,05	**d**	0,04	**d**	0,39	**b**						
VvbZIP11	0,13	**ab**	0,06	**cd**	0,14	**ab**	0,03	**cd**	0,18	**a**	0,03	**d**	0,10	**bc**	0,10	**bc**						
VvSUSY2	0,48	**b**	0,37	**b**	0,46	**b**	0,10	**b**	0,46	**b**	0,25	**b**	1,27	**a**	0,21	**b**						
VvCWINV1	0,15	-	0,18	-	0,09	-	0,31	-	0,05	-	0,14	-	0,12	-	0,19	-						
VvCAS2	0,04	**ab**	0,04	**ab**	0,03	**bcd**	0,01	**d**	0,06	**a**	0,02	**cd**	0,05	**ab**	0,02	**bcd**						
VvAGPase	0,17	**b**	0,06	**cd**	0,28	**a**	0,05	**cd**	0,08	**bcd**	0,08	**bcd**	0,15	**bc**	0,03	**d**						

References

Carra, A., Gambino, G., Schubert, A., 2007. A cetyltrimethylammonium bromide based method to extract low-molecular-weight RNA from polysaccharide-rich plant tissues. Analytical Biochemistry **360**. https://doi.org/10.1016/j.ab.2006.09.022

Caudwell A., 1961. Les phénomènes de rétablissement chez la Flavescence dorée de la vigne. Ann. Epiphyt. **12,** 347–354.

Covington E., Roitsch T. & Dermastia M. 2016. Determination of the Activity Signature of Key Carbohydrate Metabolism Enzymes in Phenolic-rich Grapevine Tissues. Acta Chimica Slovenica. 2016. 757-762. 10.17344/acsi.2016.2484.

Chuche, J., Thiéry, D., 2014. Biology and ecology of the Flavescence dorée vector Scaphoideus titanus: a review. Agronomy for Sustainable Development **34**. https://doi.org/10.1007/s13593-014-0208-7

Delaney, T. P. (1997). Genetic dissection of acquired resistance to disease. Plant Physiology, **113**(1), 5.

Dermastia, M., Škrlj, B., Strah, R., Anžič, B., Tomaž, Š., Križnik, M., ... & Pompe-Novak, M. (2021). Differential response of grapevine to infection with 'Candidatus Phytoplasma solani'in early and late growing season through complex regulation of mRNA and small RNA transcriptomes. International journal of molecular sciences, **22**(7), 3531.

Eveillard, S., Jollard, C., Labroussaa, F., Khalil, D., Perrin, M., Desqué, D., Salar, P., Razan, F., Hévin, C., Bordenave, L., Foissac, X., Masson, J.E., Malembic-Maher, S., 2016. Contrasting Susceptibilities to Flavescence Dorée in Vitis vinifera, Rootstocks and Wild Vitis Species. Frontiers in Plant Science **7**. https://doi.org/10.3389/fpls.2016.01762

LaFever, R. E., Vogel, B. S., & Croteau, R. (1994). Diterpenoid resin acid biosynthesis in conifers: enzymatic cyclization of geranylgeranyl pyrophosphate to abietadiene, the precursor of abietic acid. Archives of biochemistry and biophysics, **313**(1), 139-149.

Galetto, L., Miliordos, D., Roggia, C., Rashidi, M., Sacco, D., Marzachì, C., Bosco, D., 2014. Acquisition capability of the grapevine Flavescence dorée by the leafhopper vector Scaphoideus titanus Ball correlates with phytoplasma titre

in the source plant. Journal of Pest Science **87**. https://doi.org/10.1007/s10340-014-0593-3

Gambino, G., Boccacci, P., Margaria, P., Palmano, S., Gribaudo, I., 2013. Hydrogen Peroxide Accumulation and Transcriptional Changes in Grapevines Recovered from Flavescence Dorée Disease. Phytopathology® **103**. https://doi.org/10.1094/PHYTO-11-12-0309-R

Jammer, A., Gasperl, A., Luschin-Ebengreuth, N., Heyneke, E., Chu, H., Cantero-Navarro, E., ... & Roitsch, T., 2015. Simple and robust determination of the activity signature of key carbohydrate metabolism enzymes for physiological phenotyping in model and crop plants. Journal of Experimental Botany, **66**(18), 5531-5542.

Kuzmanovic, S., Martini, M., Ermacora, P., Ferrini, F., Starovic, M., Tosic, M., Carraro, L., Osler, R., 2008. Incidence and molecular characterization of Flavescence dorée and stolbur phytoplasmas in grapevine cultivars from different viticultural areas of Serbia. Vitis **45**, 105–111.

Morone, C., Boveri, M., Giosuè, S., Gotta, P., Rossi, V., Scapin, I., Marzachì, C., 2007. Epidemiology of *Flavescence Dorée* in Vineyards in Northwestern Italy. Phytopathology® **97**. https://doi.org/10.1094/PHYTO-97-11-1422

Pagliarani, C., Gambino, G., Ferrandino, A., Chitarra, W., Vrhovsek, U., Cantu, D., Palmano, S., Marzachì, C., Schubert, A., 2020. Molecular memory of *Flavescence dorée* phytoplasma in recovering grapevines. Horticulture Research **7**. https://doi.org/10.1038/s41438-020-00348-3

Pegoraro, M., Rossi, M., Mori, N., Galetto, L., Pagliarani, C., Boccacci, P., Gambino, G., de Paoli, E., Marzachì, C., Bosco, D., 2017. Le viti risanate da flavescenza dorata sono suscettibili a reinfezioni: prove biologiche e molecolari. In Proc. of VII Incontro Nazionale Sui Fitoplasmi e le Malattie da Fitoplasmi **32** (Torino, Italy).

Pelletier, C., Salar, P., Gillet, J., Cloquemin, G., Very, P., Foissac, X., & Malembic-Maher, S., 2009. Triplex real-time PCR assay for sensitive and simultaneous detection of grapevine phytoplasmas of the 16SrV and 16SrXII-A groups with an endogenous analytical control. Vitis, **48**(2), 87-95.

Prezelj, N., Covington, E., Roitsch, T., Gruden, K., Fragner, L., Weckwerth, W., Chersicola, M., Vodopivec, M., Dermastia, M., 2016. Metabolic Consequences of Infection of Grapevine (*Vitis vinifera* L.) cv. "Modra frankinja"

with *Flavescence Dorée* Phytoplasma. Frontiers in Plant Science **7**. https://doi.org/10.3389/fpls.2016.00711

Proels, R.K., Hückelhoven, R., 2014. Cell-wall invertases, key enzymes in the modulation of plant metabolism during defence responses. Molecular Plant Pathology **15**. https://doi.org/10.1111/mpp.12139

Ripamonti, M., Pegoraro, M., Morabito, C., Gribaudo, I., Schubert, A., Bosco, D., Marzachì, C., 2020. Susceptibility to flavescence dorée of different *Vitis vinifera* genotypes from north-western Italy. Plant Pathology. https://doi.org/10.1111/ppa.13301

Roggia, C., Caciagli, P., Galetto, L., Pacifico, D., Veratti, F., Bosco, D., Marzachì, C., 2014. Flavescence dorée phytoplasma titre in field-infected Barbera and Nebbiolo grapevines. Plant Pathology **63**. https://doi.org/10.1111/ppa.12068

Rotter, A., Nikolić, P., Turnšek, N., Kogovšek, P., Blejec, A., Gruden, K., & Dermastia, M., 2018. Statistical modeling of long-term grapevine response to 'Candidatus Phytoplasma solani'infection in the field. European Journal of Plant Pathology, **150**(3), 653-668.

Santi S., De Marco F., Polizzotto R., Grisan S., Musetti R., 2013b – Recovery from stolbur disease in grapevine involves changes in sugar transport and metbolism. Frontiers in Plant Science **4**(171).

Santi S., Grisan S., Pierasco A., De Marco F., Musetti R., 2013a – Laser microdissection of grapevine leaf phloem infected by stolbur reveals site-specific gene responses associated to sucrose transport and metabolism. Plant Cell & Environment **36**: 343-355.

Schvester, D., Carle, P., Montous, G., 1963. Transmission de la Flavescence dorée de la vigne par *S. littoralis* Ball. Ann. Epiphyt. **14**, 175–198.

Vitali, M., Chitarra, W., Galetto, L., Bosco, D., Marzachì, C., Gullino, M.L., Spanna, F., Lovisolo, C., 2013. Flavescence dorée phytoplasma deregulates stomatal control of photosynthesis in *Vitis vinifera*. Annals of Applied Biology **162**. https://doi.org/10.1111/aab.12025

Yoshida, S., Ito, M., Nishida, I., & Watanabe, A., 2002. Identification of a novel gene HYS1/CPR5 that has a repressive role in the induction of leaf

senescence and pathogen-defence responses in Arabidopsis thaliana. The Plant Journal, **29**(4), 427-437.

Final considerations and future perspectives

Grapevine is exposed to several abiotic and biotic stresses. Applying correct practices of vineyard management is not always sufficient to avoid the severe consequences of these multiple threats. Therefore, investigation of plant molecular and biochemical aspects affected during the stress is the first step to further explore tolerance strategies. Stresses have a strong impact on general plant physiology, mainly resulting in photosynthesis and transport systems dysfunctionality. Thus, carbohydrate metabolism alteration influences plant stress responses. Indeed, sugars play a pivotal role in helping plants facing stresses in a direct manner, as osmolytes, or indirectly as signalling molecules or as precursors for secondary metabolites.

Purpose of this PhD project was to extend knowledge on sugar metabolism involvement in grapevine responses to biotic and abiotic stresses, through an integrative and multidisciplinary method. Molecular, biochemical and ecophysiological measurements allowed us to investigate and compare an environmental issue, water deficiency, and a phytoplasma disease, *Flavescence dorée*. Both stresses indeed have similar consequences on the general physiology of the plant. Drought and FDp cause tissue dissecation and influence sugar allocation in the plant. In brief, **chapter I** describes how different rates of water stress affect plant recovery strategies. Soluble carbohydrates and starch accumulated in the stems during the slow developing drought constituted the source of energy to fulfill recovery. In fact, after re-watering, the amount of sugars in the stems was significantly reduced, while we assisted to a strong increment of soluble sugars in the xylem sap coupled with pH acidification. On the contrary, recovery from fast developing drought appeared not directly carbohydrate-dependent, suggesting that stress severity and mostly timing (rate) influences plant capability to manage reserves for recovering.

The role of sugar metabolism in FDp-infected grapevines was evaluated in **chapter III**. Susceptibility to *Flavescence dorée* is strictly dependent on variety. We demonstrated that tolerant cultivars have a higher content of sucrose in the leaves and an enhanced sucrose-related enzyme activity. Based on these results and on some preliminary data showing sucrose accumulation in leaf coupling with a decrease in FDp titre (data not shown in this thesis), we performed two different sucrose treatments on FDp-positive Barbera, the most susceptible variety. The treatments promoted activation of T6P and trehalose metabolism in the infected plants, while FDp-negative (which we referred to as *healthy*) appeared to drive the exogenous provided sucrose towards starch accumulation.

Chapter II represents the link between the two different studied aspects. TPS gene family characterisation revealed that T6P metabolism and signaling is involved in a wide range of mechanisms and in different tissues at every phenological stage. TPS gene expression not only was affected by both biotic and abiotic stress, but its strict connection to sucrose was also confirmed.

In conclusion, results presented in this PhD thesis proved the importance of sugars in helping plants coping with stresses of various origin, not only as primary metabolites but also as signalling molecules. Moreover, the multidisciplinary role of T6P and its direct nexus with sucrose suggests new insights on the cross-talk between primary, secondary and hormone metabolism and signalling. Further investigating the different physiological and molecular plant behaviours will elucidate the significance of carbohydrate metabolism in this complex network of interactions.

Ringraziamenti

Ringrazio sentitamente il Prof. Andrea Schubert per avermi guidata lungo il mio percorso di dottorato. Grazie della fiducia e del supporto che mi hanno permesso di raggiungere questo importante traguardo.

Grazie alla Prof. Francesca Secchi, il cui amore per la scienza è per me fonte di grande ispirazione. L'ascolto e il confronto sincero non mi sono mai mancati.

Thank you prof. Thomas Roitsch for having hosted me in your lab group. Results obtained during my visiting period at the University of Copenhagen are a valuable part of this research thesis.

Dedico questa tesi di dottorato ai miei genitori. Grazie di aver sempre lottato per comprendere il mio mondo. Da sempre supportate la mia curiosità e il mio desiderio di conoscere, di volare. In ogni scelta che ho preso non mi sono mai sentita sola. Vi ringrazio perché sapendomi guidare da vicino e da lontano siete stati le mie ali.

Grazie a tutte le ragazze e ai ragazzi del laboratorio per l'aiuto e per l'amicizia che ci lega non solo dietro il bancone.

Un abbraccio particolare a Chiara, perché più volte hai saputo con dolcezza ricordarmi di affrontare la vita con tenacia, senza smettere però di nutrire quella bambina meravigliata e spensierata dentro di me. Grazie Vera, perché senza inutili fronzoli sai essere presente e generosa sempre. Mi auguro che tu ed Eric sappiate quanto è profondo il mio affetto per voi e quanto davvero un buon pezzo della riuscita di questa tesi sia dovuta alle incredibili pizze e ai pessimi film divorati sul vostro divano. Marta sei stata una delle più belle scoperte di questo ultimo anno. Adoro la semplicità con cui ogni giorno ci cerchiamo e ci troviamo, la naturalezza e la sincerità che rende la nostra amicizia per me così unica. Sai farmi sentire al sicuro, grazie.

Marco, questo dottorato ha visto l'inizio e la fine della nostra avventura insieme in Saccarelli. Grazie di essermi stato compagno in questo cammino, di cui conosci ogni sfumatura, ogni gioia e fatica. Di Flavescenza dorata ne sai ormai a tal punto che una parte di questa tesi avresti potuto scriverla tu!

Grazie Emanuele. Condividere con te le piovose domeniche di studio matto e disperato ha alleggerito tutta la stanchezza e reso concreto ogni sforzo. Sapersi prendere cura di chi ci sta accanto è una delle doti più belle e delicate che esistano. Grazie perché riesci a farmi sentire preziosa, ma forte e coraggiosa allo stesso tempo. E poiché so che ci tieni particolarmente… si metta agli atti che a te va tutto il merito della buona riuscita di molti di questi grafici, a te e al signor Python, a cui mi hai sapientemente introdotto.

Un piccolo grazie anche alla mia Margot, il mio adorato e dispettoso famiglio che da vicino mi accompagna in ogni mio giorno.

Thanks to my Danish family. We were strangers, but you welcomed me in your house, making me experiencing what 'hygge' really means. I will be grateful forever.

Thank you Barbara, for the time we shared in Copenhagen and for our cozy Sunday coffee-chat now. You are a special friend!